

**UNIVERSITY OF WEST BOHEMIA IN PILSEN
FACULTY OF ELECTRICAL ENGINEERING**

DEPARTMENT OF TECHNOLOGY AND MEASUREMENT

BACHELOR THESIS

Organic material based on carbon allotropes for sensors.

Originál (kopie) zadání BP/DP

Abstract

The broad range of carbon forms and their extraordinary electrochemical qualities are constantly being explored for the production of novel cost-effective technology applications. Sensor technology has greatly benefited from the exploitation of these qualities in the production of low-cost, highly sensitive, responsive, repeatable, large range and sturdy sensors. An overview of the qualities possessed by some zero-, one-, and two-dimensional carbon allotropes suitable for use in sensor technology is given in the first section. Section two reviews some of the most suitable technologies for carbon deposition onto substrates in the fabrication of carbon-based sensors. The third section presents the results of a practical investigation of the variation of electrical resistance with temperature for functionalized as well as non-functionalized single-wall and multi-wall carbon nanotubes deposited on the Tesla BI2 substrate by air-brush. Sulfonate and carboxyl-ate functional groups are used. A review of experiment results including the effect of functionalization on the sensing properties of carbon nanotubes is provided in the fourth and final section.

Key words

Carbon allotrope, temperature sensor, single-wall carbon nanotube, multi-walled carbon nanotube, deposition technology, functionalization, -COOH functional group, -SO₃H functional group

Abstrakt

Široká škála forem uhlíku a jejich mimořádné elektrochemické vlastnosti jsou neustále zkoumány pro výrobu nových ekonomicky efektivních technologických aplikací. Technologie senzorů velmi těžší z využití těchto kvalit při výrobě levných, vysoce citlivých, stabilních, velkých a robustních senzorů. V první části práce je uveden přehled vlastností, kterými disponují některé 0D, 1D a 2 D uhlíkové alotropy vhodné pro použití v sensorové technologii. Druhá část práce popisuje některé z nejvhodnějších technologií pro depozici uhlíku či jeho alotropů na substráty při výrobě senzorů. Třetí část představuje výsledky praktického zkoumání variací elektrického odporu s teplotou funkcionalizovaných i nefuncionalizovaných jednostěnných a víceštěnných uhlíkových nanotrubiček na substrátu Tesla B12 deponovaných pomocí air-brush. Funkcionalizované uhlíkové nanotrubičky jsou v experimentu reprezentovány CNT se sulfonovými a karboxylovými funkčními skupinami. Ve čtvrté a závěrečné části je uveden přehled výsledků experimentu včetně vlivu funkcionalizace na sensorické vlastnosti uhlíkových nanotrubiček.

Klíčová slova

Carbon allotrope, temperature sensor, single-wall carbon nanotube, multi-walled carbon nanotube, deposition technology, functionalization, -COOH functional group, -SO₃H functional group

Declaration

I declare that I have prepared this bachelor's thesis independently, using the professional literature and sources listed in the reference section of this bachelor's thesis.

I further declare that all software used in preparing this bachelor's thesis is legal.

.....
Signature

In Plzen on, 27.5.2021

Malinga Tembo

Acknowledgment

My deep gratitude goes to my supervisor Ing. Josef Šlauf for his unflinching support and guidance throughout the duration of this work.

I am also highly indebted to Ing. Jiří Štulík, Ph.D. for introducing me to scientific research methods in materials and technologies for electrical engineering.

I am extremely thankful to Ma. Madalina Tusinean for the designing the tables and some of the graphical illustrations.

I owe a deep sense of gratitude to my family for their constant support and encouragement throughout the period of my study.

Table of content

| | |
|--|----|
| Introduction | 9 |
| List of Symbols and abbreviations | 14 |
| 1. Overview of suitable organic materials based on carbon allotropes used in the field of sensors | 15 |
| 1.1. Fullerene based nanomaterial..... | 20 |
| 1.2. Carbon nanotubes..... | 28 |
| 1.2.1. SWCNTs..... | 30 |
| 1.2.2. MWCNTs..... | 32 |
| 1.2.3. CNT synthesis methods..... | 33 |
| 1.2.3.1. Carbon Arc Discharge..... | 33 |
| 1.2.3.2. Laser Ablation..... | 35 |
| 1.2.3.3. Chemical Vapour Deposition..... | 36 |
| 1.2.4. CNT functionalization..... | 38 |
| 1.3. Graphene based nanomaterials | 40 |
| 1.3.1. Properties..... | 42 |
| 1.3.2. Other graphene forms..... | 44 |
| 1.3.2.1. Graphene oxide and reduced graphene oxide..... | 44 |
| 1.3.2.2. Graphene Foam | 44 |
| 1.3.2.3. Carbon Dots..... | 45 |
| 1.3.3. Synthesis of graphene..... | 46 |
| 1.3.3.1. Mechanical Exfoliation..... | 47 |
| 1.3.3.2. CVD..... | 47 |
| 1.3.3.3. Arc discharge method..... | 48 |
| 1.3.3.4. Reduction of graphene oxide..... | 49 |
| 1.3.3.5. Functionalization of graphene..... | 50 |
| Covalent functionalization..... | 50 |
| Non covalent functionalization..... | 51 |
| Section 2 | 52 |
| 2.1. Langmuir-Blodgett..... | 52 |
| 2.2. Drop Casting..... | 55 |
| 2.3. Electrophoretic deposition..... | 57 |

| | |
|---|-----------|
| 2.4. Layer-by-Layer Electrostatic Self-Assembly..... | 59 |
| 2.5. Dip coating..... | 60 |
| 2.6. Spray Coating..... | 60 |
| 2.7. Spin Coating..... | 63 |
| 2.8. Chemical Vapor Deposition..... | 63 |
| 2.9. Direct dry transfer..... | 66 |
| | |
| Section 3: Practice verification of the temperature response of SWCNT and MWCNT..... | 68 |
| Experiment Aims..... | 68 |
| Experiment Procedure..... | 68 |
| Results and Data Analysis..... | 70 |
| Data Analysis..... | 83 |
| References..... | 85 |

Introduction

Carbon is a non-metallic chemical element listed sixth on the periodic table and represented by the letter C. The name carbon is derived from the Latin word for coal, “carbo” [1]. Carbon occurs naturally in three isotopes: ^{12}C , ^{13}C , and the radioactive isotope ^{14}C . It is a tetravalent element and forms covalent bonds with itself as well as with other elements [2]. It is considered to be the fourth most common element in the earth’s crust with relative abundance assessed to be 180 - 270 ppm [3].

People have used carbon in technology and in everyday life for many centuries. Carbon black, charcoal and graphite are some of the many materials known to have been used in prehistoric times. In those times, carbon-based materials were used as writing and drawing materials, among other uses. Today, carbon lends itself to contemporary science and technology as an invaluable elemental asset, revolutionising the nanotechnology

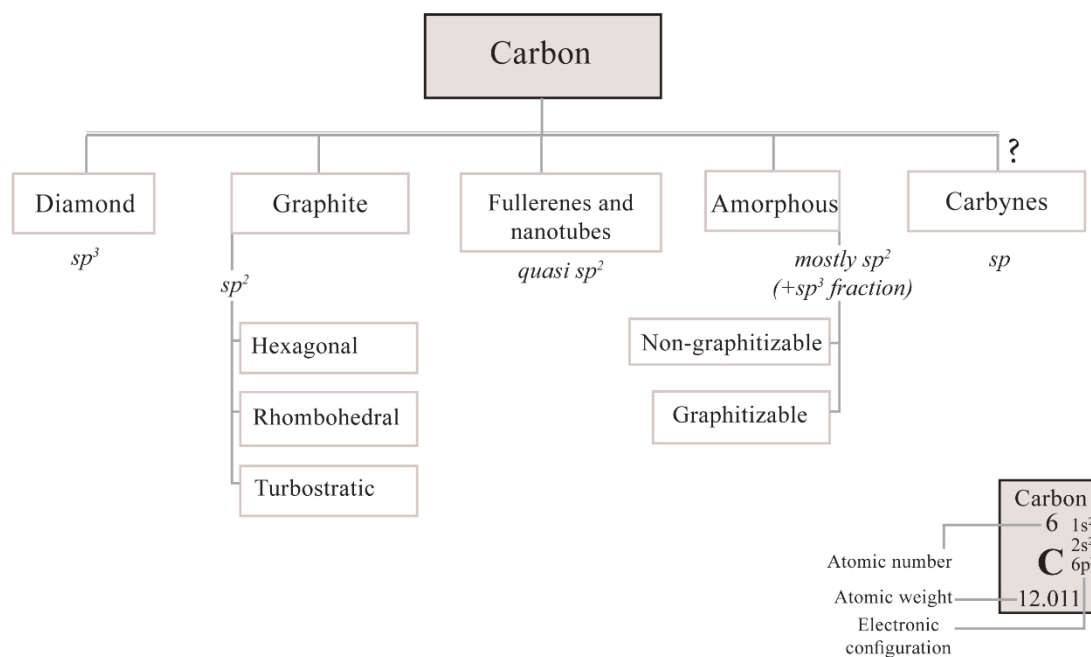


Figure i. Allotropes of carbon [34].

industry [4].

Nanotechnology is defined as the understanding and control of matter at dimensions between 1 and 100 nm where unique phenomenal enable novel applications [5]. The last 100 years have seen rapid growth in the nanotechnology industry. The increased interest in

nanotechnology research and development has consequently led to the development of outstanding industrial applications [6]. Nanotechnology has attracted so much popularity chiefly because its domain of operation is at the very foundation of matter, at the most fundamental level of organization of atoms and molecules in both living and anthropogenic systems [5]. Experiments with particles at the nanoscale reveal that these particles exhibit exceptional tunable physical properties as well as outstanding solvent interactions [7], [8]. Manipulation of materials at atomic level has brought to light the possibility to synthesize very small structures or devices from atomic or molecular building blocks using the so-called “bottom-up” approach [6], making possible the design and assembly of nanoscale functional gadgets through the emergence of technologies such as micro-electromechanical system (MEMS), to name but a few [9].

These concepts of nanotechnology were first formally introduced by the 1965 Nobel Prize Laureate in Physics [10], Richard Feynman in 1959. However, it wasn't until the 1980s that the golden era of nanotechnology launched. In 1985 Kroto, Drexler, Curl, and Smalley discovered fullerene using principles first laid out by Feynman and other pioneers in the field. Great interest in nanotechnology was further enhanced when Iijima discovered carbon nanotubes in 1991 [11]–[13]. The revolutionary discoveries of fullerene and carbon nanotubes have since placed carbon nanotechnology squarely at the helm of the nanotechnology industry [6].

Nanomaterials are generally classified as zero-dimensional if all three dimensions of the material are less than 100 nm; one-dimensional if the material has two of its dimensions less than 100 nm; two-dimensional if the material has one dimension less than 100 nm. Three-dimensional nanomaterials are usually bulky structures composed of nano-sized building block structures. Chemical functionalization of nanoparticles, permits construction of composite nanostructures of higher dimensions. Functionalization technologies also serve to alter the properties of nanomaterials [9]. Figure ii shows an illustration of zero, one and two-dimensional carbon nanomaterials together with a few inherent properties.

Carbon presents itself in many different natural and artificial allotropic forms [14]. The eight main allotropes of carbon are, 1) graphite, 2) diamond, 3) C₆₀ (buckminster fullerene or buckyball), 4) C₇₀, 5) C₅₄₀, 6) lonsdalite, 7) carbon nanotubes (buckytube), 8)

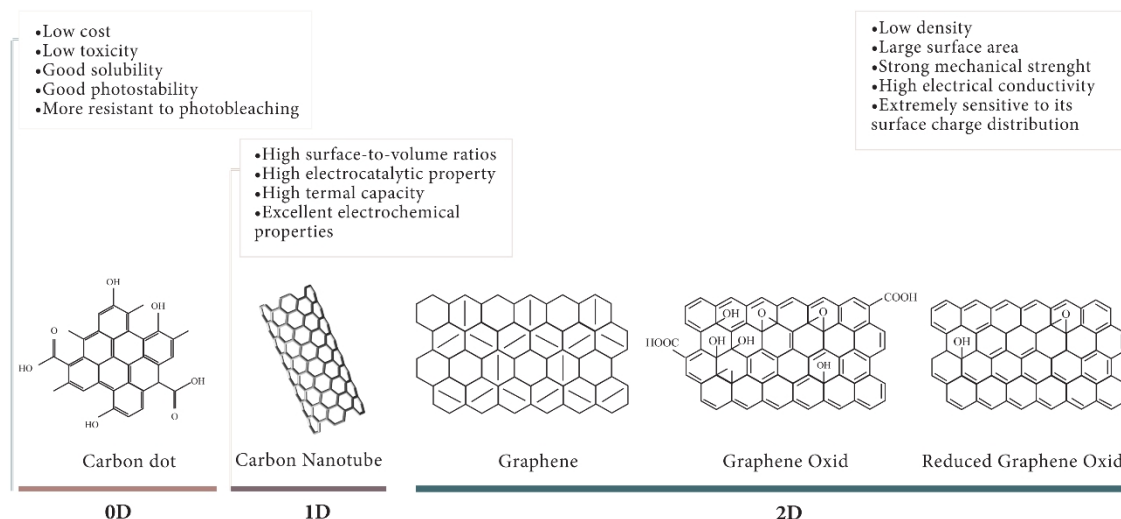


Figure ii. Properties of some 0D, 1D and 2D CNMs as potential candidates in sensor technology [179].

amorphous carbon [1]. In contrast to other nanomaterials such as metal oxide nanowires and transitional metal nanomaterials, carbon allotrope-based nanomaterials possess exceptional chemical, physical, mechanical and electronic properties [14] [15]. These brilliant properties of carbon include, but are not limited to; wide specific area, biocompatibility, high electro-chemical stability, ease of manipulation, good electrical and thermal conductivity, high mechanical resistance, low cost, suitable surface chemistry for a wide range of oxidation-reduction reactions, and environmentally friendly qualities, continue to fascinate researchers and scientists [3], [15]–[17]. Structure and size play a huge role in determining an allotropes' properties [18].

It is therefore no surprise that carbon continues attracting substantial attention owing to its direct application in the generation of new materials with exclusive properties. Carbon is also one of the most studied and used materials in the field of nanotechnology on account of the many unique properties it holds over conventional alternatives. There has, consequently, been an ascent in the use of conjugated carbon materials over the last 25 years not least in the fields of material science, nanoelectronics and nanobiotechnology [4], [9], [19].

The outstanding thermal, optical, mechanical, and electrical properties of the carbon nanostructures are constantly being investigated for deployment in sensor [9], [20]–[23] technology, among other uses [24]–[31].

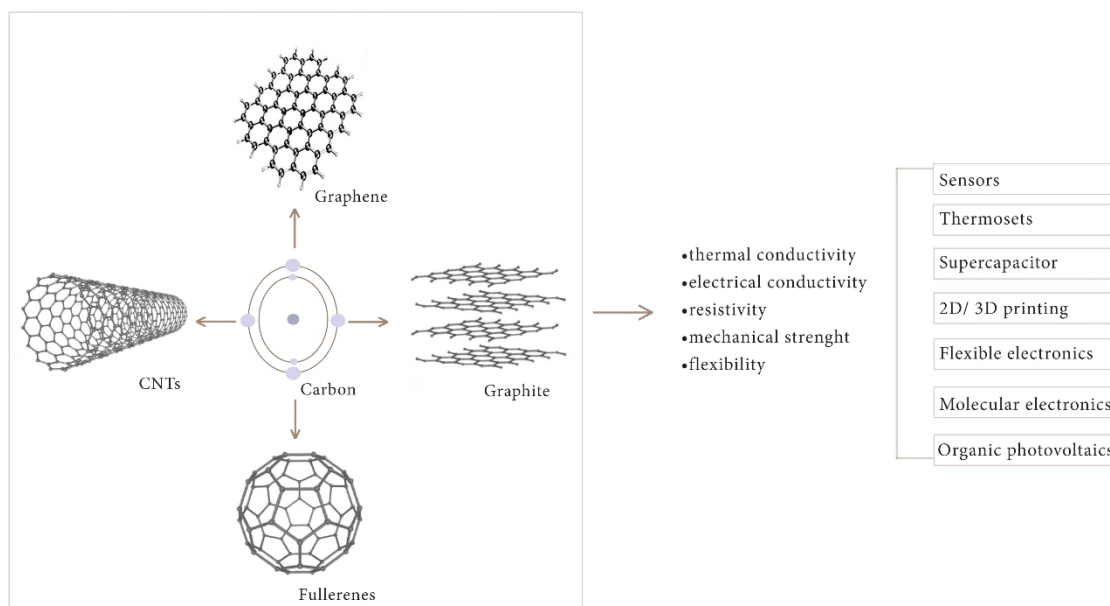


Figure iii. Various carbon allotropes, their electronic properties and applications in electronic industries. [3]

A sensor is defined to be a device that responds to stimulus, generating a signal that can be analysed [16]. The two general categories for carbon nanomaterial-based sensors are electrical and electrochemical sensors [16]. Sensor operation relies on the interaction of an analyte and sensing material via physical or chemical means. The resultant signal, in proportion to the analyte concentration, can then be transduced before amplification and processing for user interface [23]. It is required of a good quality sensor to have fast response to external stimulus, low recovery time, *in situ* analysis, and the ability to detect an analyte in proportion as low as possible. A sensor must also be easy to operate, and of preferably small relative size. These high-quality sensing properties are possible thanks to carbons' superior chemical and physical qualities [15], [9]. Furthermore, carbon can be

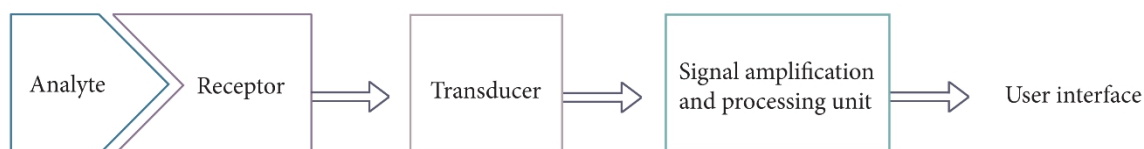


Figure iv. Working of a basic sensor block schematic [23].

Table i. Analyt and corresponding quantity in sensor technology [9].

| Analyt | Quantity (Transduction) |
|---|---|
| Acoustic | Wave (amplitude, phase, polarization), Spectrum, Wave Velocity |
| Biological & Chemical | Fluid Concentrations (Gas or Liquid) |
| Electric | Charge, Voltage, Current, Electric Field (amplitude, phase, polarization), Conductivity, Permittivity |
| Magnetic | Magnetic Field (amplitude, phase, polarization), Flux, Permeability |
| Magnetic Electro-magnetic (Gamma, X-ray, UV, Visible, IR, RF) | Refractive Index, Reflectivity, Absorption, Wave (amplitude, phase, polarization) |
| Thermal | Temperature, Flux, Specific Heat, Thermal Conductivity |
| Mechanical | Position, Velocity, Acceleration, Force, Strain, Stress, Pressure, Torque |

functionalised to a high degree in order to achieve excellent target specificity for desired analyte. [15], [32].

Part one of this thesis gives an overview highlighting the unique properties of some carbon allotropes suitable for use in sensor technology. An overview of a representative 0-, 1- and 2-dimensional carbon allotropes is given. In the second part, a review of some wet and dry approach deposition technologies suitable for carbon allotropes used in sensor technologies is presented. The third and final part is a practical verification of the temperature dependence, by measuring output resistance, of pristine as well as functionalised single- and multiple-walled carbon nanotubes. Sulfonate and carboxyl-ate functional groups are used.

List of Symbols and abbreviations

| | |
|---------------------------------------|---|
| D..... | Dimension |
| NM..... | nanomaterials |
| C ₆₀ | Buckminsterfullerene |
| CNM..... | Carbon based nanomaterial |
| CNT..... | Carbon Nanotubes |
| FCC | Face Centred Cubic structure |
| PAHs | Polycyclic Hydrocarbons |
| LUMO..... | Lowest Unoccupied Molecular Orbital |
| HOMO..... | Highest Occupied Molecular Orbital |
| IPR..... | Isolated Pentagon Rule |
| PAHs..... | Polycyclic Hydrocarbon |
| SWCNT..... | Single-Walled Carbon Nanotube |
| MWCNT..... | Multi-Walled Carbon Nanotube |
| DWCNTs | Double-Walled CNTs |
| C _h | Chiral Vector |
| a ₁ , a ₂ | unit vectors |
| θ | Isolated Chiral angle |
| NIR | Near-Infrared Radiation |
| GO | Graphene oxide |
| rGO | reduced Graphene Oxide |
| CD | Carbon Dot |
| GQD | Graphene Quantum Dots |
| HOPG | Highly Oriented Pyrolytic Graphite |
| LB | Langmuir-Blodgett |
| EPD | Electrophoretic Deposition |
| LbL | Layer-by-Layer |
| LbL-ESA | Layer-by-Layer Electrostatic Self-Assembly |
| IDES | Integrated Electrode Structure |
| COOH..... | Carboxylic Acid |
| SO ₃ H..... | Sulphur (trioxide) Acid |
| SWCNT-COOH..... | Sulfonate Functionalised Single-Wall Carbon Nanotube |
| MWCNT-COOH..... | Sulfonate Functionalised Multi-Wall Carbon Nanotube |
| SWCNT- SO ₃ H..... | Carboxyl-ate Functionalised Single-Wall Carbon Nanotube |
| MWCNT- SO ₃ H..... | Carboxyl-ate Functionalised Multi-Wall Carbon Nanotube |
| Ch | Channel |
| NTC | Negative Temperature Coefficient |

1.0. Overview of suitable organic materials based on carbon allotropes used in the field of sensors.

Amorphous carbon and two crystalline carbon forms, graphite and diamond, have classically been the three known naturally occurring forms of carbon [33]. The individual chemical and physical properties of the two crystalline forms of carbon, graphite and diamond, differ immensely despite both consisting exclusively of carbon atoms. Amorphous carbon, however, lacks structural crystallinity and often contains notable quantities of hydrogen [34].

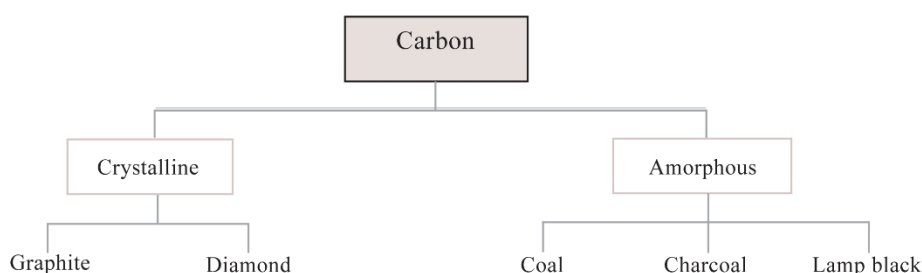


Figure 1.0.1 Some examples of crystalline and amorphous carbon allotropes [180].

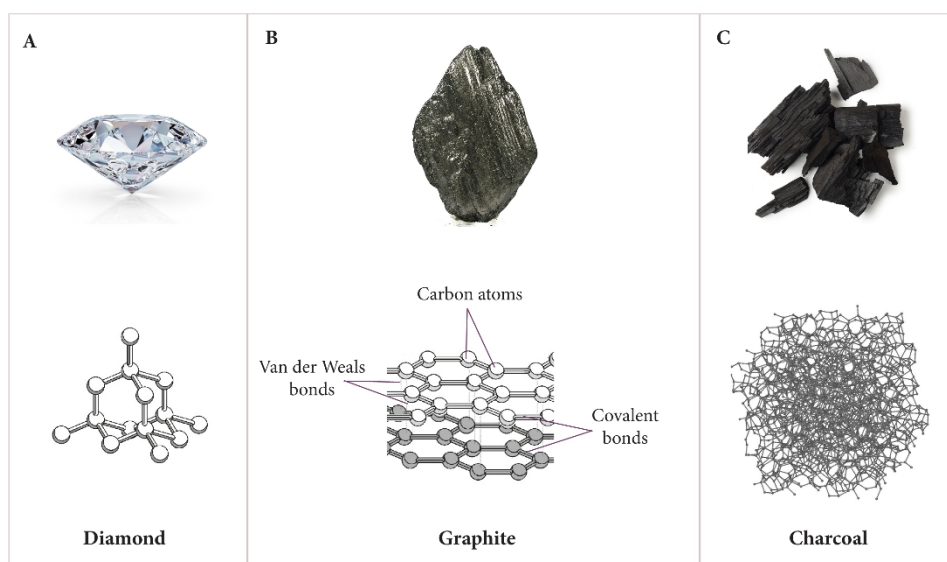


Figure 1.0.2. Schematic diagram of the classically known carbon forms, (a) diamond, (b) graphite, (c) amorphous carbon example, charcoal.

Carbon, a group 14 (IV A) element, is the most versatile of all known elements, presenting many bonding possibilities [34], [35]. Its extent of catenation is unrivalled by any other element. Carbon not only bonds with nearly all other elements of the periodic table, but also with itself in almost limitless variations. It also has the ability to form long chains of atoms, thus displaying polymerization. Further still, carbon bonds with both electropositive and electronegative elements [34] [36]. Carbon atoms are capable of forming single, double and triple carbon-carbon bonds where the average bond energies are reported to be approximately 350 kJ mol^{-1} , 610 kJ mol^{-1} , 840 kJ mol^{-1} between single, double and triple bonds, respectively [37].

Even though chemically speaking, graphite and diamond are similar, they manifest completely different physical parameters [4] [36]. Graphite and diamond, are two physically different substances but composed entirely of the same atom, carbon. Graphite and diamond are thus said to be allotropes of carbon. Allotropes occur when the atoms of a substance that has only one kind of atom arrange differently [4]. Carbon nanomaterials (CNMs) can be classified with respect to the number of dimensions, which are not confined to the nanoscale range ($<100 \text{ nm}$) [21]. Some allotropes of carbon can be classified yet still with respect to their shape, size, and the orientation of their carbon bonds [1]. More accurately, allotropes are classified on the basis of the hybridisation of their carbon atoms. Based on this classification scheme, each one of the three main carbon valence states is characterised by a unique and specific allotrope form. For instance, single bond sp^3 hybridisation as is observed in the bulk 3D structure of diamond, double bonds in sp^2 hybridisation of the 2D layers of graphene structure and the sp hybrid state of the linear chain 1D carbene structure. Buckyball fullerenes are considered quasi-zero-dimensional (0D) and nanotubes quasi-one-dimensional (1D) allotrope [15] [38]. Both buckyball fullerenes and carbon nanotubes manifest quasi sp^2 hybridisation [34]. Valence atoms of some carbon allotrope such as amorphous carbons, diamond like carbon and nanocrystalline diamond aren't always in the sp , sp^2 or sp^3 hybridization states. They maybe in the so-called mixed and intermediate states, sp^n where $1 < n < 3$ [39] [22].

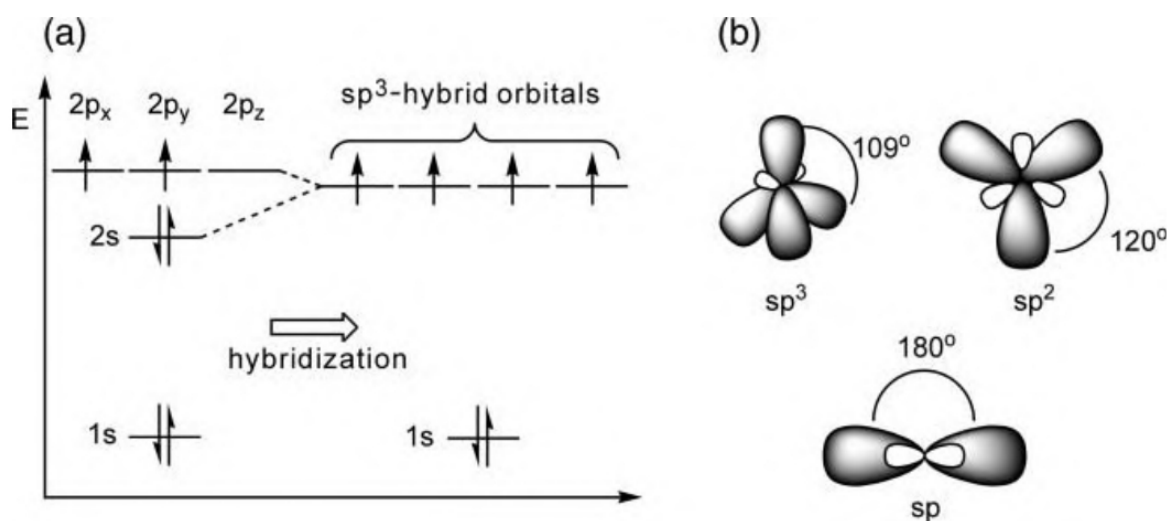


Figure 1.0.3. (a) Diagram of atomic orbitals and sp^3 hybridization, (b) hybrid orbitals of carbon [181].

The energy level distribution of the 2s and 2p electronic shells are responsible for the many structures carbon has to offer. The 4 valence electrons, with atomic configuration $2s^2 2p^2$, are able to transition energy states at minimal energy cost. These electrons can be involved in sp, sp^2 and sp^3 hybridisation due to carbon having energy bands that are so close in energy, consequently enabling carbon to occur in numerous allotropic forms [38] [39] [40].

Research and development in the field of carbon nanotechnology is actively investigating the synthesis and applicability of novel as well as known CNMs [41]. CNM surfaces, however, need functionalization before deployment for use in most technologies. Furthermore, CNTs can be modified by conjugation with organic or metallic nanoparticles [42]. Modification and functionalization is not only essential to remedy their insolubility and tendency to aggregate, but also to ultimately enhance their properties (e.g., mechanical, chemical, optical properties, electrical, physical etc) [3], [42]. The broad structural dimensionality and ease of functionalization enables the adaptation of these brilliant electromechanical properties possessed by CNTs at nanoscale, via composite materials, for use at microscopic scales [43]. Carbon based allotropes have

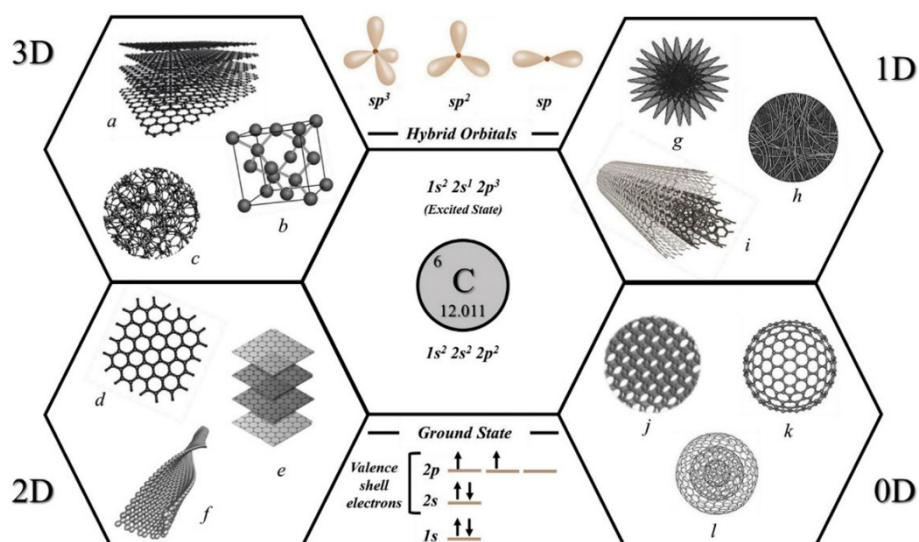


Figure 1.0.4. 0 to 3D carbon allotropes used in electrochemical (bio)sensors: (a) graphite, (b) diamond, (c) amorphous carbon, (d) graphene, (e) sandwich-like graphene, (f) nanoribbons, (g) nanohorns, (h) nanofibers, (i) nanotubes, (j) carbon nanodots, (k) fullerene and (l)nanooion. The electrons in the valence shell, excited state and possible hybrid orbitals found in carbon allotropes are shown at the center of the scheme [182]

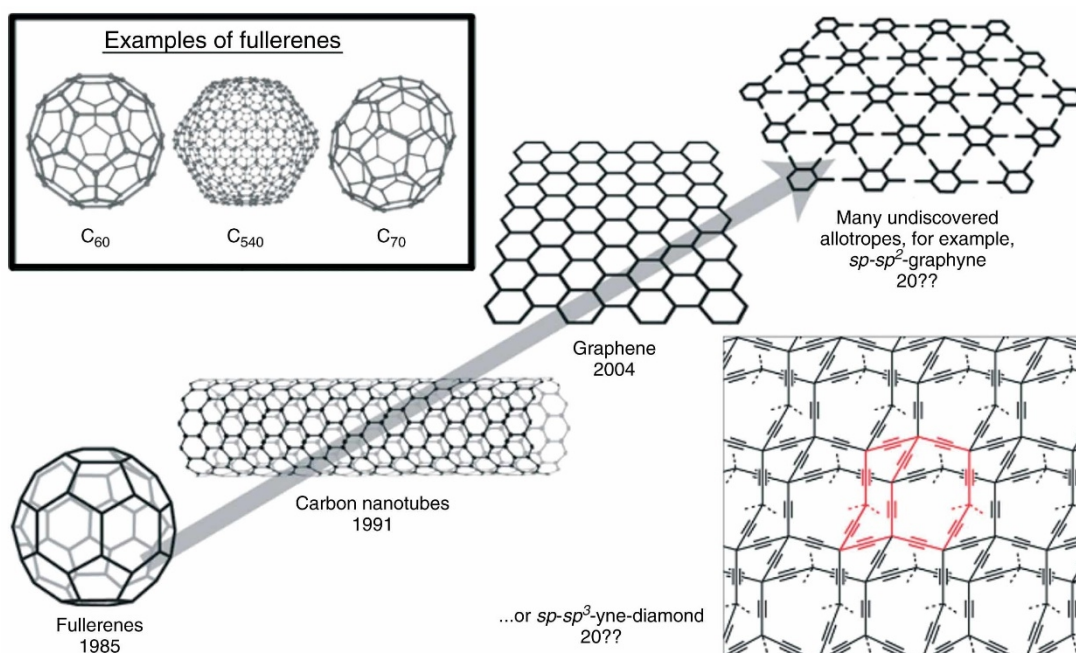


Figure 1.0.5. Timeline of some of the structures of nanostructured carbon allotropes [95].

reportedly been used in different sensing applications for targets such as temperature, pressure, biomolecules, environmental pollution to mention but a few [3], [9], [44], [45]. Physicochemical properties of an allotrope depend strongly on the allotropes' structure and size [18]. In this section, an overview of the properties of the 0D CNM C_{60} fullerene, 1 D carbon nanotubes (CNTs), and 2D graphene and its derivatives, is given. Their surface properties, rather than bulk properties, are as they play a significant role in sensor applications [40].

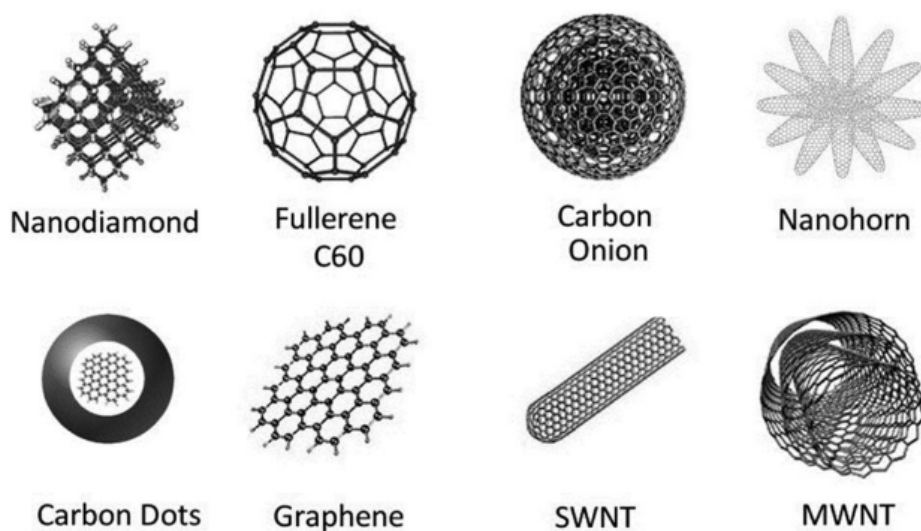


Figure 1.0.6. Members of the carbon nanomaterial family [21]

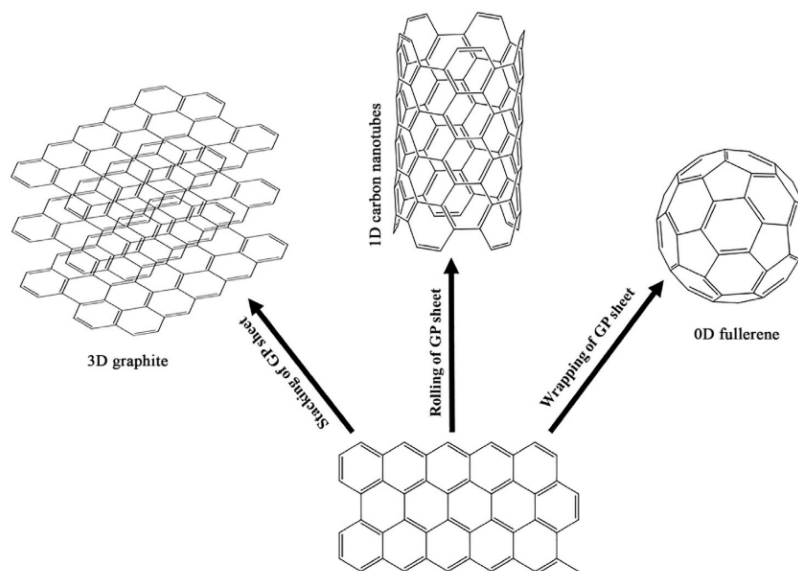


Figure 1.0.7. Stacking, rolling and wrapping of graphene sheets [138].

1.1. Fullerene based nanomaterial

Fullerenes are a family of carbon allotropes that generally exist in two distinct categories based on their shape, displaying distinct chemical-physical properties. Closed, ellipsoidal or hollow spherical shaped fullerenes are called buckyballs while the tubular fullerenes are called carbon nanotubes (CNTs) or buckytubes [1], [40], [46], [47]. Carbon nanofibers and carbon nanobuds are some of the other fullerenes synthesised for scientific research and use [2]. Fullerenes can be thought of as rolled up graphene sheets [18].

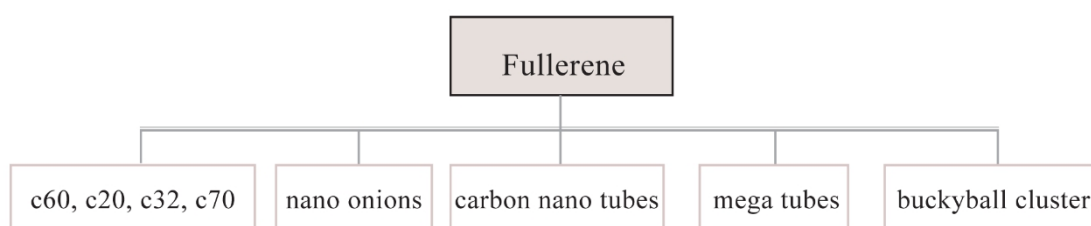
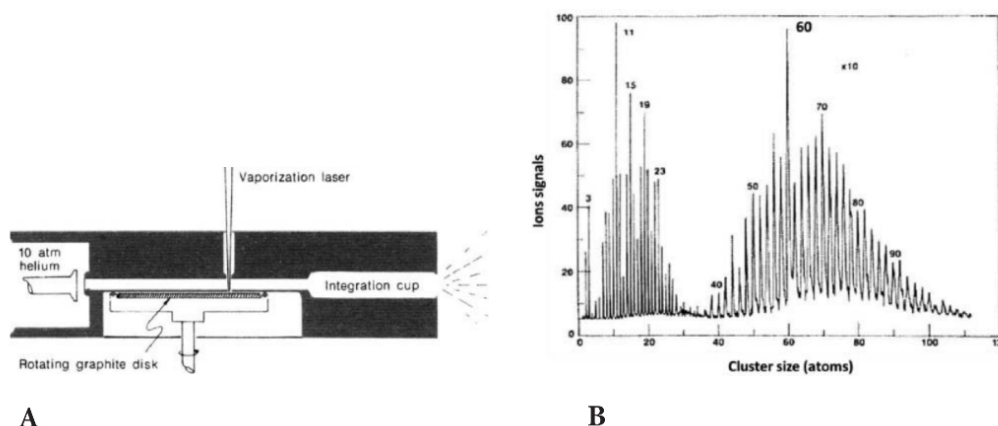


Figure 1.1.1. Some types of fullerenes [1].

The presence of the fullerene C_{60} had been predicted as far back as 1970 by Eiji Osawa [48] of Japan in his paper on superaromaticity. However, it wasn't until 1985 when during an experiment to simulate the conditions under which the formation of red stars occurs, that Kroto et al. [12] discovered fullerene C_{60} . The experiment involved vaporisation of the surface of a solid block of graphite by irradiation into a plasma of atoms and free ions. Upon cooling the plasma, mass spectrometry analysis of the resulting clusters showed a sharp spike commensurate with 60 atoms of carbon and in second place another spike consistent with 70 atoms of carbon [12], [49], [50]. The more stable molecule C_{60} was observed to assume the shape of a soccer ball whereas the C_{70} was more ellipsoidal as illustrated in figure 1.1.3. This discovery marked the start of intense research into CNMs [51] and was later awarded the 1996 Nobel Prize in Chemistry [52].



A **B**
 Figure 1.1.2. (a) Schematic representation of apparatus used to generate and analyse carbon-cluster and in the discovery of fullerenes. (b) Mass spectrum and the preponderance of C_{60} . [47]

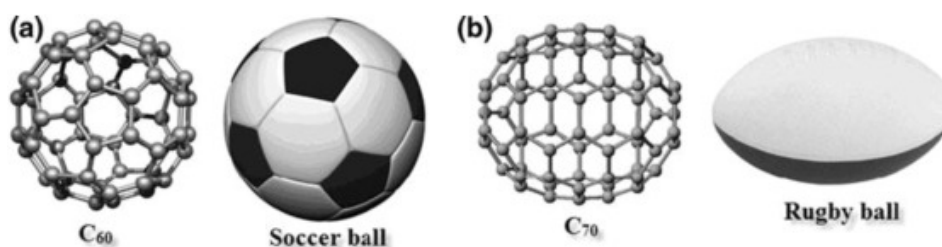


Figure 1.1.3. Structure of (a) C_{60} and its resemblance to a soccer ball, and (b) C_{70} and its resemblance to a rugby ball [23].

Kroto et al. [12] named the newly discovered molecule C_{60} , “buckminsterfullerene” in honour of the architect, Richard Buckminster Fuller, who had designed geodesic domes of similar structure. Despite being closed caged, all buckyball fullerenes are 5-fold symmetrical and have so far been shown to comprise an even count of carbon atoms, C_{2n} . C_{60} fullerene, for instance, exhibits spheroidal geodesic geometry with a diameter of 7.1 Å or approximately 0.7 nm. Buckyball fullerenes are thus generally taken to be 0D CNMs as all of their three spatial dimensions are below 100 nm. Buckyball fullerenes can be considered to be the smallest stable CNM structures and are right at the molecule-nanomaterial boundary [43]. These structures have been shown to be consistent with Euler's polyhedron formula [51] which states that, “exactly 12 pentagons, and a variable h , number of hexagons must be involved if a polyhedron is to build a closed structure from pentagons and hexagons” [49]. The number of hexagons required for a fullerene molecule

of n carbon atoms is, $h=(n-20)/2$ [53]. Of the buckyballs, C_{60} and C_{70} are the most common fullerenes with C_{60} being the smallest fullerene whose structure obeys the Isolated Pentagon Rule (IPR). IPR imposes the restriction that no two pentagons can be placed adjacent to one another. It is by Euler's polyhedron formula and IPR that it can be understood why C_{60} fullerene is observed to be the most stable buckyball fullerene and also why buckyball fullerenes with less than 60 carbon atoms are structurally very unstable, taking up asteroidal shapes whereas higher members are pentagonal in shape [51]. The smallest fullerene possible, yet highly unstable, is C_{20} [54].

C_{60} fullerene molecule is a truncated icosahedron (I_h), made up of 20 hexagon rings and 12 pentagon rings upon which the closed cage symmetric structure depends. C_{60} fullerene is the most symmetric molecule [55] with a 120 various symmetric operations [49], [50]. At every vertex of the fullerene C_{60} 's structure is a carbon atom containing 1 π bond and 2 σ bonds [56]. Being of icosahedral structure, the carbon atoms of C_{60} fullerene permit distortion of the molecular geometric structure towards tetrahedral geometry, i.e. pyramidalization [47]. Buckyball fullerene pyramidalization angle, $(\theta_{\sigma\pi} - 90)$, depends on the number of carbon atoms present in the fullerene and determines the fullerenes' geometrical structure. The angle between the σ and π orbitals in C_{60} fullerene is 101.6° giving a pyramidalization angle of 11.6° [18]. Addition or removal of hexagons contorts the symmetry of C_{60} fullerene effectively altering size and reducing structural stability [49].

In order to build the truncated icosahedral structure of C_{60} fullerene, each carbon atom is covalently bonded to 3 of its neighbouring carbon atoms by sharing 3 of its 4 outer electrons [47], [49]. C_{60} X-ray diffraction patterns reveals two types of bonds present in C_{60} fullerene. The first type, shorter of the two bonds and of length 1.39 \AA , is that between adjacent hexagons, denoted the C_6-C_6 bond. This bond type displays double bond characteristics although it's not purely a double bond. The second type of bond is found between adjacent pentagons and hexagons. It is 1.45 \AA and denoted as C_5-C_6 bond. It shows single carbon bond characteristics even they though strictly speaking it isn't. Owing to pyramidalization, the carbon atoms in C_{60} fullerene aren't purely sp^2 hybridised. Instead, a pseudo sp^3 component is also present. C_{60} and higher fullerene may be assumed to possess hybridization between sp^2 and sp^3 . To achieve the truncated icosahedral structure of C_{60} fullerene, connection angles in sp^2 hybridised carbon atoms are adjusted from 120° in sp^2 orbitals to 109° in sp^3 orbitals. More accurately the hybridization is understood to be

$sp^{2.3}$ [47], [57]. This hybridisation effectively reduces structural strain and enhances C_{60} fullerenes' stability. The delocalised π electrons play a role in structural stabilization by

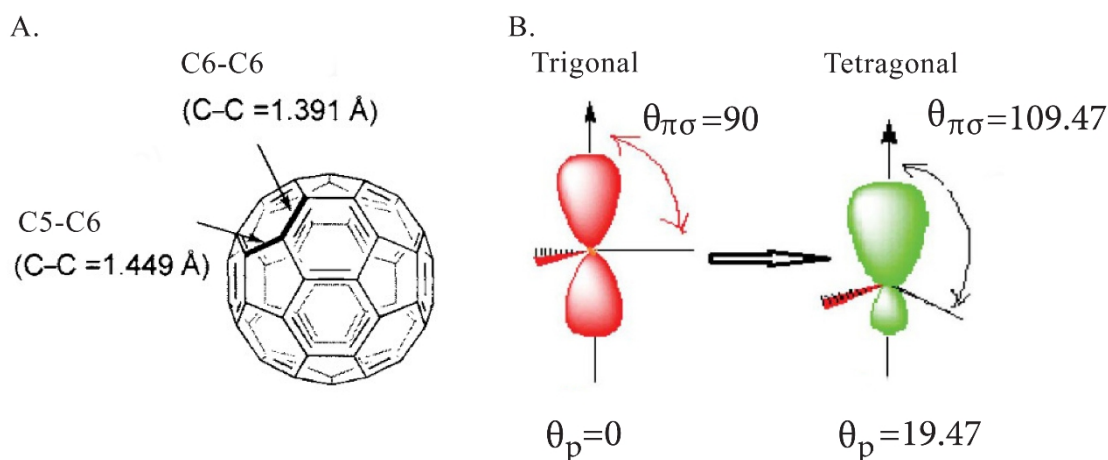


Figure 1.1.4. (a) The two bond types in C_{60} [78].

(b) pyramidalization in C_{60} [47].

resonance [43], [47], [49], [50], [56].

Properties enhancement and turnability of buckyball fullerenes is mainly done through chemical functionalization mostly by the introduction of functional groups or other carbon nanomaterials, ions etc, to the buckyball cage. Chemical functionalization has the effect of synergistically improving the overall properties of functionalised fullerene while still maintaining the individual properties of the constituent properties [58]. Catalytic activity, magnetic, thermal, mechanical and intense light absorption are some of the properties that have been shown to improve via chemical functionalization [51], [58].

Fullerene crystals, fullerites, are a 0D crystalline form of carbon with Face Centred Cubic structure (FCC). The buckyball fullerenes are present at each vertex and face of the crystal [51]. Masuhara et al. [59] showed how to experimentally produce crystals of the same shape and size using a reprecipitation method. By the use of nanoarchitectonics, Cheng-Tien et al. [60] reported the assembly of 1D nanowhiskers, 2D fullerene nanosheets and 3D fullerene cubes from 0D fullerene crystals as building blocks. Face selective chemical etching of 0D fullerene crystals was performed to achieve these materials. The chemically etched nanomaterials showed outstanding dispersibility and vapor sensing properties in addition to providing a cheaper and scalable alternative to costly techniques used in the manufacture of microstructures [60]. The above two examples show the

versatility in the wide spectra of uses for which fullerenes can be adopted for use through surface manipulation as well as functionalization.

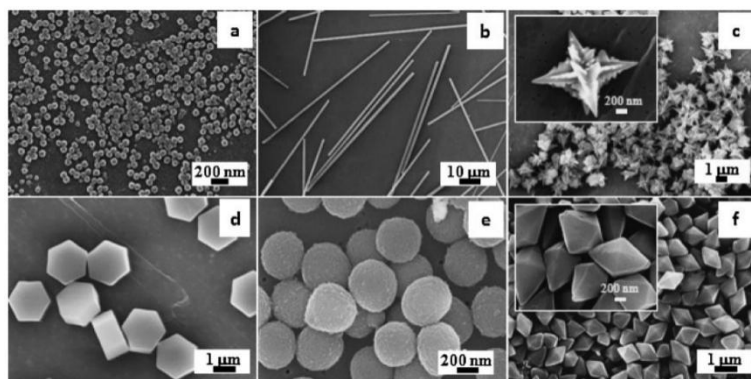


Figure 1.1.5. Masuhara et al.'s fullerene fine crystals of uniform and controlled size [59]

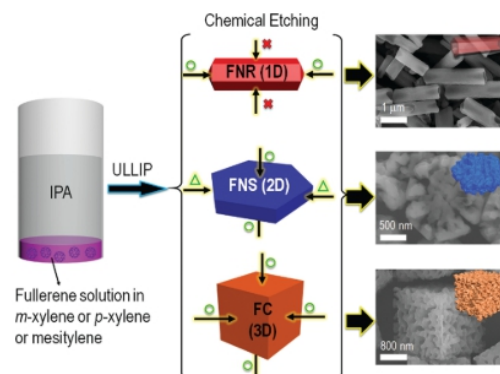


Figure 1.1.6. Schematic representation of the synthesis process of 1D, 2D, and 3D fullerene nanostructures and their face-selective etching with ethylene diamine [60]

Natural occurrences of fullerene have been reported in several scientific papers [61]–[64]. Geological sources were identified as far back as 1992 when Buseck et al. identified fullerene (C_{60} and C_{70}) in Precambrian rock from Russia [65]. Meteoritic as well as geological sources have been the main sources of natural occurring fullerenes, although at really low concentrations. Localised energetic events such as lightning, soot from wildfires and impacts of extra-terrestrial bodies are thought to be the responsible for these occurrences [66]. Buseck offers a comprehensive review on natural occurrence of fullerenes [66].

Before fullerenes could be widely studied, fullerene production technologies of sufficient yield had to be sought. Kroto et al.'s [12] initial laser ablation (figure 1.1.2) of graphite experiment produced an insufficient yield to attract meaningful research as fullerenes could only be detected through mass spectroscopy analysis [67]. It wasn't until 5 years later, in 1990, that Huffman and Krätschmer [68] produced sufficient macroscopic quantities of fullerene, that the era of scientific fullerene exploration launched [67]. The "Krätschmer–Huffman method" is essentially synthesis of fullerene by electric arc heating of graphite. It involves the vaporisation of graphite electrodes by means of resistive heating in inert (helium) environment. An electric arc is generated between the electrodes

producing a soot. Benzene solvent was used to extract the fullerene contained in the resultant soot. Mass spectral analysis revealed the presence of C₆₀ and C₇₀ in the final yield in proportions of 10:1, respectively [67]. In the same year, 1990, Smalley and co-workers reported the design of another fullerene production mechanism they called “C₆₀ generator” [69]. They synthesised fullerene by resistive arc heating of graphite by generating an electric arc between graphite electrodes completely enclosed in a reaction chamber in an inert environment. Organic solvents were used to extract fullerenes from the soot produced in the C₆₀ generator [67]. One of the modern methods of fullerene production is the synthesis by laser irradiation of polycyclic hydrocarbons (PAHs). PAHs have shown to be better at the synthesis of new fullerene homologues as compared to graphite vaporisation methods. Through the use of flash vacuum pyrolysis, PAHs of a desired carbon structure can be “rolled up” by laser irradiation [70]. Other production methods include sputtering, electron beam evaporation, soot combustion of hydrocarbons and electron beam ablation [71]–[74]. Arc plasma or radio-frequency-plasma methods are usually the most used commercial methods [1]. Sorting and purification methods such as column chromatography, selective chemistry and high performance chromatography are some of the procedures after fullerene production to isolate monodisperse fullerenes [22]. The demand for low-cost, high-quality fullerene production of sufficient yield is a challenge synthetic production methods seek to accomplish [53]. Readers are referred to Alonso et al.’s [53] detailed review on the synthesis of fullerenes. The relatively high-cost and low yield of available commercial production methods of buckyball fullerene is a major practical hinderance [75].

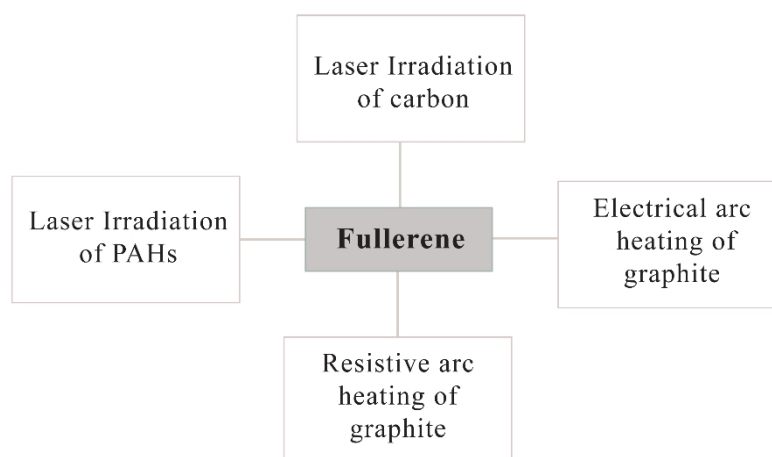


Figure 1.1.7 Main synthetic routes for fullerene production [70].

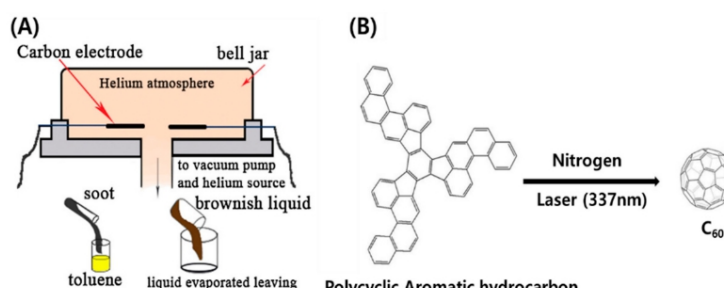


Figure 1.1.8. schematic representation of two fullerene synthesis routes (a) Huffman–Krättschmer method based on evaporation of graphite. (b) laser irradiation of PAHs.

Many fullerene- C_{60} 's unique chemical and physical properties are heavily influenced by its 3D topology and electronic structure [76], [77]. Fullerene structures that obey IPR manifest more sp^3 bonding characteristics like high angle strain and more reactive carbon sites as opposed to the poorly stable fullerenes violating IPR [70]. The curved surface of fullerene is responsible for the pyramidalized carbon atoms. The unique chemical properties, such as the effects of orbital rehybridization of fullerene, are owed to the pyramidalization of the fullerene molecule. Orbital rehybridization, from sp^2 to $sp^{2.3}$, forces the p-lobes to spread more on the exterior more than they do on the interior, effectively promoting overall electronegative behaviour. Low lying pi orbitals with pronounced s orbital character also contribute to electronegative behaviour. Its high affinity for nucleophiles is partly due to the fact that 72 electrons are required to form a closed configuration but yet only 60 pi electrons are present [47]. Orbital rehybridization in fullerene C_{60} (2.7 eV), for instance, lowers the “lowest-unoccupied molecular orbital” (LUMO) energy level. Fullerene C_{60} also displays fivefold “highest-occupied molecular orbital” (HOMO) and triply degenerate LUMO level able to gain six electrons reversibly and bring about stable multi-anions [78], [79]. Fullerene electron transfer and charge shift is accelerated as a direct result of the spherical fullerene framework. However, charge recombination is slowed down [80]. The spherical shape and electron deficiency facilitates exhaustive reaction with free radicals [43].

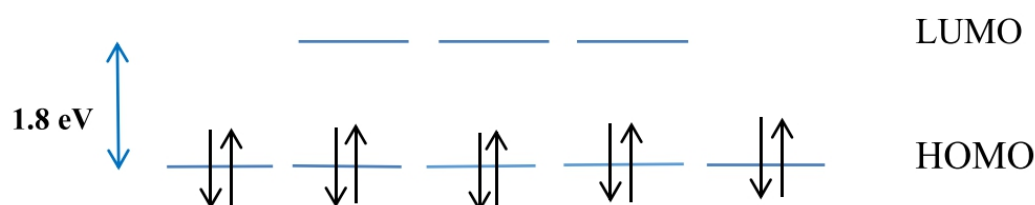


Figure 1.1.9. HOMO and LUMO gap in fullerene- C_{60} [183]

Physically, fullerene-C₆₀ shows elasticity when compressed up to 75% its size. Mathematical models indicate that it has a bulk modulus of 668 GPa making it harder than diamond whose bulk modulus is 160 GPa [77], [81]. Generally fullerenes can withstand pressure of up to 3000 atmospheres [77]. Fullerene is the only soluble allotrope of carbon under ambient conditions and thus can be used to prepare carbon films in solution. However, elemental fullerene is hydrophobic and is insoluble in many solvents, such as polar solvents. It is soluble in non-polar solvents such as carbon disulphide, o-dichlorobenzene, toluene and xylene. Solutions of fullerene C₆₀ are deep-purple/violet whereas those of C₇₀ are brick red in colour [49], [70], [82]. Fullerene size and morphology are responsible for its unique optical properties such as the large indices of refraction, broad absorption of light in the UV-VIS region [43], [76]. When exposed to light fullerene-C₆₀ produces singlet oxygen [82], a trait not least suitable *in vivo* biosensing application. fullerene-C₆₀ also polymerise when exposed to ultra-violet light [83].

Fullerenes in pure form are not very useful because of their tendency to form aggregates, their poor solubility in most organic solvents and their hydrophobic nature. Fullerene-C₆₀, for instance, contains 30 equivalent electrochemical bonds. The carbons at these junctions can participate in addition and redox reactions. These reactions make it possible to functionalise fullerene to possess the desired properties making fullerene versatile for more applicable use. Fullerene functionalization can be done covalently or non-covalently. Through functionalization, fullerene can be made lipophilic, water soluble, prepare it to as polymer dopant etc [76], [82], [84]. For instance, addition of amine groups to fullerene C₆₀ makes it hydrophilic [76].

1.2. Carbon nanotubes

Carbon nanotubes (CNTs) are a 1D allotrope of carbon. They are one atom thick rolled-up graphene sheets, of cylindrical tubular shape [1], [85]. CNTs are often capped with buckyball fullerene hemispheres at both ends during their formation [51]. They exist either as multiple-walled CNTs (MWCNTs) or single-walled CNTs (SWCNTs), both of which were discovered by Iijima et al. in 1991 [13] and 1993 [86], respectively [87]. Iijima first discovered MWCNTs as a by-product during the synthesis of fullerene, by the arc discharge method [88]. SWCNTs are a single rolled-up layer of graphene sheet and MWCNTs consist of more than two concentric rolled-up layers. Two concentric rolled-up layers are known as double-walled CNTs (DWCNTs) [89]. The diameter range of CNTs varies from about 0.4 nm to about 70 nm and can have variable lengths in the order of micros [47], [90].

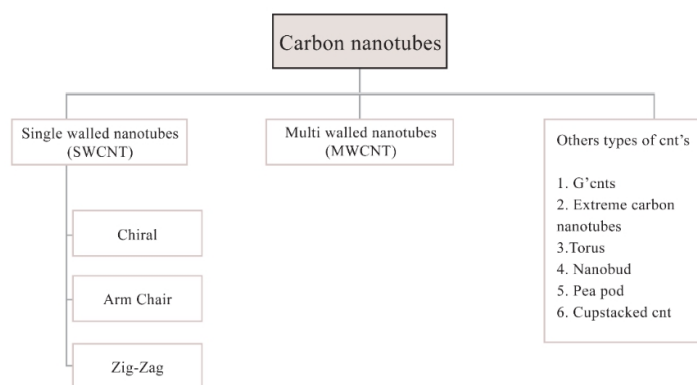


Figure 1.2.1. Types of CNTs [1].

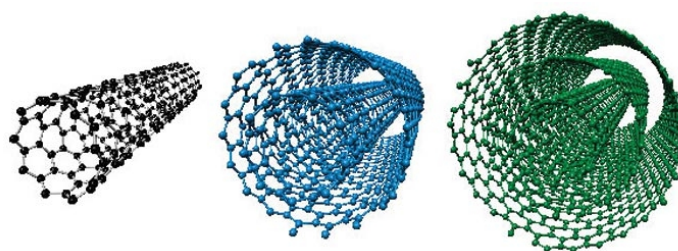


Figure 1.2.2. SWCNT, DWCNT and MWCNT [184].

Although different types of CNTs are entirely made up of sp^2 hybridised carbon atoms, each atom sharing three electrons to establish trigonally coordinated σ bonds with three adjacent carbon atoms with strong covalent bonds between the atoms, they exhibit varying

physical and chemical properties depending on their structure [75], [90]. The delocalisation of π bonds throughout the CNT structure is responsible for the optical and electrical properties inherent. These strong bonds, however, limit chemical reactivity of pristine CNTs [88].

In comparison to other fibrous materials, CNTs have extremely high tensile strength and elastic modulus values owing to the sp^2 type of orbital hybridisation [91]. They are considered the second hardest material after graphene, capable of withstanding pressure of up to 24 GPa. Their brilliant electrical and thermal properties have found important applicability in superconductivity [47]. The highest length-to-diameter ratio, 132 000 000:1 [1], construction of any material has been achieved with CNTs. Owing to their smaller diameter, SWCNTs have a much higher length-to-diameter ratio than MWCNTs [75]. Mechanically, CNTs rank among the strongest fibres thanks to the sp^2 bonds that are present between their carbon atoms. This high length-to-diameter ratio makes CNTs one of the most anisotropic nanomaterials ever produced [1], [87]. Important unique characterises of CNTs as compiled by Tiwari et al. [47] are shown in table 1.1.1.

CNTs do not disperse in organic or inorganic solvents due to their surface properties. Although both ends of CNTs contain moieties, which are hydrophilic, the wall that makes up the larger portion of the CNTs surface is hydrophobic because the strong van der Waals interactions solidly hold the CNT wall together. Electronically, the properties of CNTs depend heavily on physical structure, chirality, length and diameter [87]. Structural chirality influences the CNT conductivity while CNT morphology is determined by the chosen preparation methods [92]. The ability of graphene to absorb light of all wavelength together with its outstanding electron transfer properties makes CNTs attractive materials for further scientific investigation and application to sensor [21].

More generally, CNTs are an advantageous material for use in sensor technologies because of small size, presenting a large surface area, quick response, and high sensitivity at ambient temperature. Brilliant electron transfer characterises render CNTs as brilliant candidates for electrode use in electrochemical sensors [93]. CNTs possess qualities that make them favourable for *in vitro* and *in vivo* use as biosensors, e.g., size, tunability and the ease with which they can be functionalised to avoid toxicity [94], [95].

1.2.1. SWCNTs

Table 1.2.1.1 Some remarkable mechanical, physical and electronic properties [75].

| | |
|-------------------------|---|
| Specific surface area | 200-900m ² J ⁻¹ |
| Specific gravity | 0.8-2g-1cm-2 |
| Electrical conductivity | 2 x 10 ⁻² -0.25Scm ⁻¹ |
| Thermal conductivity | 6600Wm ⁻¹ K ⁻¹ |
| Elastic Modulus | >1TPA |
| Tensile strenght | >100GPa |

SWCNTs are rolled up single graphene sheets that have a typical diameters of between 1 to 3 nm, and are about 10 μm in length [75]. Structurally, all the carbon atoms on the cylinder surface are placed in equivalent positions in hexagonal rings. Buckyball fullerene hemispheres which may be present, during formation, on both ends of the SWCNT contain pentagonal rings favouring chemical reactivity [92]. SWCNT atoms in the hexagonal rings are not planar due to the presence of sp³ hybridisation component. This has the overall effect of making the surface SWCNTs more reactive than planar graphene sheet [92].

To form a SWCNTs, a graphene sheet can be rolled in a number of different ways with respect to lengths along graphene crystal lattice unit vectors (in the honey comb structure) as shown in figure 1.6 [75]. Therefore, the structure of any type of SWCNT can be described in terms of chirality (hexagon orientation with respect to the tube axis [75]) with the aid of the chiral vector index, (n, m), where n and m are integers. Chirality is determined by the rolling angle or rather orientation of carbon atoms around the circumference [88]. Chirality, c_h , not only indicates the angle between the hexagons and the CNT axis [43] but also the alignment of the π-orbitals. Figure 1.2.1.1 illustrates chirality. To roll-up a sheet of graphene along a vector $c_h = na_1 + ma_2$, the first and the last carbon atom on c_h must be overlaid [90]. The electrical properties are a function of the CNTs chirality depending on the value of the chiral vector index (n, m). Chiral vector

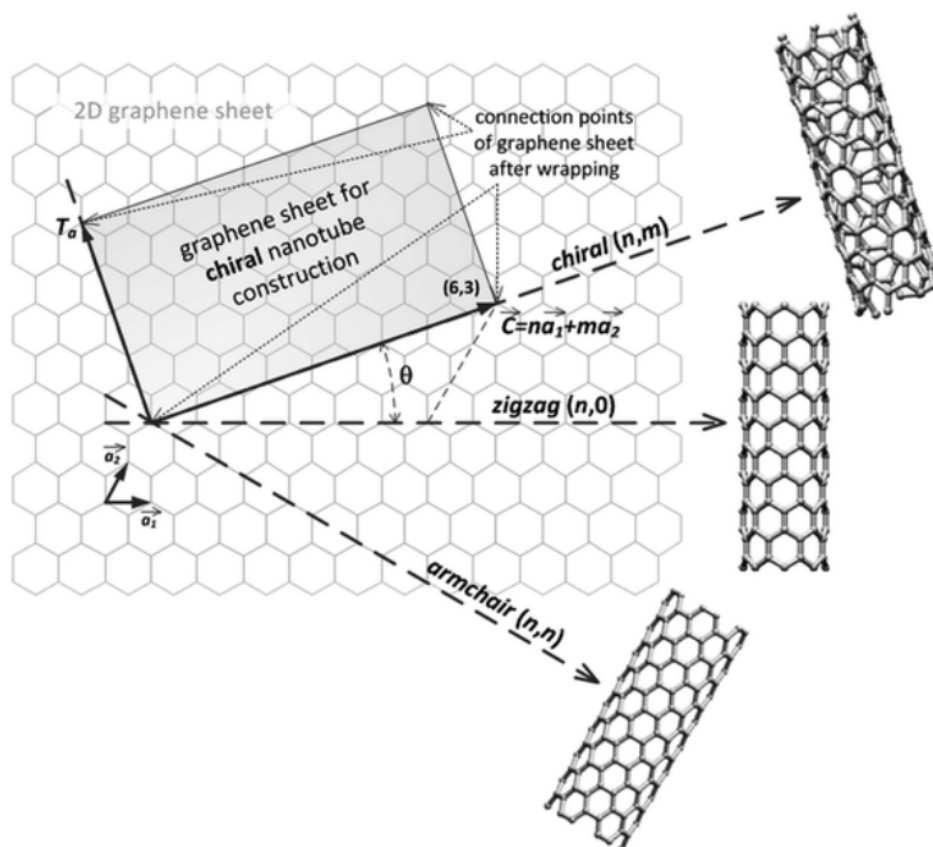


Figure 1.2.1.1. Derivation of a CNTs from a single graphene sheet. The chiral vector dictates structure of SWCNT. [174].

indexes (n, n) and $(n, 0)$ result in arm-chair and zigzag configurations, respectively. Any other configuration is considered helical also known as chiral [92]. Figure 1.2.1.1 shows these configurations. Chirality can be rolled up in different ways to make the CNTs either semiconducting or conducting. A SWCNT, (n, m) , is considered metallic if $m=n$ or $(n-m)$ is a multiple of 3; otherwise, the CNT is a semiconductor. Arm-chair SWCNTs even display higher values of electrical conductivity than that of copper [75]. Electrical conductivity is also a function of SWCNT's diameter and helicity [93]. The emission wavelengths of CNTs vary based on the diameter and chirality. SWCNT diameters may vary from nanometers to micrometers [95].

The distinctive resonance enhanced Raman spectrum exhibited by SWCNT is very stable thanks to the sp^2 carbon lattice. SWCNTs have shown great potential as implantable sensors in single molecule detection due to their intrinsic near Near-Infrared Radiation (NIR) (900–1600 nm) fluorescence, the sensitivity of their band-gap structure to local dielectric environment and their unique quenching properties [95].

DWCNTs exhibit properties roughly equivalent to those of SWCNTs. The main difference is DWCNTs manifest superior chemical resistance in comparison, making them more advantageous [1].

1.2.2. MWCNTs

MWCNTs are intrinsically more complex than SWCNTs. They may house from two to unlimited number of graphene sheets [92]. They have typical diameters of between 5 to 25 nm, and variable lengths from nm to 10 μm [75], [92]. MWCNTs can exist in two geometric configurations. The first is, more than one SWCNT is arranged coaxially such that the diameter of the innermost SWCNT is the smallest and that of the outermost SWCNT has the greatest diameter. This configuration has no upper limit on the number of concentric layer possible [92]. The second possibility is the rolling up of graphene sheet on itself like a paper roll. The inter-tubular separation in MWCNTs is similar to that of the inter-plane separation of graphite (0.34-0.35nm), and is due to van der Waals forces [1], [95].

The carbon layers that make up MWCNTs have inconsistent chirality and thus don't display electric properties as extraordinary as SWCNT. However, MWCNT show extraordinary mechanical properties far superior to those of SWCNTs as reported by Hyung et al. [96], rendering them more useful in strain sensor technology [88], [97]. Thermally, the properties of MWCNTs have been observed to be extremely similar to that of graphene, but quite different to those of SWCNTs [85]. Even though MWCNT do not have qualities as varied and high as SWCNTs, they are easier to process owing to their larger size. MWCNTs contain range from 20 to 40nm and have lengths in the range of 1 to 50 [92].

Apart from the commonly studied SWCNT and MWCNT, other CNTs of varied shapes such as ropes, stripes, springs, bamboo structures, hollow-tube, herringbone etc have been reported [51].

1.2.3. CNT synthesis methods

The chosen methods of CNT synthesis and the subsequent processing techniques determine morphology and properties of the output CNTs. It is to this cause that ever improving methods of CNT production are constantly being sought to improve yield selectivity and purification methods in order to effectively lower the cost of bulk production and processing. This is important for greater control over the quality and properties (structural and electronic) of the CNT final yield [98]. The main hurdle to date with production method available is their lack of total control over structure, diameter and chirality of their CNT yields [99]. Present day synthesis methods produce statistical distributions of chirality [100]. An et al. [99] gives a comprehensive review of the methods and technologies aiming to gain more control of yield parameters.

The three most common bulk production methods of CNTs are arc discharge, laser ablation, and chemical vapour deposition [42].

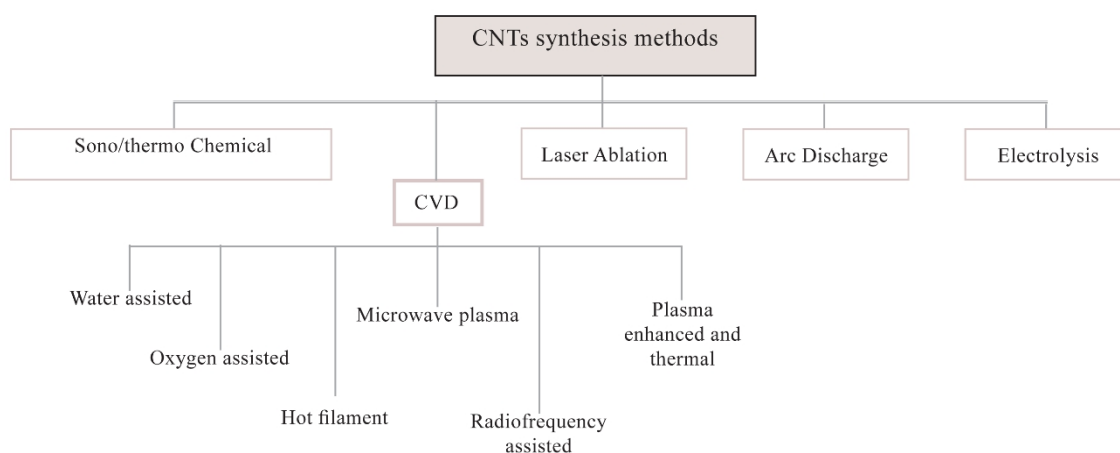


Figure 1.2.3. Different methods for CNTs synthesis.[47]

1.2.3.1. Carbon Arc Discharge

First reported by Iijima in 1991 when he unintentionally produced MWCNT during the synthesis of fullerene [13], [98], [101]. Carbon arc discharge is the simplest and most popular method of CNT production. It was Ebbesen and Ajayan [102] who first demonstrated the gram level production of MWCNTs by the carbon arc discharge method

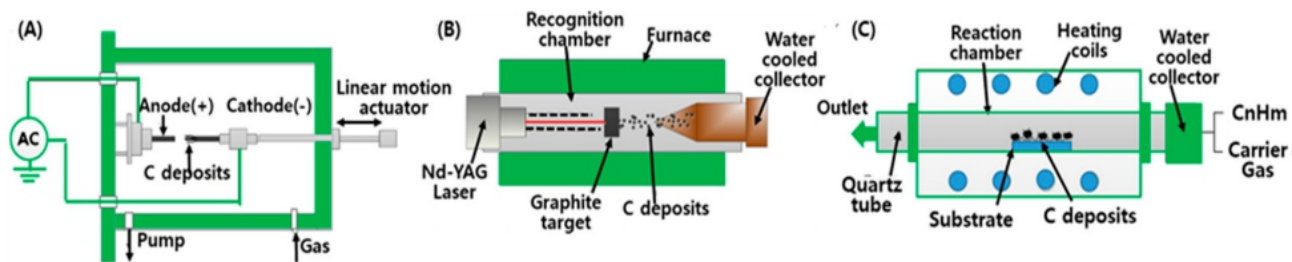


Figure 1.2.3.1. Schematic representation main CNT synthesis methods: (a) arc discharge, (b) laser ablation, and (c) chemical vapor deposition [42].

in 1992. A year later Bethune and co-workers [103] practically succeeded at CNT production in useful quantities.

Carbon arc discharge method involves the growth of CNTs on graphite electrodes by vaporisation of the graphite using direct current (D.C). The synthesis occurs in a vacuum chamber filled with an inert gas such as helium or argon at low pressure (50 - 700 mbar) [47]. An inert environment speeds up reaction (carbon deposition [100]) because of its high ionisation potential [88]. Upon stabilization of chamber pressure, a D.C potential difference is set up between the electrodes. The anode is slowly moved towards the cathode to strike the electric arc [100]. When the graphite anode and cathode are about less than a millimetre apart, a 100 A current flows through the electrodes conveying a large amount of heat through the discharge, creating a plasma arc [56], [104]. The temperature generated in the plasma exceeds 3000 K and vaporises the carbon atoms on the anode, depositing them on the cathode. As the anode depletes, during the course of the production, its position relative to the cathode should be adjusted so as to maintain optimal inter electrode separation for plasma arc uniformity. Once the required length of synthesised CNTs is collected, at the cathode, the D.C power supply source is disconnected and the electrodes are water cooled [85], [104].

Both SWCNTs and MWCNTs of high quality can be synthesised via carbon arc discharge. Diameters of MWCNTs produced by this method vary from 10 to 200 nm while those of SWCNTs vary from 0.7 to nm. CNT length is dependent on time of synthesis [75]. MWCNTs are produced without the aid of a catalyst whereas SWCNTs are produced with the aid of a metal catalysts on the cathode or electrode. Yield quality of the SWCNTs is greatly affected by parameters such as metal concentration at the electrodes, inert gas pressure etc [101], [104].

The major drawbacks of arc discharge method of CNT production are the labour-intensive recovery and purification required to isolate pure CNTs from the residue by products such as amorphous carbons and non-tubular fullerenes. These processes in part compromise the structural integrity of the produced CNTs [104]. Furthermore, the evaporation of carbon at very high temperature tends to promote the formation of bundled CNTs of limited use [75]. This method requires large amounts of graphite and also consumes a lot of energy [56].

Ishigami et al. [105] reported a modified version of the carbon arc discharge set up, replacing the vacuum chamber and inert gas with a liquid medium so as to find better ways of CNT collection and processing.

1.2.3.2. Laser Ablation

Smalley and co-workers [106] first outlined the use of laser ablation for CNT production in 1995. They reported the production of SWCNTs of diameters between 5 and 20 nm as was observed by X-ray diffraction and transmission electron microscopy analysis.

The laser ablation method setup is very similar to that of the carbon arc discharge except that laser ablation uses a laser beam to evaporate a graphite pellet target containing cobalt or nickel catalyst. The vaporisation is conducted in an inert (He or Ar) gas environment where a pulsed or continuous laser beam is aimed at the target in a furnace at over 1000 °C and 67 kPa. The cloud of carbon and catalyst metal vapour produced is accumulated on a water-cooled copper collector in another section of the reactor. The catalyst in, vapour form, prevent the closing of the CNTs in formation as it condenses slowly. Production ceases when the chamber is cooled or the catalyst structures become too large [47], [88], [100], [104]. The by products are amorphous carbons, fullerenes and carbon polyhedrons with enclosed metal particles [100].

The SWCNT yield produced by this method show a high degree of structural perfection [107]. The typical SWCNT yield is roughly 70% [108]. Increasing laser force has been observed to increase yield diameter of the SWCNT product [56]. Other factors like wavelength and power of the laser, chemical constituents of target material, chamber

pressure, distance between laser source and target material, fluid dynamics near the carbon target etc, have been observed to affect the amount and quality of the SWCNTs produced [104].

Good quality CNTs with yields of up to 70% can be obtained via laser ablation [88]. However, researchers are constantly seeking ways to improve the classic version of this setup to so as to improve upon the pitfalls and thus increase production efficiency. One example is given in ref [109].

Regardless of the advantages of carbon arc discharge and laser ablation, these procedures require vast amounts of graphene and energy and are thus costly. In addition, the yield needs further refinement in order sort-out unwanted carbons and catalysts [85]. Laser ablation has not, so far, been reported to produce MWCNTs.

1.2.3.3. Chemical Vapour Deposition

To overcome the major pitfalls (high-cost, high energy consumption and yield purities) inherent in the classic carbon arc discharge and laser ablation methods, chemical vapour deposition (CVD) was developed rather modified to synthesis CNTs [88]. Scientific reports on the use of catalytic CVD go back as the 1880 when Sawyer and Man [110] used CVD to coat lamp filaments with carbon and metal to extend the life of lamps [111]. CVD was first used in the synthesis of CNTs by Yacaman [112] and co-workers in 1993.

CVD is basically the decomposition of volatile precursor over a catalyst in a chamber containing an inert gas [92], [104]. In the case of CNTs production, the volatile precursor is a hydrocarbon such as CO, acetylene, ethylene, methane etc. The production involves imparting the precursor hydrocarbon with thermal energy at temperatures between 550 and 750°C in order to decompose it into reactive radical species (carbons) over a heated wafer substrate coated with Ni, Co or Fe nanomaterial catalyst [100]. Upon hydrocarbon decomposition, the carbon is dissolves into the molten nano catalyst until a certain saturation point is reached. The catalyst serves as a nucleation site to initiate the growth of CNTs. At this point a semi fullerene cap forms before carbon atoms with honeycomb structure appear to begin CNT precipitation. The growth of the CNT continues as long as the reaction chamber is supplied precursor hydrocarbons. Further purification and filtration

is required to separate the CNTs from the catalysts and hydrocarbons [56], [75]. An exhaustive review of sorting and purification techniques is given in citation [98].

CVD's ability to control diameter-size for desired CNTs is made possible by adjusting the size of the metal catalyst nanoparticles, effectively altering CNT properties. Diameters of 0.5 - 5nm for SWCNTs and 8 – 10 nm for MWCNTs are possible [113]. Methane hydrocarbon is used in the synthesis of SWCNTs whereas acetylene or ethylene for MWCNTs [56]. Well separated large quantities of direction controlled CNTs can be produced by CVD [85], [98].

The nature of the chosen precursor hydrocarbon and chosen nanoparticle catalyst material are the main parameters that influence the production of CNTs by CVD [87]. Length of produced CNTs is dependent on time taken to grow them [62].

CVD is preferred to carbon arc discharge and laser ablation because growth-in-place synthesis of CNTs at lower temperatures and lower pressures is possible [47], [56]. Despite the high quality CNTs obtained by the use of the carbon arc discharge and laser ablation procedures, the necessity to evaporate carbon atoms at temperatures above 3000 °C is energy consuming and thus expensive. Worse still the clamping up of CNTs produced via carbon arc discharge or laser ablation limits their use [75].

Table 1.2.3. Synthesis methods summary [104].

| Method | Arc Discharge | Laser Ablation | CVD |
|----------------|--|--|---|
| Yield rate | >75% | >75% | >75% |
| SWCNT or MWCNT | Both | Both | Both |
| Advantages | Simple, inexpensive, high-quality nanotubes | Relatively high purity, room-temperature synthesis | Simple, low temperature, high purity, large-scale production, aligned growth possible |
| Disadvantages | High-temperature, purification required, tangled nanotubes | Method limited to the lab scale, crude product purification required | Production limited to MWCNTs, defects |

1.2.4. CNT functionalization

Despite CNTs having valence carbon electrons that are delocalised in the π bond all over their structure and thus displaying outstanding optical and electronic properties, they display poor chemical interaction with external the physical environment [88]. This poor interaction displayed by pristine CNTs is due firstly to the fact that pure CNTs have no functional groups attached to them and secondly, due to strong Van der Waals forces and $\pi - \pi$ interaction that exist among the CNTs [114]. Some of these pristine CNTs have been reported to have a Lennard-Jones bind potential of approximately 500 eV/ μm [115]. As a result, pristine CNTs are highly hydrophobic and tend to agglomeration or bundle up while dispersing in solvents or when merging with a polymer, in effect preventing interaction with other molecules [114]–[116]. Pristine CNTs are very toxic in nature and accumulate in living organisms [117]. In order to circumnavigate these problems, the surface of pristine CNTs is functionalised. Functionalization is the process that modifies the surface of CNTs in order to improve their solubility/isolation or dispersion in aqueous solution. Functionalization renders CNTs useful under the physiologically relevant conditions for adaptation to a specific application. It is achieved by adding functional groups to the CNT surface walls, tips or even defects [90], [115].

Covalent and non-covalent methods are the most commonly used functionalization methods for CNTs.

Covalent functionalization involves modification of the CNT sidewalls defect sites or at the caps. It deals with the formation of a chemical bond between the carbon skeleton of CNTs and a functional group [114]. This effectively disrupts the pure CNT properties like luminescence and Raman detection shift plots which are reportedly lessened [118], making covalently bonded CNTs less favourable for use in photothermal or imaging application [119]. The loss in qualities is caused by alterations in the conjugated π -grid of pristine CNTs. Despite these losses, functionalization such as oxidation by a strong acid presents new possibilities for further modification of the CNTs with amines, amino acids etc [114]. Oxidation has the effect of imparting physical strain upon the sp^2 hybridised carbon atoms due to tension in the curvature, converting the sp^2 hybridised carbon atoms to sp^3 making the CNT more susceptible to further reactions [114]. Functionalization with strong acids

also has the effect of reducing CNT length, opening the CNT ends and creation of carboxyl groups there [117].

Addition reactions with hydrophilic groups can be used to improve solubility and avoid some of the side effects of acid functionalization [117].

Covalent functionalization can also be used to improve dispersion of CNTs in aqueous solutions by covalently bonding them to surfactants, peptides and proteins on their surface [117].

Unlike covalent functionalization, non-covalent functionalization is non-invasive, in that it can be done without altering the sp^2 hybridised carbon network of the CNT wall [119]. From this it follows that non-covalently functionalised CNTs preserve their electronic structure, inevitably leaving the physical electronic and optical properties

unaltered [90], [92]. This surface functionalization procedure is based on adsorption and

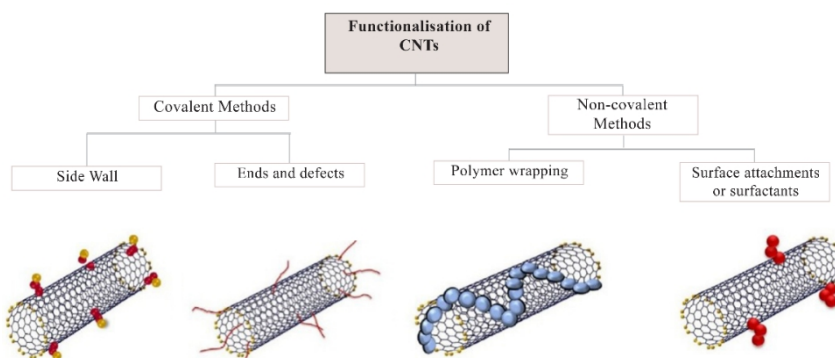


Figure 1.2.4.1 Functionalization methods of CNTs [185]

weak interaction forces such as π - π stacking, Van der Waals force, hydrophobic interaction, electrostatic, charge transfer or hydrogen bonds. It is therefore not surprising that the load that non-covalently functionalised CNTs can take on might be low. This functionalization happens by the adsorption of surfactant molecules on the outer walls of CNTs or the wrapping of polymer chains around the nanotubes [114], [119].

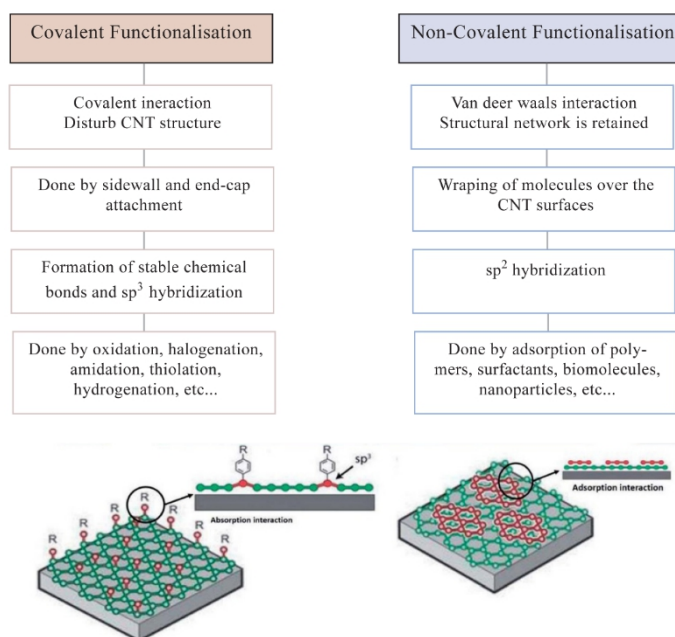


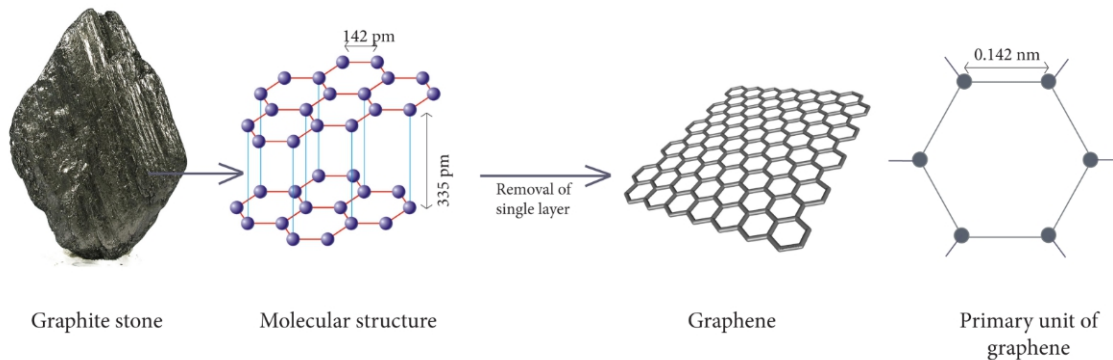
Figure 1.2.4.2 Covalent and non-covalent functionalization properties [154].

1.3. Graphene based nanomaterials

Graphene is a 2D, nanomaterial, allotrope of carbon. It presents as a hexagonal network (honeycomb crystal lattice) of monolayer sp^2 hybridised carbon atoms, with a distance of 0.142 nm between any two carbon atoms. These atoms are densely packed in a benzene ring formation [51], [87]. Simply put, graphene is a one-atom-thick graphite layer [120]. It is thus considered to be a building block of other graphitic carbon allotropes. It can transform into 3D graphite by stacking, into 2D CNTs by rolling and into 0D buckyball fullerene by wrapping [121]. Before Prof. Andre Geim and Prof. Konstantin Novoselov observed and characterised graphene in 2004 [122], its existence had been theoretical and its physical realisation deemed impossible owing to predicted thermodynamic instability [51]. The two researchers isolated graphene by means of micro mechanical peeling of graphite [123]. Geim and Novoselovs' ground-breaking discovery was awarded the 2010 Nobel Prize in Physics [124]. However, theoretical studies on graphene go back as far as 1947 when Canadian theoretical physicist P. R. Wallace wrote a paper [125] on the band theory of graphite. In his paper he calculated the band structure of graphene ('a monolayer of

graphite', as he termed it) as a basis for the understanding of bulk graphite [126]. It wasn't until 1986 that the chemist Hanns-Peter Boehm first coined the term graphene [126], [127]. For a complete review on the prehistory of graphene, reference is made to Geims' paper [126] on the matter.

Figure iv. Schematic representation graphite stone to the primary unit cell of graphene [47].



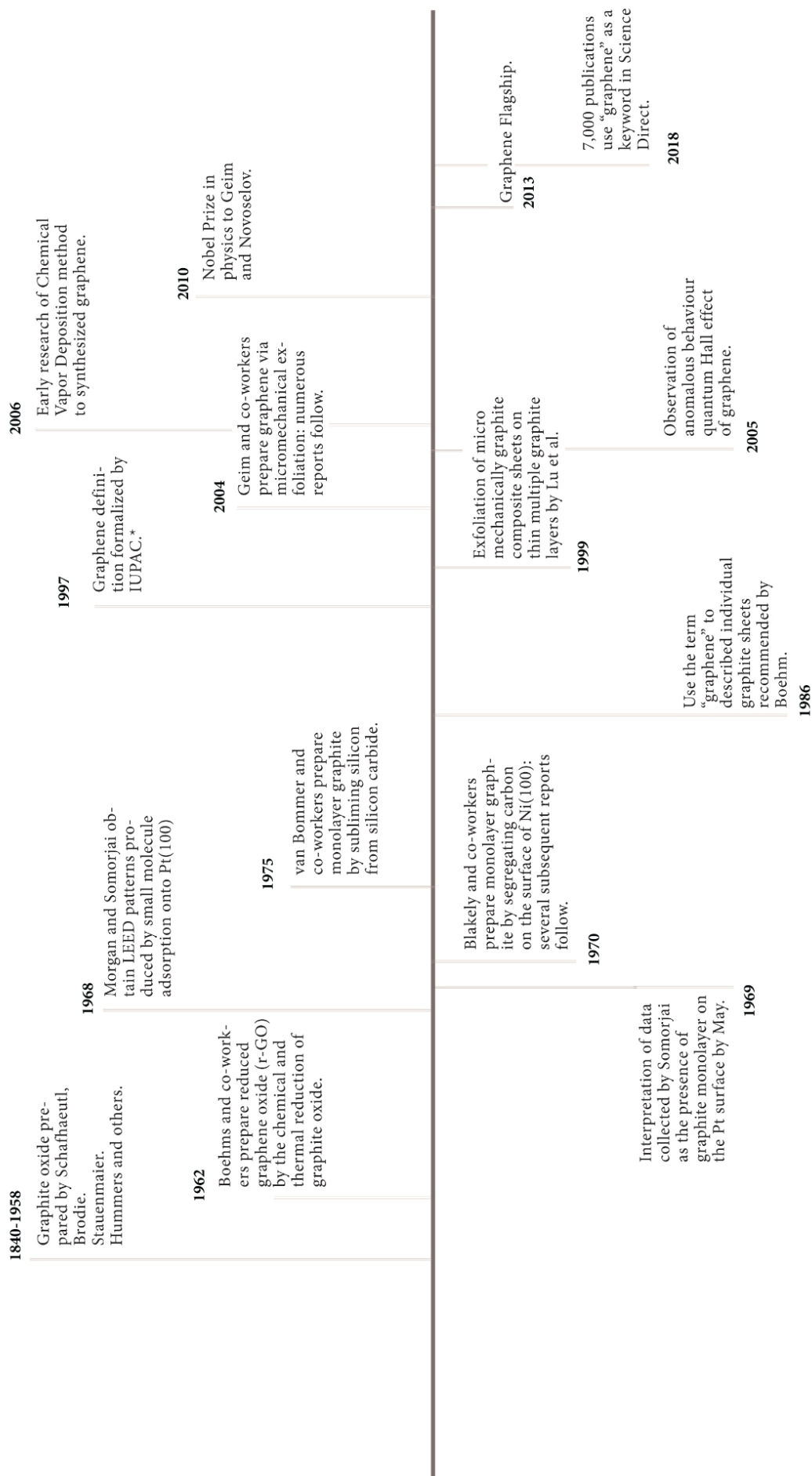


Figure v. Timeline in the development of graphene [17].

1.3.1. Properties

The physical and electrochemical properties of graphene favour its adaptation for use in sensor technology among many other uses. Being only atom-thick, graphene's unusual properties are proving to be a superior worthy replacement for already existing materials. Graphene is finding applicability in nanocomposite technologies, nanoelectronics, optoelectronics devices, solar cells, drug delivery technologies, sensors and many others [128]–[133].

A backbone of overlapping sp^2 hybridised carbon bonds holds the graphite single sheet in place. The special properties are mainly due to the 2p orbitals. These orbitals establish the π state bands that delocalise over the graphene structure. This is directly responsible for graphene's physical, thermal, high charge carrier mobility, impermeability to gasses and optical transparency qualities [134]. The low energy dynamics of graphene electrons manifest some interesting properties. The π and π^* bands meet at a single point at the Fermi energy, consequently leading to the extraordinary electron transport properties, and zero effective electron mass [133]. The touching of the valence and conduction bands make graphene a semimetal [51].

Single planar graphene boasts of a specific area of approximately $2630 \text{ m}^2 \text{ g}^{-1}$ making it suitable for use in gas sensing and biosensing applications because of high electrocatalytic behaviour. Its dimensionality, mechanical flexibility, high Young's modulus of approximately $E = 1.0 \pm 0.1 \text{ TP}$ at an estimated thickness of 0.335 nm [134] renders it a great agent for wearable as well as stretchable electronic sensors [135]. In addition, the planar architecture of graphene enables its processing into 1D fibres, 2D films and 3D structures that can be integrated into various kinds of sensors as per need. It is well expected that being a material one atom thick, graphene is one of the thinnest materials with an approximate thickness in the range 1 to 1.6 nm [133]. Furthermore, its single-atomic thick structure promotes outstanding absorption characteristics of gases and other analytes for sensing applications.

Graphene has distinctive optical properties, widely used in sensor technology owing to its high optical transparency displaying absorption of 2.3% of white [136]. Transmittance

of more than 95% have been reported for graphene at films of 2nm [133]. These high transmittance values are owed to the fine structure constant of graphene [47].

At ambient conditions, graphene's zero band gap structure is responsible for its extra-high electron mobility of $200,000 \text{ cm}^2 \text{ V}^{-1} \text{ s}^{-1}$ making it a superconductor [51], [133], [137]. Its room temperature electrical conductivity is reportedly 7200 S.m^{-1} , and thermal conductivity ranging between $(4.84 \pm 0.44) \times 10^3$ and $(5.30 \pm 0.48) \times 10^3 \text{ WmK}^{-1}$ for a single graphene sheet [133], higher than any of the other allotropes [47]. It also has a sheet resistance as low as $30 \Omega/\text{sq}$. [138]. Furthermore graphene's electronic structure allows for a tuneable band gap, highly sensitive to magnetic fields [123].

The ultra-low electronic noise exhibited by graphene makes it ideal for the sensitive detection of various analytes to a high degree of precision [137].

Table 1.3.1. Some physical, mechanical and electrical properties of Graphene [186].

| | |
|-----------------------------|--|
| Electron mobility | $>15,000 \text{ cm}^2 \text{ V}^{-1} \text{ s}^{-1}$ (at room temperature) |
| Carrier density | 10^{13} cm^{-2} |
| Thermal conductivity | $(4.84 \pm 0.44) \times 10^3$ to $(5.30 \pm 0.48) \times 10^3 \text{ W m}^{-1} \text{ K}^{-1}$ |
| 2D elastic stiffness | 340 N m^{-1} |
| 2D density | $7.4 \times 10^{-19} \text{ kg } \mu\text{m}^{-2}$ |
| Area per unit mass | $2600 \text{ m}^2 \text{ g}^{-1}$ |
| Young's Modulus | 1 TPa |
| Breaking strenght | 42 N m^{-1} |
| Breaking strain | 25 per cent |
| Optical absorption spectrum | Almost flat from 300 to 2500 nm with a peak at approximately 270 nm |

1.3.2. Other graphene forms

1.3.2.1. Graphene oxide and reduced graphene oxide

GO is by far the most used substance for the large-scale production of graphene-like materials [4]. It is also a 2D allotrope of carbon. The structure of GO is similar to that of graphene, mostly made up of an aromatic sp^2 backbone. GO has oxygen containing functional groups such as hydroxyl, carbonyl and carboxyl groups. However, electronic and material properties of graphene and GO differ considerably as a result of these slight differences (presence of functional groups and defects in sp^2 structure [14]) [134]. In comparison to graphene, GO shows lower material and electronic properties because the tertiary alcohols in GO break up the sp^2 hybridisation. This results in a reduction in the number of π -bonds and consequently number of delocalised electrons. It is also thanks to the functional groups that GO has brilliant dispersion in water and most solvents enabling the preparation of nanocomposites [134]. Thermal or chemical reduction is used to partially restore the disrupted π -network. This process yields reduced graphene oxide (rGO). The electronic and material properties of rGO are closer in relation to graphene that are those of GO. GO and rGO are suitable for use in sensor technology because the presence of functional groups increases the affinity of graphene oxide-based materials to analyte substances. Furthermore, functionalization of graphene oxide-based enables precise tuning of properties on demand [14], [95].

1.3.2.2 Graphene Foam

Graphene foam is a 3D structure based on graphene. It was synthesised to exploit the enhanced thermal and electrical properties of graphene-like properties in 3D for various uses. Graphene foam shows changes in resistance upon local perturbation. This quality is used in temperature as well as electromagnetism sensor technology applications. Graphene foam is also a superhydrophobic material in addition to being flexible while mechanically robust [14], [95].

1.3.2.3. Carbon Dots

Carbon Dots (CD)s can be grouped as graphene quantum dots (GQD) or carbon quantum nanodots (CQD). Graphene Quantum dots (GQDs) are single layers of graphene broken up into tiny pieces. GQDs as small as 10nm can be fabricated [139]. They belong to the 0 D family of CNM with a diameter range of 1 – 10. CDs are electron confined fluorescent nano particles [1]. They exhibit a sp^2 hybridised electron configuration but sometimes exhibit sp^3 carbon configuration. They are quasi-spherical in shape and have dimensions of less than 10nm. They are made of amorphous cores and allow for functionalization of their surface with groups such as C–O, C=O and C–OH. The functional groups play an important role in sensing applications as they are able to form coordination bonds with specific molecules. Synthesis methods include thermal plasma, hydrothermal synthesis, pyrolysis, microwave synthesis and the less expensive soot of the candle flame. Furthermore, they serve as nanodiamond alternatives. [1], [75], [138]

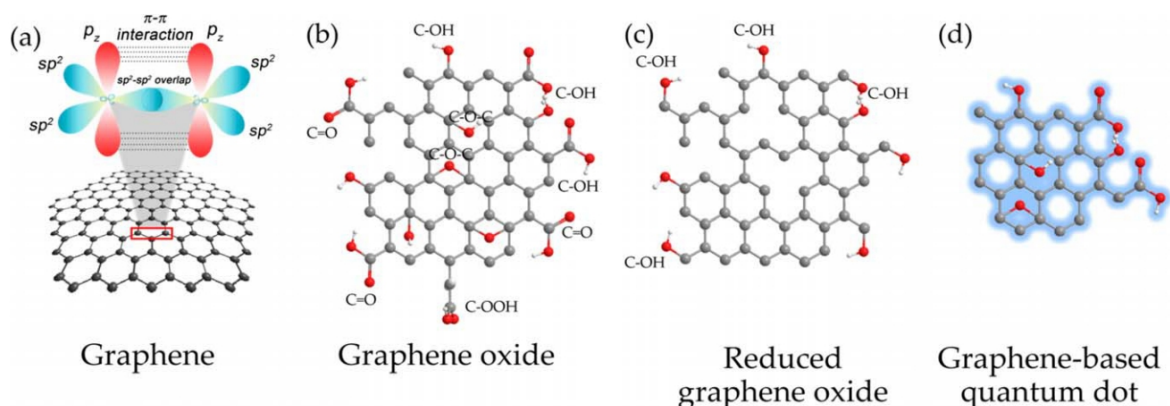


Figure 1.3.2. Structures of Graphene based nanomaterials. (a) pure Graphene with sp^2 hybridization (b) GO (c) rGO (d) Graphene based carbon quantum dot [75].

1.3.3. Synthesis of graphene

Graphene's unique properties and structure make it an ideal choice for use in sensor and transduction technologies. However, unlike most CNMs used in sensor technology, bulk graphene doesn't possess desirable traits and therefore almost always requires surface functionalization for deployment. The preparation method chosen, doping and number of layers are the main variables by which the properties of graphene can be tailored to suit a specific sensor application requirement [140]. Some of the more common methods of graphene preparation are; thermal redox, unzipping of CNTs, thermal CVD, plasma CVD, exfoliation, cleavage, thermal decomposition etc [140], [141]. These methods have merits and demerits with respect to yield amount, length of production time, electrochemical properties of yield, complexity, expense etc [140].

Upon synthesis, unlike CNTs, graphene does not contain metallic impurities that

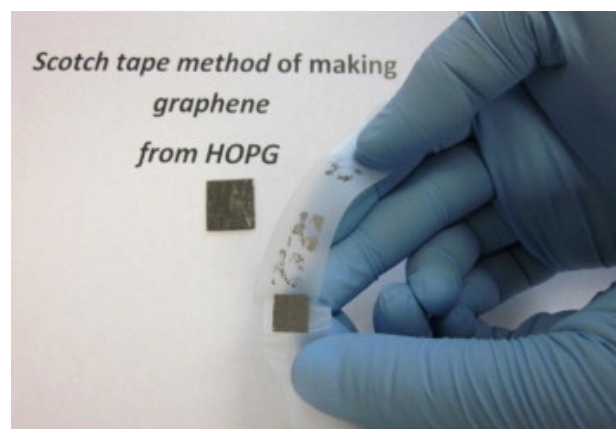


Figure 1.3.3. Scotch tape method of making graphene from HOPG [143].

would otherwise interfere with sensor data or require extra purification [133]

Graphene synthesis methods can be categorised in two groups, namely; the bottom-up approach (synthesis using hydrocarbon gases) and the top-down (decomposition of graphite) approach [51]. The top-down approach involves the decomposition of graphite raw material into graphene sheets. The most prominent top-down methods are micromechanical cleavage, exfoliation of graphite intercalation compounds, arc discharge,

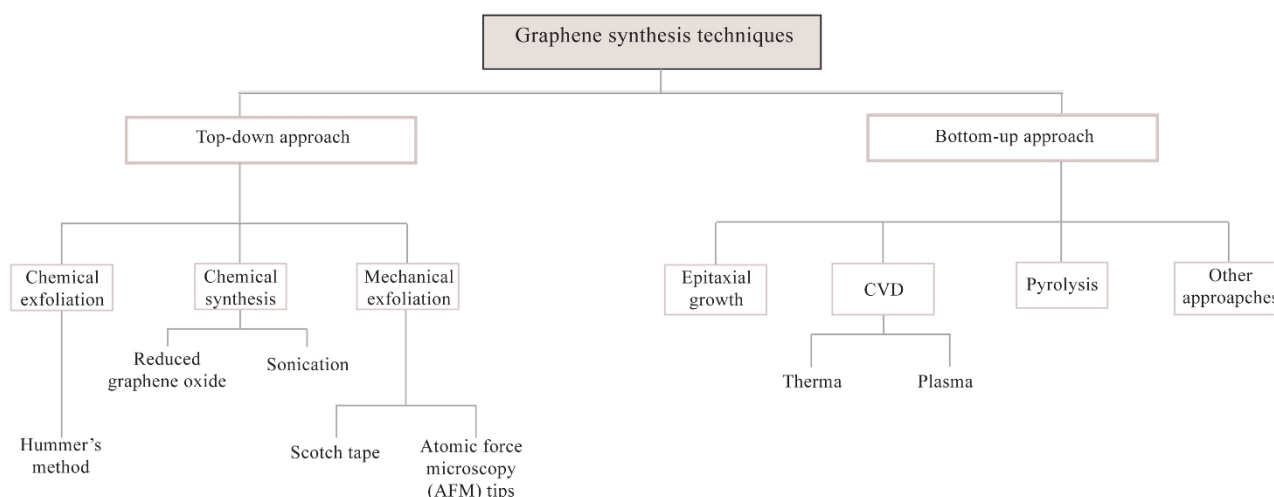


Figure 1.3.4. Process flow diagram of graphene synthesis methods [88].

unzipping of CNTs, graphene oxide exfoliation and solvent-base exfoliation. The bottom-up approach involves the use of hydrocarbon gases as raw material to produce graphene and includes methods like CVD and epitaxial growth on Silicon Carbide [17].

1.3.3.1. Mechanical Exfoliation

Also called the “scotch-tape” method is one of the simplest methods. This method involves stripping of highly oriented pyrolytic graphite (HOPG) with scotch tape and then repeatedly stripping off layers from the tape until a graphene sheet is obtained. Upon dissolving the tape, the graphene is then extracted [88], [140], [142].

However, for commercial production of graphene, this method would prove very expensive, labour intensive and suffer low yields [138].

1.3.3.2. CVD

This procedure involves the decomposition of a hydrocarbon (gas or spray liquid) at high temperature and the subsequent growth of carbon atoms derived upon nucleation onto a metal substrate. The metal substrate also serves as a catalyst. Precursor material maybe in a carbonaceous gas such as ethylene, methene etc or liquid form such as hexane etc [133], [134]. Growth mechanism of graphene development is heavily dependent on the substate used [134]. The most commonly used substrates are Cu foil or Ni film on Si/SiO₂ wafer.

When Ni substrate is used, the carbon atoms dissolve into the Ni crystal assuming an epitaxially arrangement before forming graphene [133]. Preparation variables such as precursor concentration, substrate composition, temperature and gas composition influence can vary the yield. Changes in precursor concentration has been reported to vary the number of layers. CVD can take place at normal pressure or in vacuum conditions [133].

The many types of CVD include plasma-enhanced CVD, hot wire CVD, thermal CVD, radio-frequency CVD, radio-frequency CVD, hot/cold wall CVD and ultrasonic spray pyrolysis [133], [134]. The yield is in the form of graphene thin films on a substrate or graphene powder [133]. The yield is in the form of graphene thin films on a substrate or graphene powder. CVD techniques to synthesis high quality graphene sheets have been developed. Currently, graphene produced by CVD is available commercially [22].

Expensive synthesis equipment, high cost and complex synthesis process are some of the biggest challenges facing CVD with respect to graphene production [47], [123]. It, however, is one of the best methods for ultra-pure large area graphene production [47], [134].

Unzipping of CNTs into single-layer graphene [133].

This principal stems from the fact that CNTs are rolled up graphene sheets. One-way to accomplish this is by treatment of CNTs with harsh acids under the right thermodynamic conditions. Unzipping of MWCNTs by H_2SO_4 treatment followed by $KMnO_4$ in order to produce graphene by oxidation has also been reported [143]. Other methods include the Argon plasma etching method [133].

For an in-depth reading on the unzipping of CNTs see ref [143], [144].

1.3.3.3. Arc discharge method

Is an inexpensive flexible method by which a number of CNTs are produced. This method, involves the use of nearly pure graphene rods at high voltage placed a very close distance to one another in a reaction chamber. The very high potential difference between the rods sets up an electric field that in turn induces a spark to set up the arc. The product

fallouts from this process include a mixture of nanostructures which are then sorted for graphene extraction [133]. Varying parameters such as purity of the graphite rods, discharge chamber atmosphere, varying the chamber gas combinations and concentrations etc can varies the yield parameters [145].

1.3.3.4. Reduction of graphene oxide

Graphene can also be synthesised by the chemical reduction of graphene oxide (GO) with, however, many more defects than that synthesised directly from graphite [75]. GO is a form of graphene that contains hydroxyl, epoxy functional groups on its basal plane and carbonyl and carboxyl groups on the edges. These groups cause the formation of colloidal solutions in water and polar solvents [75], [133].

Commercially, strong acidic oxidants are used to convert graphite into GO [140]. GO is then, via exfoliation, turned into monolayer graphene sheets. Graphene like single layers are then produced by the subsequent *in-situ* reduction [134]. By Hummers method [146] or the modified versions [17], [147] of it.

Other methods of GO reduction reported include, laser, thermal and electrochemical methods [133].

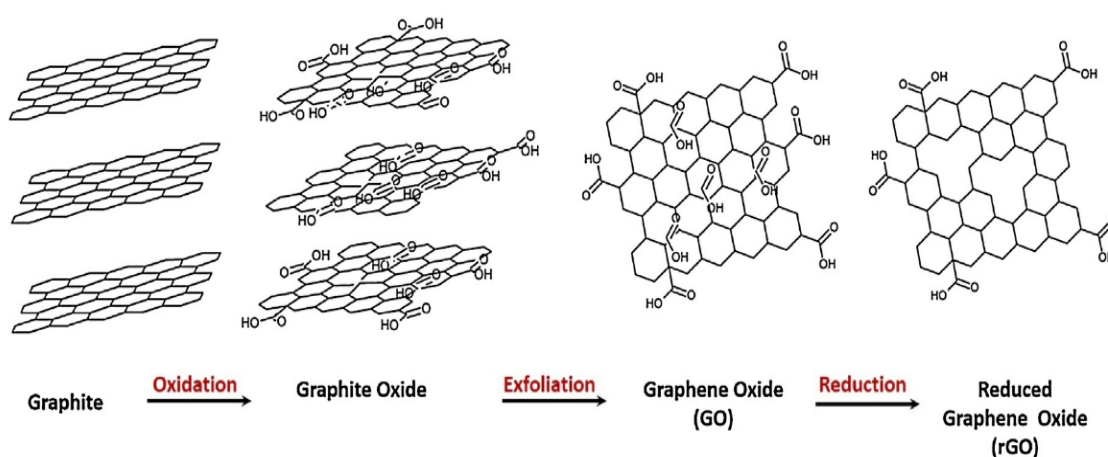


Figure vi. Graphite to reduced graphene oxide procedure [124].

Large scale preparation of graphene is mainly done via redox chemistry [140].

Table 1.3.3. Common synthesis methods for Graphene [163].

| Method | Advantages | Disadvantages |
|-------------------------|---|---|
| Mechanical cleavage | No defects | Neither scalable nor capable for mass production |
| Solution exfoliation | Less defects | Low efficiency and hard to control the number of layers |
| Epitaxial growth | No defects for every single graphene island | Discontinuous |
| CVD | Compatible with the current CMOS technologies | High cost and complex transfer process |
| Total organic synthesis | Potentially suitable for mass production | Many defects |
| Reduced GO | Low cost and suitable for mass production | The majority of defects can be removed |

1.3.3.5. Functionalization of graphene

Surface modification, i.e., functionalization, is important in order to tailor the physiochemical properties of graphene to a specific application. It enables the alteration of cohesive forces between graphene sheets (GS) preventing the agglomeration and restacking of GS [133], [142] and promote the dispersibility of graphene in common organic solvents with the aid of functional groups [148]. Fusion with recognition molecules in sensor application. Procedures like heteroatom doping and oxidation enriches GR based materials with functional groups to tune and create hybrid sensor properties [140]. Graphene based NMs may be functionalised by the more stable yet electromechanically disruptive covalent method or the degradable non-disruptive non-covalent functionalization method [123].

Covalent functionalization

Covalent functionalization occurs with the aid of the formation of a covalent bond on basal plane and/or at the end edge of a GS. Surface functionalization involves the rehybridization of one or more sp^2 hybridised carbon atoms into sp^3 thus causing an alteration in the electronic configuration [133]. The two main ways in which this can be achieved are; (I) covalent bond formation between the C=C bonds of pure graphene and dienophiles (or free radicals), (II) covalent bond formation between the oxygen groups of

GO (as well as rGO), and organic functional groups [149][148], [149]. Heteroatom doping also achieves covalent functionalization [140].

Non covalent functionalization

Non covalent functionalization involves connecting graphene to functional groups through Van der Waals force, π - π stacking, hydrophilic - hydrophobic interactions. This functionalization achieved via weak bonding that is non-evasive in that it leaves the graphene structure undestroyed thus returning all of graphene's properties suitable for sensor technology. The hydrophobic nature of pure graphene is cured through non covalent functionalization by linking upon it hydrophilic functional groups. π - π stacking between GS is another problem remedied [140], [142], [148]

Table 1.5.2. Some advantages and disadvantages of CNM functionalization.

| | Advantages | Disadvantages |
|---------------------------------|------------------------------------|-------------------------------------|
| Covalent functionalization | •Formation of high stability bonds | •Loss of inherent properties |
| | | •Possible structural damage to CNMs |
| | | •Re-agglomeration of CNMs in matrix |
| Non- covalent functionalisation | •Structural network is retained | •Weak coating stabilities |
| | •No loss of electronic properties | |
| | •Simple procedure | |
| | •Minimum damage | |

2. Deposition Techniques

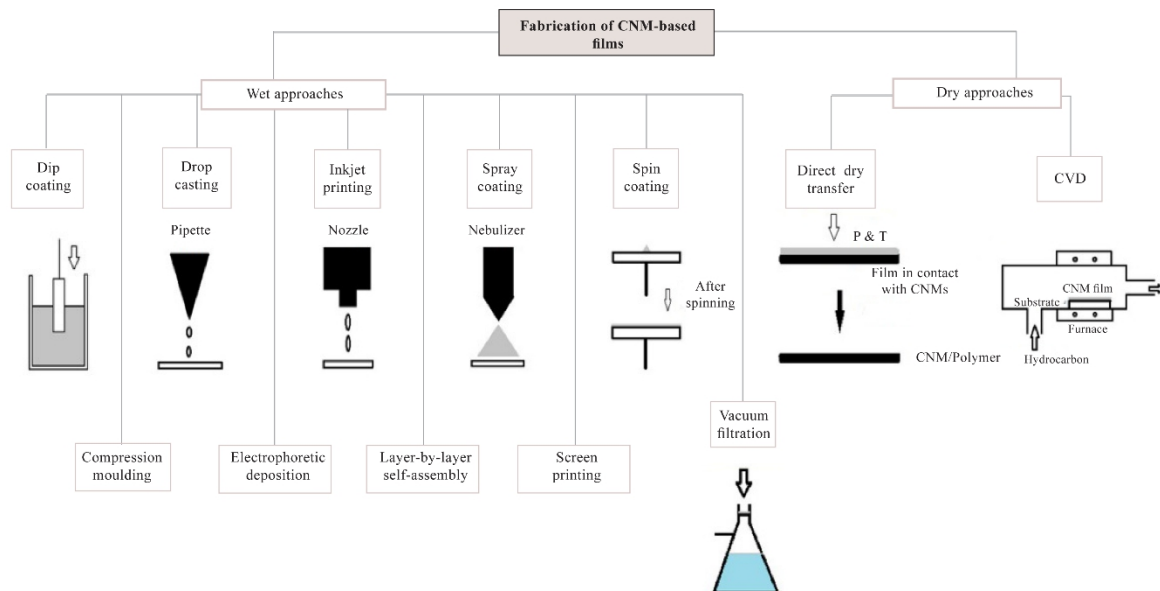


Figure 2.0. Fabrication methods of CNM-based films [88].

Deposition technologies are divided into wet and dry techniques as shown in figure XX above. Wet techniques involve the creation of thin films from the liquid phase of CNMs whereas dry techniques seek to create films directly from CNM assemblies [88]. To produce highly sensitive, stable and repeatable CNM based sensors, suitable preparation techniques should be used. The Chosen deposition technique has a huge impact on sensor performance as it controls parameters like, uniformity and thickness of the coating. This section gives an overview of some of the deposition techniques used for CNM in sensor technologies [87].

2.1. Langmuir-Blodgett

The Langmuir-Blodgett (LB) depositing technique was first introduced by Irving Langmuir and Katharine Blodgett after whom it is named. This method involves the deposition of amphiphilic monolayers of particles trapped at the air/water interface onto a solid substrate by means of a vertically dipping the substrate immersed at the sub-phase [150], [151]. The amphiphilic materials used often are those with hydrophobic tails and hydrophilic heads[87].

The deposition procedure is conducted in two main steps. The first involves dissolving the amphiphilic material in a volatile solvent, ideally one with positive spreading coefficient and insoluble in the subphase. The solution is then spread onto the air/water surface followed by solvent evaporation which enables the formation of the amphiphilic material monolayer. Upon the attainment of thermodynamic equilibrium, the monolayer-thick film is isothermally compressed in order to form a stable monolayer film. The compression has the effect of altering its shape all the while altering its phase states. The second stage involves transfer of the film onto the solid substrate. To attain this, the solid substrate is dipped into the sub-phase and is then raised out subsequently depositing the monolayer film onto the substrate. During this stage, surface pressure is monitored via isobars and is kept constant by adjusting the moveable barrier to achieve the target pressure, figure 2.1.2. Surface pressure is an important parameter in determining the quality of the coating. More monolayers may be coated onto the substrate by repeating the transfer process. Figure 2.1.2. shows the three different coating techniques by the LB procedure [87], [150], [151].

A similar mono-layer deposition technique called Langmuir - Schaefer method involves horizontal deposition of a thin film onto a substrate as opposed to the vertical deposition of LB as shown in figure 2.1.2. (b).

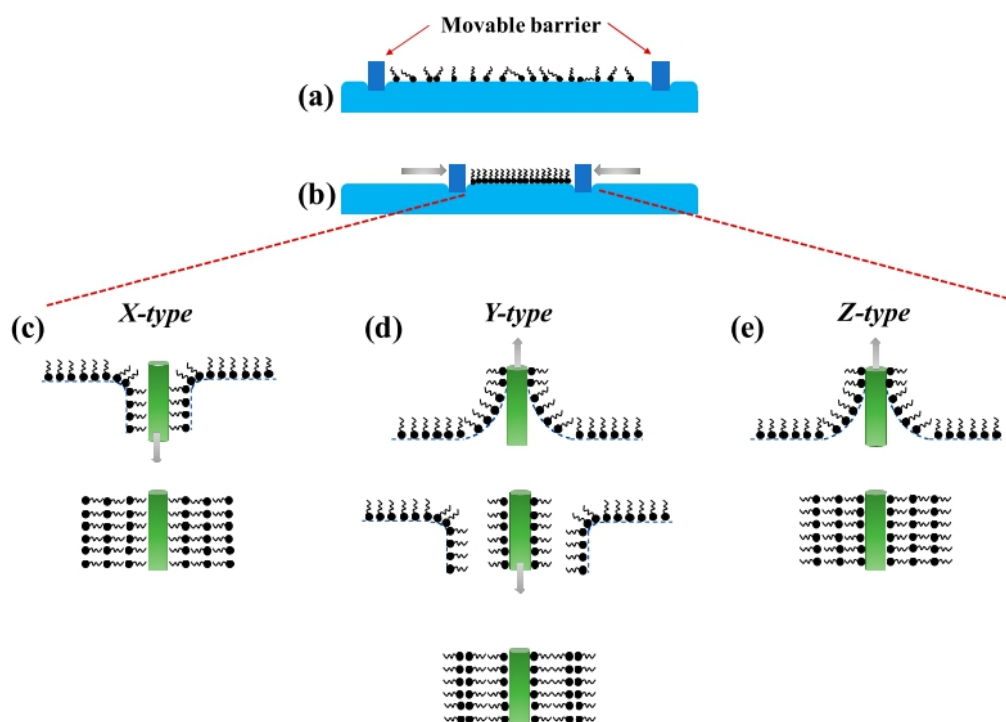


Figure 2.1.1 Langmuir-Blodgett film deposition scheme. (a) Spreading of molecules to the surface of sub-phase, (b) surface compression with constant pressure to yield a condensed and stable monolayer film, (c) X-type LB film deposition, (d) Y-type LB film deposition. [87]

Yap et al. [87] outlines the deposition of CNM onto an optical fibre substrate for the preparation of CNM based optical fibre for environmental and biological sensors. Deposition thickness control in the range 1-3 nm was reported.

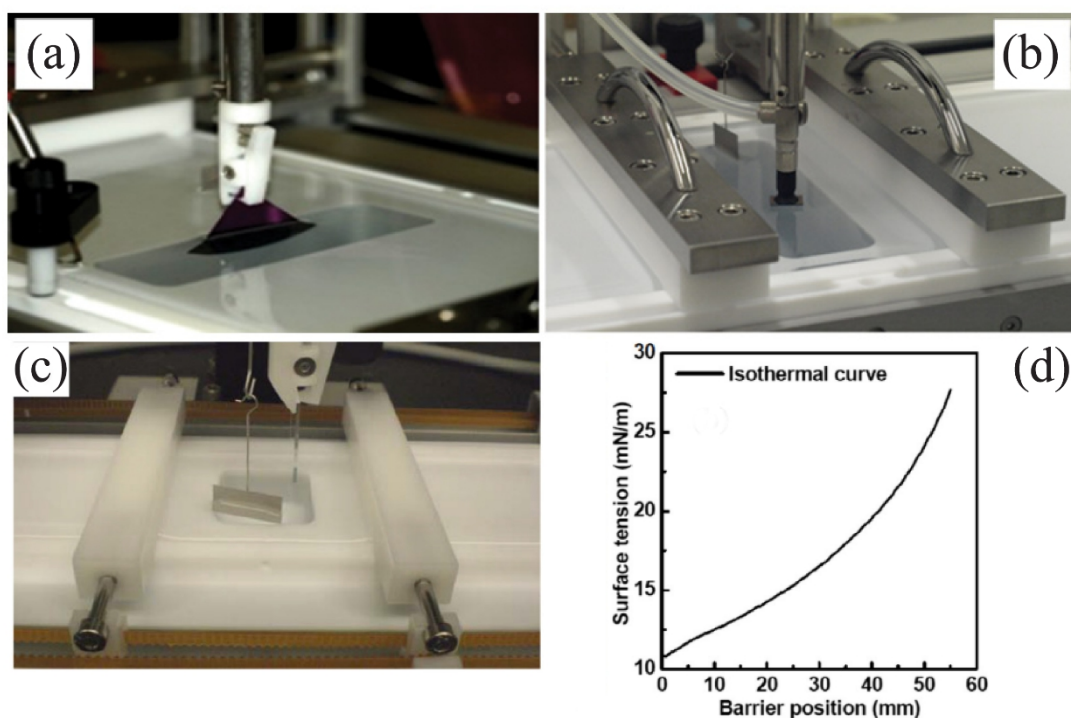


Figure 2.1.2. (a) LB and Langmuir-Schaefer (b) transfer processes. (c) Illustration of LB deposition and its corresponding surface pressure isobar reading in (d). [150].

Kim et al. [151] reported an improvement upon the classic LB method to ease the rapid deposition of dense monolayers of MWCNTs. They demonstrated the layer-by-layer deposition of MWCNT-SiO₂-MWCNT onto a substrate by taking advantage of the Marangoni stresses caused by surfactants at fluid-solid-gas interfaces and the auto assembly of nanoparticles.

Unlike other deposition techniques like CVD, LB is carried out at room temperature, it is simple and in its simplest form requires only one chemical compound. LB can be used for the production of composites and water soluble materials [87], [150]. It is however a very slow process requiring a skilled operator to operate it. The films produced by this method mostly demonstrate poor thermal stability [87].

2.2. Drop Casting

Drop casting is another wet approach method of thin film fabrication from the liquid phase of CNMs. This is a cheap, easy and tuneable deposition procedure most suitable for small areas of about 1cm^2 . This method involves dispersing a specific quantity of suitable CNM into a volatile solvent and then literally dropping it on a prepared substrate, using a pipette. The drop is then left to evaporate off the substrate, under controlled conditions of temperature and pressure, leaving behind CNM deposited onto the substrate. Drop casting is another wet approach method of thin film fabrication from the liquid phase of CNMs. This is a cheap, easy and tuneable deposition procedure most suitable for small areas of about 1cm^2 . This method involves dispersing a specific quantity of suitable CNM into a volatile solvent and then literally dropping it on a prepared substrate, using a pipette. The drop is then left to evaporate off the substrate, under controlled conditions of temperature and pressure, leaving behind CNM deposited onto the substrate. Varying the CNM concentration or volume of dispersion or indeed repeating the procedure could be done to

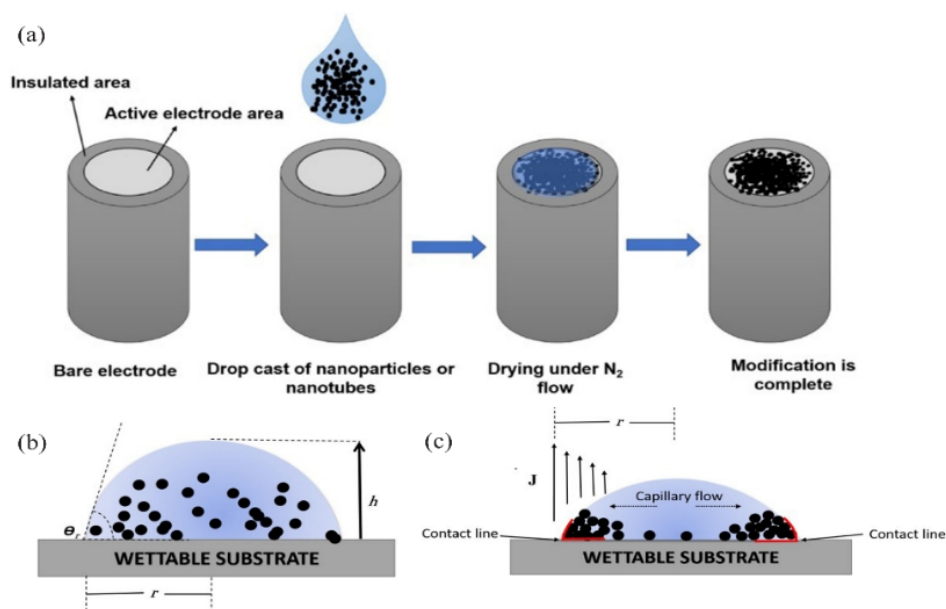


Figure 2.2.1. A schematic showing the drop casting of nanoparticles or nanotubes onto an electrode [155].

vary the thickness of the coating. Complete wetting and hydrophobic properties of the

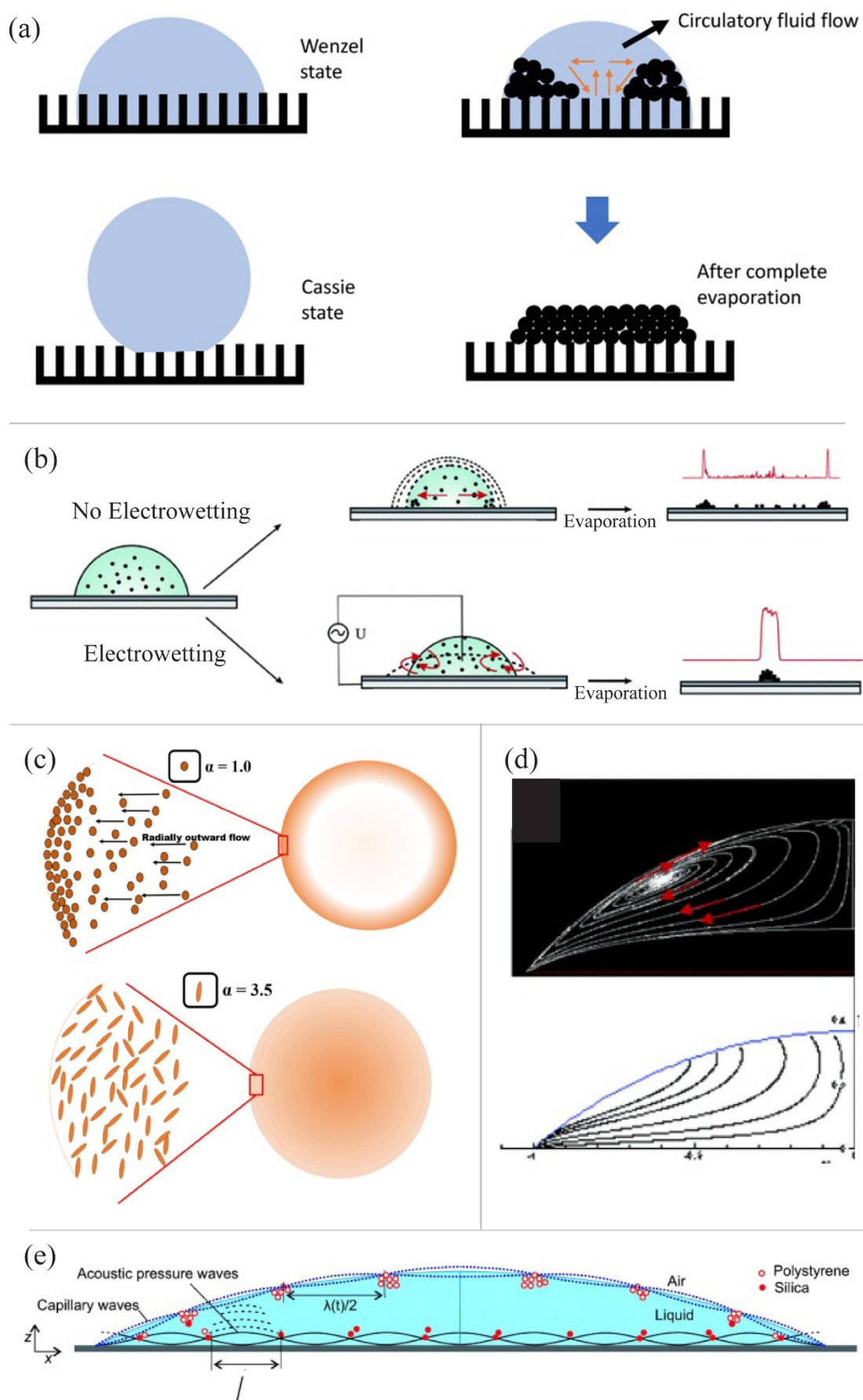


Figure 2.2.2. Schematics of Kumar et al.'s modification of the drop casting technique: (a) hydrophobic surface modifications (b) Electrowetting modification (c) use of anisotropic particles (d) Marangoni flow considerations (e) surface acoustic waves in the evaporating droplet [155]. .

substrate must be taken into account to determine solvent properties for the chosen CNM [87], [152], [153].

It is very difficult to obtain a uniformly thick coating across the substrate using this procedure. This is due to differences in the rates of evaporation on different substrate points and also due to fluctuations in concentration. High is always a chance for formation of voids. These reasons make drop casting unsuitable for use across large areas [153], [154].

Kumar et al. [155] demonstrate ameliorations to the drop casting technique when used to deposit nanomaterials onto electrodes for electrocatalytic analysis and electrochemical sensing. Potential remedies to suppress formation of coffee ring and its effects, during the deposition of nanoparticles in the course of the creation of particle modified electrodes, are outlined. Five modifications are given. Chemically modified super hydrophobic surfaces, electrowetting, anisotropic particle interactions or use of surfactants, establishment of surface acoustic waves into the evaporating droplet and the Marangoni effect are proposed.

2.3. Electrophoretic depositions

Electrophoretic deposition (EPD) is a two-step wet approach method. The two main steps are, electrophoresis followed by deposition. In the first stage, electrophoresis, colloidal charged particles or molecules are dispersed in a suitable solvent (or aqueous solution). They then migrate towards an electrode under the influence of an electric field. Deposition occurs at the target electrode surface by particle accumulation and coagulation, forming a coherent homogeneous deposit [156], [157].

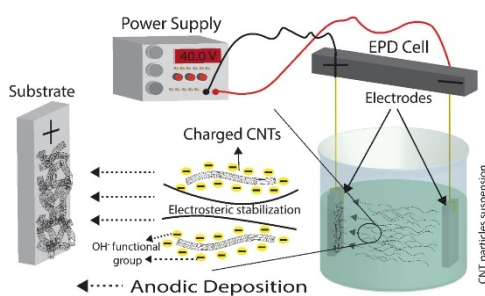


Figure 2.3.1. Illustration of the anodic EPD process of CNTs [157].

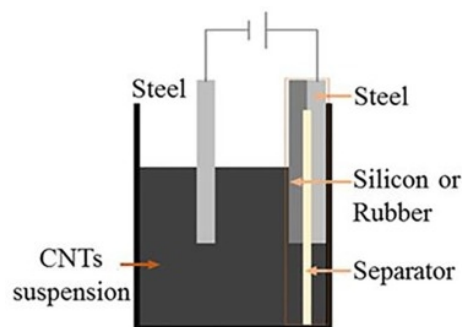


Figure 2.3.2. Zhao et al.'s modified EPD setup for deposition on semi-/non-conducting substrates [159].

The basic EPD setup is shown in figure XX. It consists of a power-supply connected to two parallel electrodes. Deposition can either be set up to occur at the cathode (cathodic electrophoretic deposition) or at the anode (anodic electrophoretic deposition) depending on the polarity of the particles in the suspension [158].

Deposition uniformity and the ability to control deposition thickness on the surfaces of irregular and regularly shaped substrates alike, achieving microstructural homogeneity, are some of the main advantages of EPD. In addition, EDP has the potential to infiltrate porous substrates. It is also a simple and inexpensive deposition procedure [156].

Zhao et al. [159] reported a modified EPD procedure on nonporous semiconducting and nonconducting substrates in which they coated CNTs onto bare rubber and silicon using their enhanced EPD setup. The setup was as shown in figure 2.3.2. Two steel electrodes of surface area dimensions $1\text{ cm} \times 3\text{ cm}$ and $500\mu\text{m}$ were used and placed a distance of 0.5 cm apart. They were supplied a voltage of 50 V . The anode was clipped to either rubber ($500\mu\text{m}$ thick) or silicon ($525\mu\text{m}$ thick) substrate with a porous solvent prewetted separator placed between them. The experiment was conducted at ambient conditions each experiment varying substrate, deposition time, suspension solvents and CNTs (SWCNT and MWCNT). The CNTs successfully deposited on the nonconductive surfaces as shown in table 2.3. From the experiment results, it was concluded that the separator between the steel electrode and substrate is a necessary modification to enable deposition onto semiconducting and nonconducting surfaces by EPD.

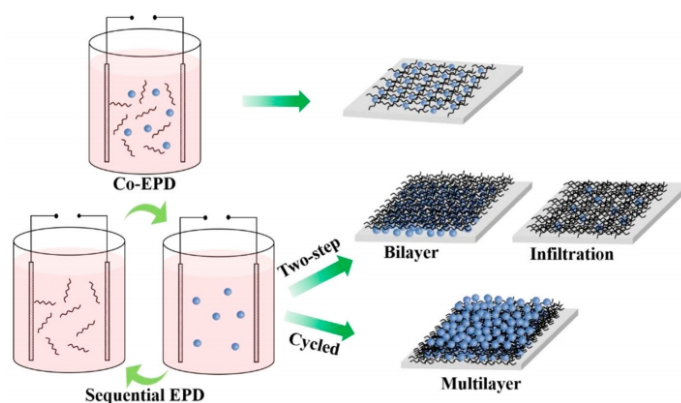


Figure 2.3.4. Schematic illustration of common EPD strategies applied for the production of CNT-based composite coatings [157].

Table 2.3. The coated samples from Zhao et al.'s modified EPD setup and the corresponding process parameters [159].

| Sample # | Substrate | Deposition time (min) | Suspension solvents | Types of CNT |
|----------|-----------|-----------------------|---------------------|--------------|
| 1 | Silicon | 60 | Ethanol | SWCNT |
| 2 | Silicon | 15 | Ethanol | SWCNT |
| 3 | Silicon | 15 | Water | SWCNT |
| 4 | Silicon | 15 | Acetone | SWCNT |
| 5 | Silicon | 5 | Acetone | MWCNT |
| 6 | Silicon | 15 | Acetone | MWCNT |
| 7 | Silicon | 25 | Acetone | MWCNT |
| 8 | Rubber | 10 | Acetone | MWCNT |
| 9 | Rubber | 15 | Acetone | MWCNT |
| 10 | Rubber | 20 | Acetone | MWCNT |
| 11 | Steel | 3 | Acetone | MWCNT |

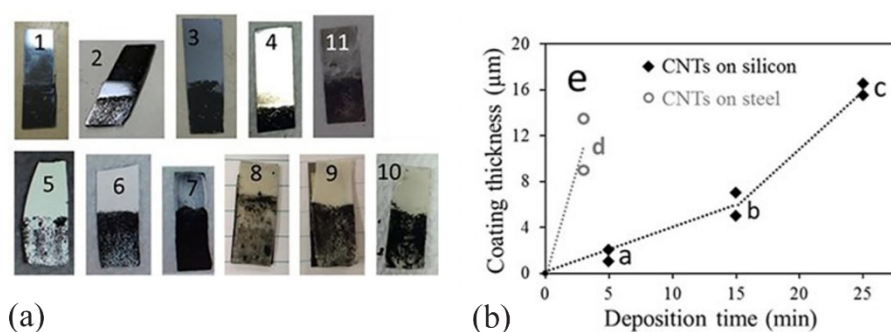


Figure 2.3.5. (a) Photos of the CNTs coated samples from Zhao et al.'s modified EPD setup. (b) deposition thickness as a function of time [159].

2.4. Layer-by-Layer Electrostatic Self-Assembly

Layer-by-Layer Electrostatic Self-Assembly (LbL-ESA) is a thin film fabrication technique whose operating principle is based upon the electrostatic interaction, hydrogen bonding or covalent bonding between two materials of opposite charges. Thin layer deposition can be achieved in several ways such as, spray-coating, dip-coating and spin-coating. Multilayer coating can be done at ambient temperature and unlike the LB technique, even coating can be conducted on a substrate regardless of its shape and size. Apart from CNMs, other materials such as biological molecules, metals, ceramics, nanoparticles etc can be deposited by LbL-ESA [88], [160].

Yap et al. [87] outlines the deposition procedure for CNMs by LbL-ESA onto optical fibre substrate for environmental and biological sensing. The substrate is first treated to

induce a negatively charged surface. The substrate is thereafter submerged into a polycation solution until molecule adsorption occurs. A deionised water bath is done before it is submerged into a polyanion electrolyte solution. The last stage deposits a bilayer by LbL-ESA deposition. To obtain more layers, the process can be repeated.

2.5. Dip coating

Dip coating is a well-known thin film coating procedure. It is conducted in three main steps. The first step involves immersion of the substrate, at constant speed, into a solution containing the coating material where it is left for a predetermined time. Deposition occurs as the substrate is retrieved from the solution at constant speed to ensure homogeneous coating. The coat thickness is directly proportional to the speed at which the substrate is being retrieved from the solution. This is followed by drainage of excess solution off the surface of the substrate by baking or forced air drying. Excess solvent is left to evaporate off the surface and a thin film is deposited onto the substrate [161]–[163]. Number of dipping cycles, rate of solvent evaporation, solution contents, viscosity, concentrations, temperature, etc. also affect film properties and thickness [161], [164].

Though similar to most wet deposition techniques, dip coating is remarkably faster. It is also simple and cheap and thus may not be suitable for use in situations requiring high quality substrate deposits. Nonuniformity in coating thickness is the main disadvantage of dip coating. It is however suitable for use in laboratory set up and for large scale requirements for which low quality depositions are sufficient [161], [162].

Wang et al. [165] demonstrated the production of GO films by dip coating hydrophobic quartz substrate into an aqueous GO dispersion. The films obtained showed really high-quality conductivity and transparency in addition to being chemically and thermally stable.

2.6. Spray Coating

Spray Coating is a wet thin-film solution processing deposition technique.

This procedure involves spraying CNM onto a heated substrate with a nebuliser. Thin film formation occurs on the substrate by pyrolytic decomposition of the spray droplets [88].

Using spray deposition, Abdellah et al. [166] fabricated flexible CNT based gas sensors by large scale spray deposition. It was demonstrated that high quality gas sensors on flexible substrates can be achieved by spray deposition. The flexible gas sensor showed immediate response to target the analyte as well as repeatability for known analyte

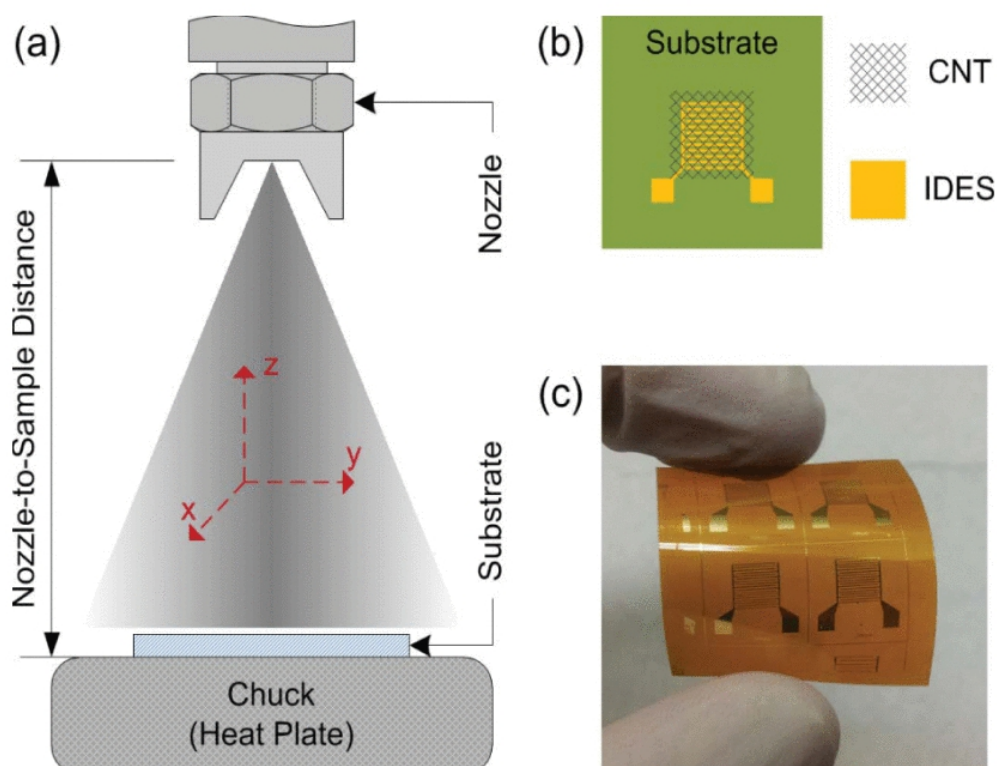



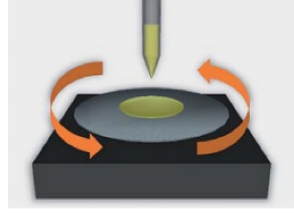

Figure 2.6.1 (a) Schematic drawing of the spray setup, indicating the three-axis motion control.

(b) The general device architecture of Abdellah et al.'s gas sensor, incorporating an interdigitated electrode structure (IDES). (c) Four flexible sensors fabricated in one. [166]

concentrations.

Pham et al. [16] demonstrated the preparation of a quick and simple chemically converted graphene film by spray deposition on a preheated substrate. GO was reduced to chemically converted graphene films of low sheet resistance, and high transmittance at a wavelength of 550nm.

Table 2.6. Principle and main characteristics of dip, spin and spray coating deposition methods [187].

| | Dip coating | Spin coating | Spray coating |
|----------------------------|---|---|--|
| Principle of the technique |  Film formation during hoisting of the substrate after immersion in the liquid coating solution (multi-faced coating) |  Spreading of the liquid coating solution by the centrifugal force acting on a spinning substrate (single-face coating) |  Atomization and transport of the liquid coating solution toward the substrate (single-face coating) |
| Characteristics | <ul style="list-style-type: none"> •Simple equipment •Low waste •Reproducibility and uniformity with simple automation -Mostly for simple shapes -High volume of liquid required | <ul style="list-style-type: none"> •Simple equipment •Low volume of liquid required •Reproducibility and uniformity with simple automation -Considerable waste -Mostly for flat substrates | <ul style="list-style-type: none"> •Flexibility (properties of the liquid) •Also for more complex shapes -High amount of parameters -More complex equipment -High waste |

Wang, Sparkman and Gou [167] present a modified version of the basic spray deposition technique with application to the manufacture of strain sensors using CNTs. They developed an inexpensive, highly efficient and scalable digitally controlled spray deposition technique.

An x-y plotter equipped with 12 array bubble jet nozzles was designed. As with the classic set up, a substrate heater was also included. It was shown that the manufactured sensors' gauge factor could be tuned by varying the layers of CNTs. Deposited CNT layers were varied between 10-50 and resulting in a gauge factor range of 0.61-6.42.

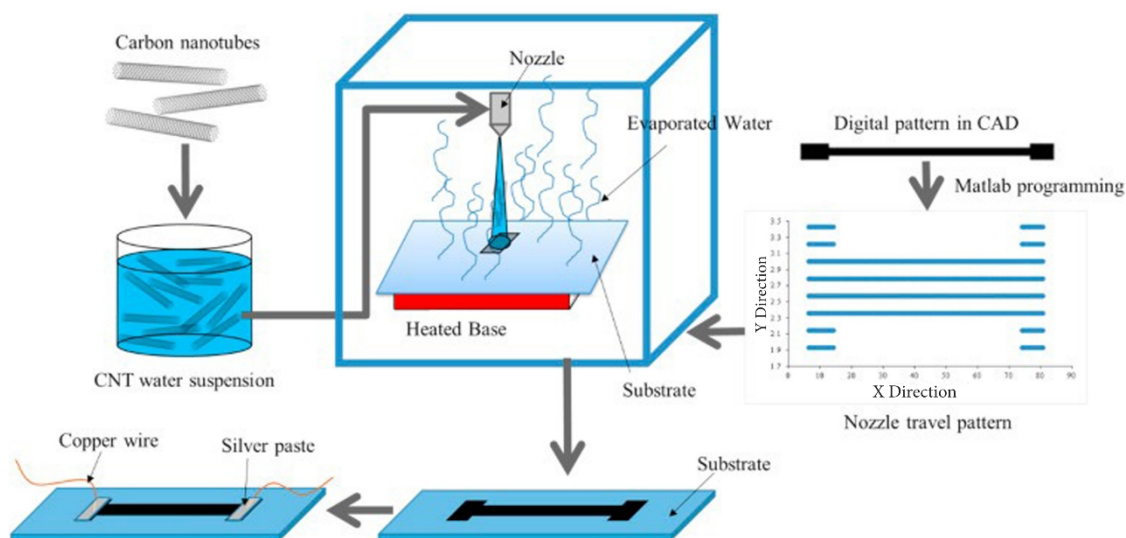


Figure 2.6.2. Schematic of Wang et al.'s digital fabrication of CNT strain sensors through the spray deposition modelling (SDM) technique [167].

2.7. Spin Coating

Spin coating utilises centrifugal force for its operation. It is well known for depositing thin films of even thickness on flat substrates. The procedure involves placing a small puddle of CNT based solution, of known concentration, on a substrate. The substrate is then spun at high, predetermined speeds, in order to spread the solvent evenly over the entire substrate by centrifugal force. Film properties, such as thickness, are mainly determined by the nature of the solvent and spin parameters [163], [164]

Spin coating, ideal for preparation of CNT polymer composite films. However, it is an impractical procedure for large area film depositions. It is also very cumbersome to use for multi-layer deposition purposes. Worse still the material efficiency of spin coating is low as a substantial amount of raw material is lost by not landing on the substrate.

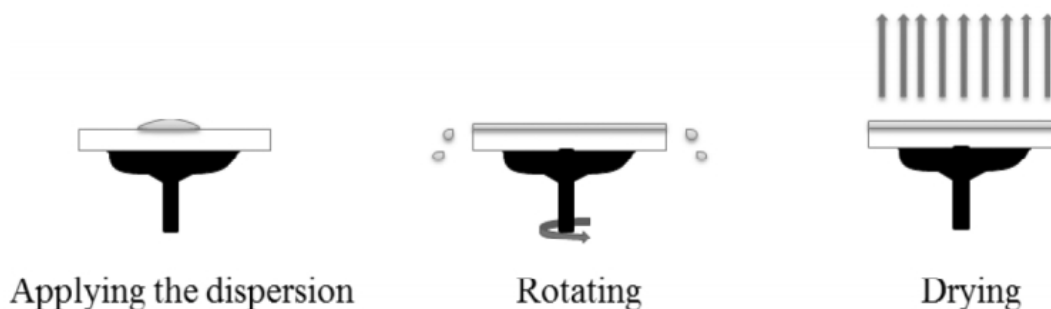


Figure 2.7. Schematic diagrams of thin film preparation using spin coating procedures [188].

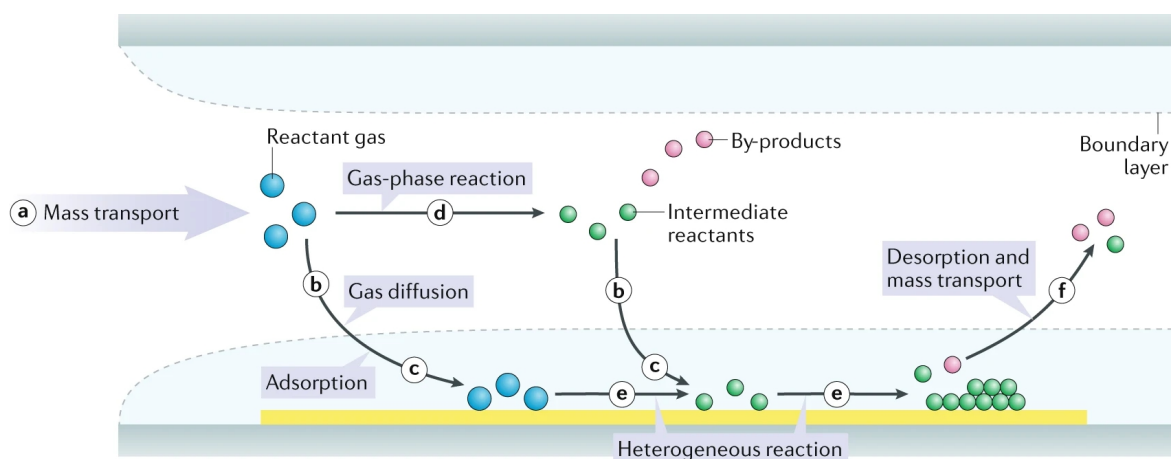
2.8. Chemical Vapor Deposition

CVD is a popular dry approach materials processing technology. In materials science, CVD denotes various techniques that deposit solid material, in gaseous phase, onto a solid substrate. In addition to thin film deposition onto substrates, CVD is also used to produce powders, composite and high-purity bulk materials. [168], [169].

CVD involves the deposition of a solid thin film produced from the chemical reaction of a gas phase precursor, over a heated substrate. CVD differs from physical vapour deposition (PVD) in that PVD uses a solid precursor material which is vapourised right

before deposition. Tunability of the CVD processes renders it more superior to PVD processes like sputtering and evaporation procedures [170].

The first stage in CVD involves feeding the reactor chamber, at roughly ambient temperature, with a reactant precursor gas which may be diluted in a volatile carrier gas. Upon entering the reaction chamber, the reactant may undergo gas-phase reactions or diffuse into the substrate right away through the substrate boundary layer. Gas-phase reaction requires, a high temperature and this may be supplied by various sources such as resistive, radiation or radio frequency induction heaters etc. Plasma energy and laser sources may also be used. The gas-phase reaction leads to the formation of intermediate reactants as well as volatile gaseous by-products which are removed via the reaction chamber exhaust system. Alternatively, the reactant precursor gas could diffuse into the



substrate via the boundary layer. At this stage, in both gas-phase reaction and direct diffusion, the intermediate reactants or reactant gas adsorb onto the heated substrate.

Figure 2.8.1. Basic schematic of the workings of the CVD. (a) reactant precursor gas input via a gas delivery system. (b) diffusion of precursor gas across the boundary layer and (c) adsorption onto the heated substrate. (d) formation of intermediate reactants via gas phase reaction. (e) surface diffusion and heterogeneous reaction. (f) Desorption followed by expulsion of unreacted species via the exhaust system [170].

Following reactions at the gas-solid interface, the deposition of a film on the substrate surface through nucleation, coalescence and growth is initiated. Unreacted reactants and reaction by-products are discarded via the exhaust [169], [170].

At industrial scale, CVD is the most widely used deposition technology for CNMs considering the controllable deposition sizes and structure [171]. The general CVD method was tailored to CNMs in order to overcome most of the shortcomings of method like laser

ablation, arc discharge which lack high efficiencies, low yield purity, high and energy consumption cost [88], [172].

For deposition and growth of carbon allotrope nanoparticles, many variations of the basic CVD procedure exist and depend on the nature of the material. Some examples are given below.

Kleckley et al. [173] reports two CVD arrangements for the deposition of fullerene. A hot-filament CVD setup whose apparatus consists a stainless-steel chamber, vertically installed tungsten filament providing about 2000 °C. Pure high-grade hydrogen and methane are used as precursors for the diamond thin film deposition on stainless steel substrate. The microwave enhanced CVD apparatus utilised the inner walls of quartz tube as substrate with methane, hydrogen and argon precursor supplied with a 100 W of microwave.

CNT deposition by CVD enables the production of highly tenable CNTs. CNT properties can be tuned by varying the CVD parameters such as choice of catalyst, substrate, precursor concentration and flow rate, deposition time etc. A metallic substrate and gaseous carbon precursor are used in the presence of a catalyst. When the precursor decomposes onto the substrate, CNTs growth may occur by two mechanisms, tip-growth or base-growth. Heterogenous reactions and diffusion of the carbon atoms through the metal particles leads to the formation of the CNT structure [174].

Large area graphene monolayer may be produced from carbon-based gasses such as methane or ethylene precursors exposed over a metal catalyst such as copper (Cu) or nickel (Ni) at high temperatures. Upon nucleation on the metal surface, the carbon atoms rearrange into large domains to form graphene sheets [134].

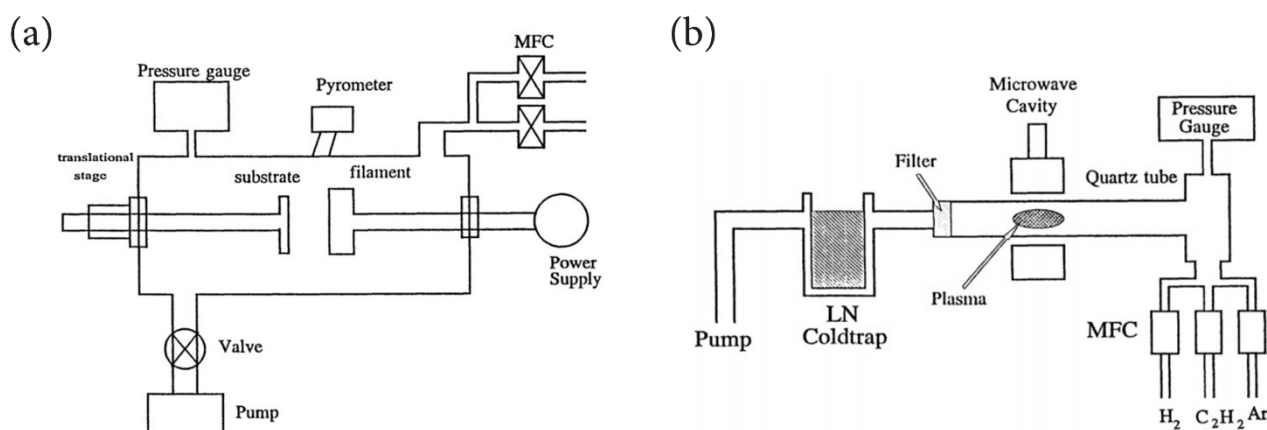


Figure 2.8.2. Kleckley et al.'s (a) hot-filament and (b) microwave-enhanced CVD apparatus [173].

The main advantages of CVD over other deposition technologies are the high purity deposits, conformal coating and high efficiency. However, it requires expensive raw materials and it produces toxic by-products [168].

2.9. Direct dry transfer

Direct dry transfer is a dry deposition approach that is mostly used for the deposition of graphene monolayer obtained from Cu substrate, produced via CVD, onto other target surfaces such as dielectrics, flexible substrates etc.

This basic procedure involves coating the grown graphene on original Cu substrate with a support layer, releasing the graphene from Cu substrate. The graphene and support layer are transferred to the target surface before the support layer is removed [175].

Fechine et al. [175] demonstrate, in an experiment the direct dry transfer of graphene on Cu substrate, produced by CVD, onto polymeric substrates. A polymer is attached to the graphene and subjected to high pressure and temperature, above the polymer melting point. The set-up is then left to cool to ambient conditions before the Cu substrate is mechanically peeled off.

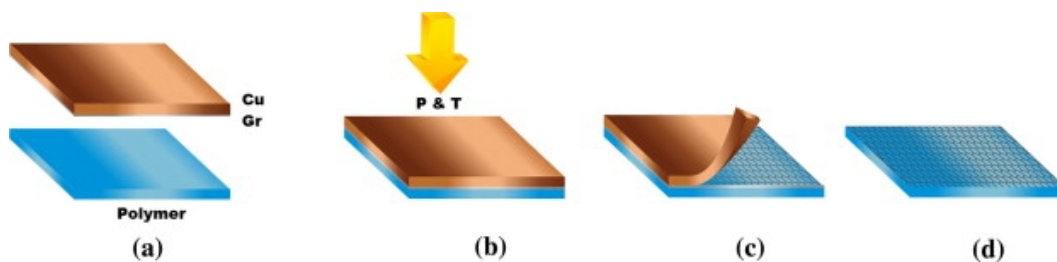


Figure 2.9. Fechine et al.'s direct transfer steps of CVD grown graphene onto a polymer target surface [175]

| | Evaporation | Cathodic arc deposition | Chemical vapor deposition | Polymer deposition | Electrodeposition | Thermal spraying |
|---|---|---|--------------------------------------|-------------------------------|-------------------|-------------------|
| Mechanism of production of deposition species | Thermal energy | Thermal energy | Chemical reaction | Thermal energy | Solution | Flames or plasmas |
| Deposition rate | Can be very high (up to 750,00 A/min) | Can be very high | Moderate (200-2500 A/min) | Very high (up to 100,000 A/s) | Low to high | Very high |
| Deposition species | Atoms & ions | Ions | Atoms | Monomers/polymers | Ions | Droplets |
| Throwing power for: Complex shaped objects | Poor, line of sight coverage except by gas scattering | Good, but nonuniform thickness distribution | Good | Good | Good | No |
| Into small blind holes | Poor | Poor | Limited | Poor | Limited | Very limited |
| Metal deposition | Yes | Yes | Yes | No | Limited | Yes |
| Energy of deposited species | Low (~0.1-0.5 eV) | Can be very high | Can be high with plasma assisted CVD | Low | Can be high | Can be high |
| Bombardment of substrate/deposit by inert gas ions | Generally no | Yes | Possible with PECVD | No | No | Yes |
| Growth interface perturbation | Not normally | Yes | Yes (by rubbing) | No | No | No |

Figure 2.9.1. Overview of some deposition technologies and their qualities. [189]

3. Section 3: Practice verification of the temperature response of SWCNT and MWCNT

Experiment Aims

To practically verify the temperature response of chosen CNMs (SWCNT and MWCNT) and to determine the effect of CNT functionalization on the temperature response.

Experiment Procedure

The first part of the procedure involved preparing the sensor platform. The sensor platform was fabricated by air-brush spray deposition of CNTs onto the Tesla BI2 [176] substrate platform. A total of 20 platforms were prepared. 10 were based on SWCNT and another 10 on MWCNTs.

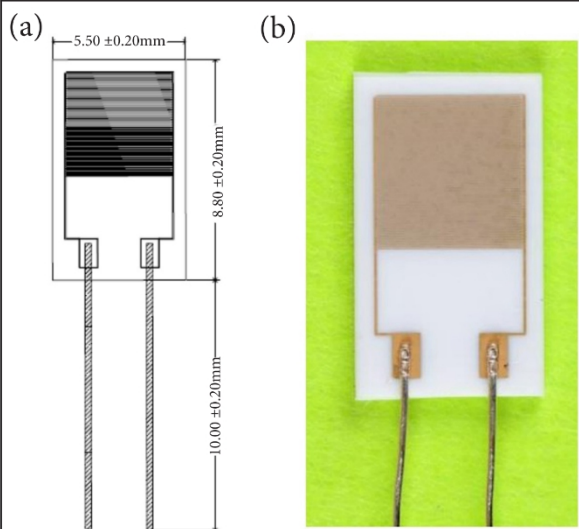
| | | |
|---|------------------------------|--|
|  | Application | Typical application areas for this platform are different types of gas sensors and measurement of relative humidity and quality of air |
| | IDE electrodes | width / gap: 25 μ m / 25 μ m layer structure: NiCr / Ni / Au |
| | Temperature range | 30 °C to +200 °C |
| | Dimensions | 5.5 x 8.8 x 0.6 mm |
| | Input terminal leads | Ag wire \varnothing 0,25 (0,15) mm |
| | Length of input leads | 10 \pm 2 mm |

Figure 3.1. BI2 substrate platform (a) dimension schematic, (b) some of its manufacturer given properties. [176]

The prepared sensor samples were then placed in a climatic chamber for 24 hours during which the temperature of the chamber varied between 9 and 89 °C, with a time period, T, of 5 hours. A record of the climatic chamber temperature was sampled at a frequency of 12 temperature reading per second and saved to a digital file. The corresponding sampling date and time were also logged.

The ten sensor samples of SWCNT and MWCNT were placed in individual climatic chamber channels and were subjected to the same climatic chamber temperature environment. Responsivity of the sensor samples with respect to the temperature of the climatic chamber was established by sampling the resistance of the sensor samples every 20 seconds. The corresponding sampling date and time were also logged and stored to separate digital files for each channel.

Upon completion of the experiment, the record logs from the climatic chamber and the individual channels containing the CNT sensor samples were analysed.

Table 3.1. CNT functionalization and corresponding climatic chamber channel.

| Channel number | CNM-Functionalisation |
|----------------|-------------------------|
| 1 | MWCNT-COOH |
| 2 | MWCNT-COOH |
| 3 | MWCNT-COOH |
| 4 | MWCNT-COOH |
| 5 | MWCNT-SO ₃ H |
| 6 | MWCNT-SO ₃ H |
| 7 | MWCNT-SO ₃ H |
| 8 | MWCNT |
| 9 | MWCNT |
| 10 | MWCNT |

| Channel number | CNM-Functionalisation |
|----------------|-------------------------|
| 1 | SWCNT |
| 2 | SWCNT |
| 3 | SWCNT |
| 4 | SWCNT-SO ₃ H |
| 5 | SWCNT-SO ₃ H |
| 6 | SWCNT-SO ₃ H |
| 7 | SWCNT-COOH |
| 8 | SWCNT-COOH |
| 9 | SWCNT-COOH |
| 10 | SWCNT-COOH |

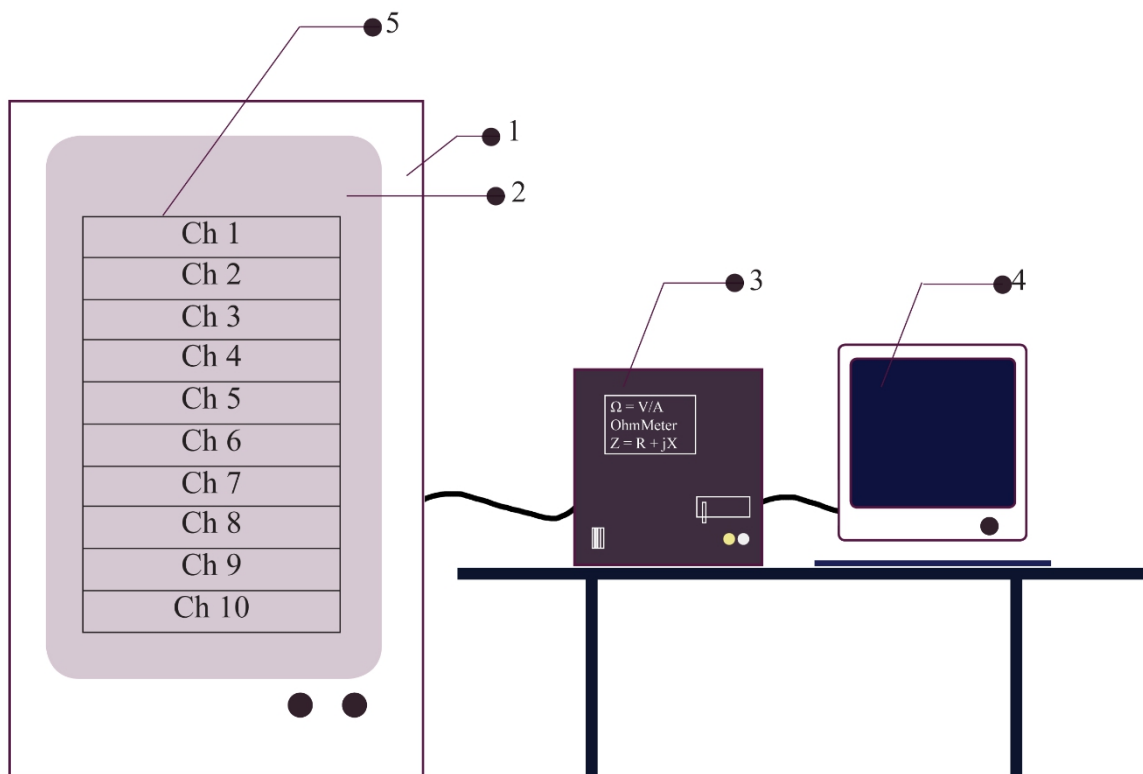
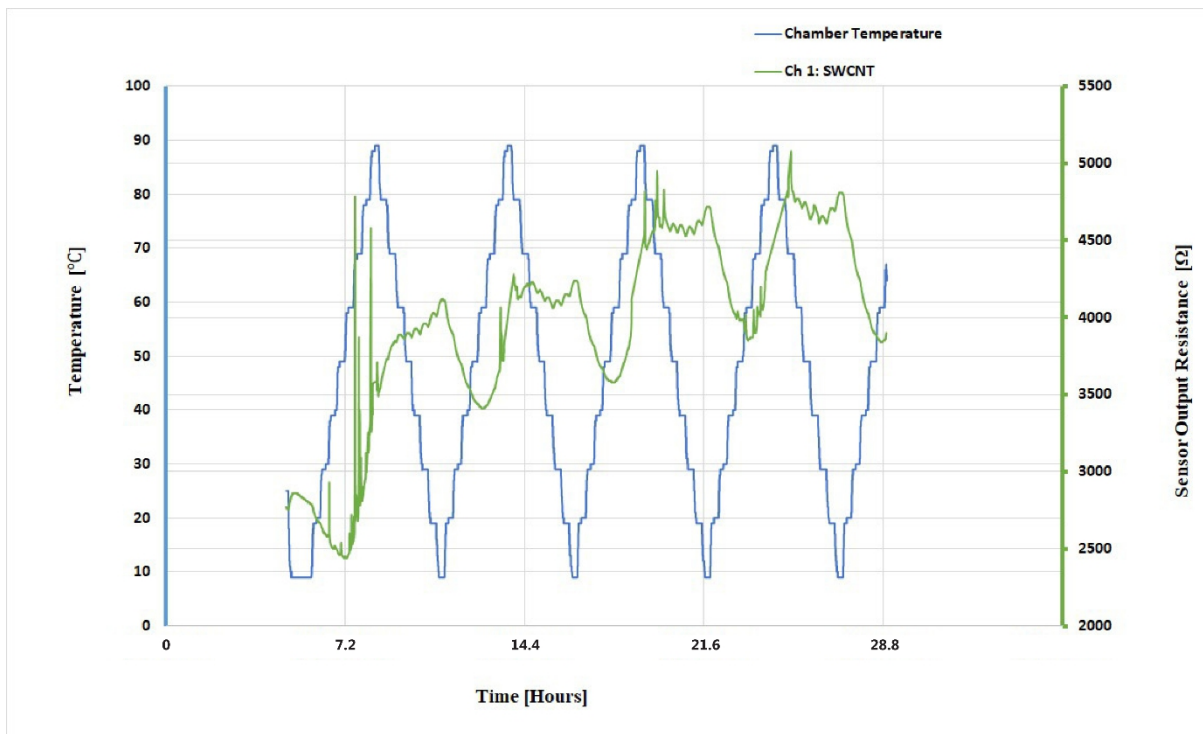


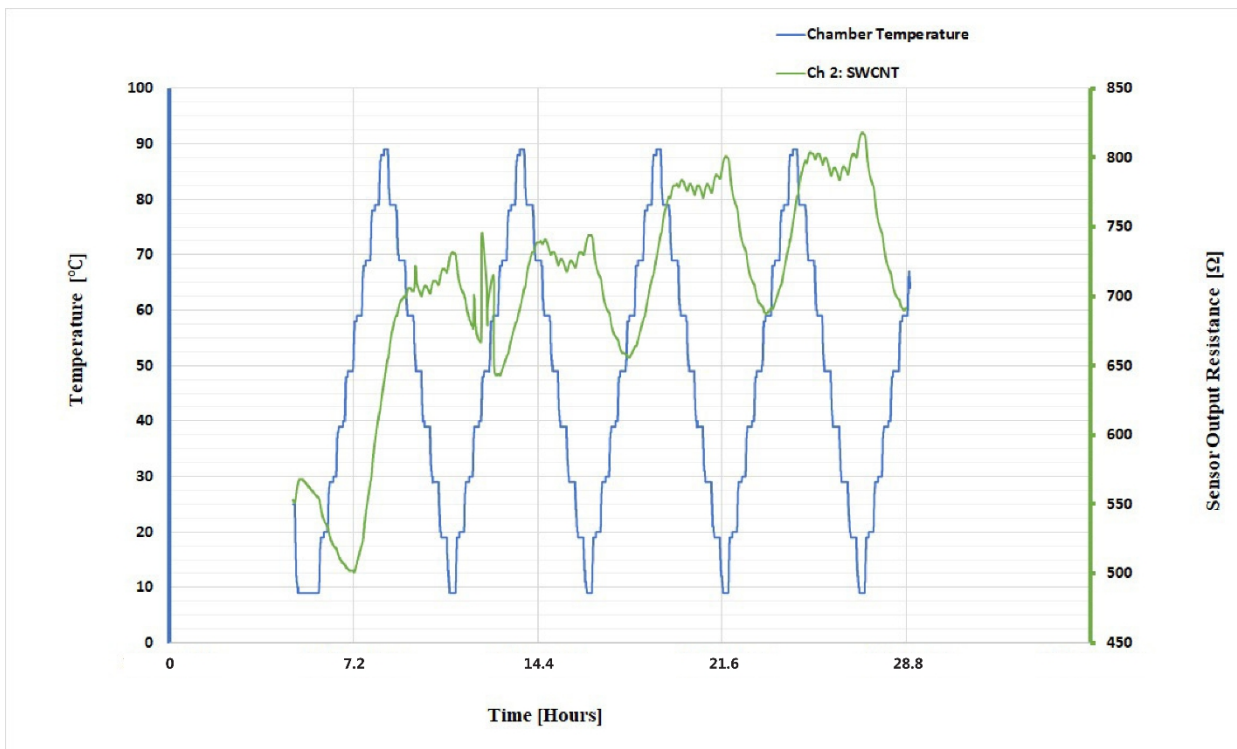
Figure 3.2 Schematic of measurement set-up: (1) Climatic chamber body, (2) Chamber area, (3) Digital analyser, (4) Computer, (5) Climatic chamber channels.

Results and Data Analysis

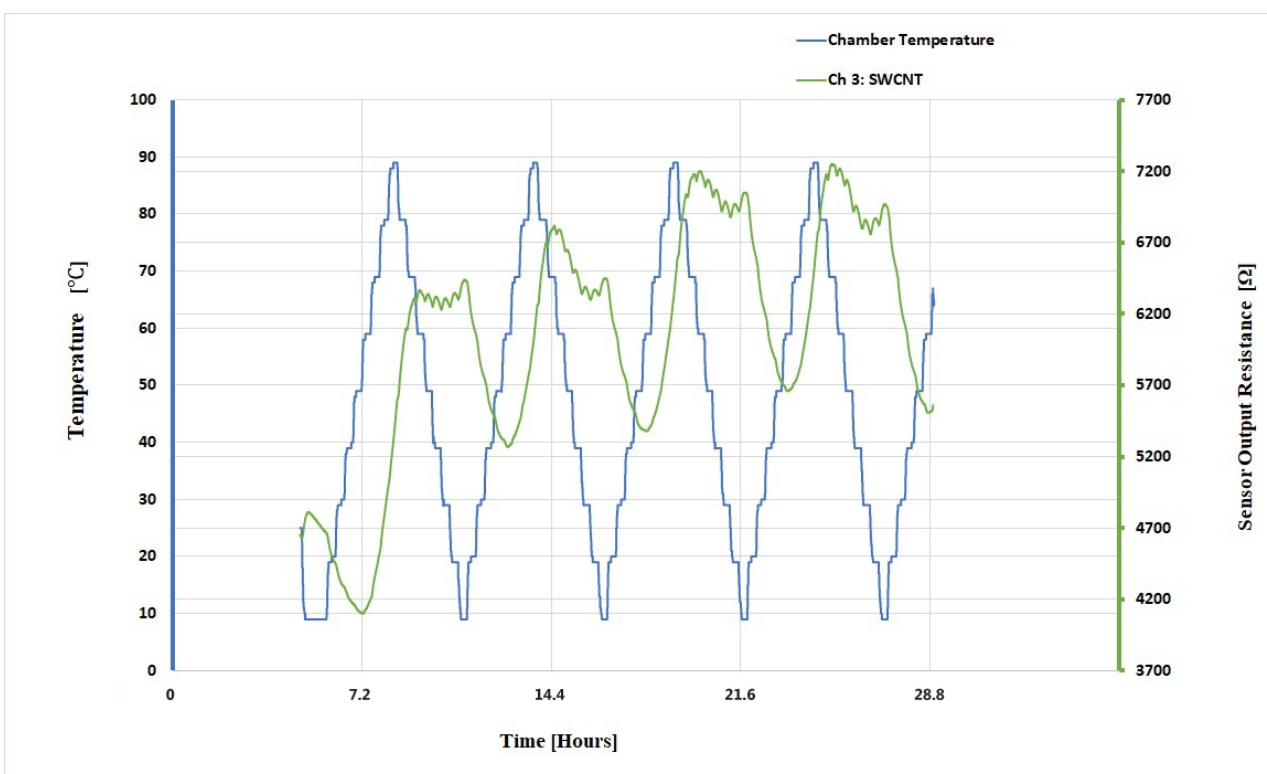
This section presents graphical results obtained from the laboratory exercise. The dual axis graphs display time on the common x-axis, climatic chamber temperature on the major y-axis and sensor resistance of the minor y-axis. Ten such graphs, for each of the ten channels, is given for the SWCNTs. A final graph is then shown to compare the effect of functionalization on responsivity of the samples. The same presentation is also given for all the ten MWCNTs samples as well.



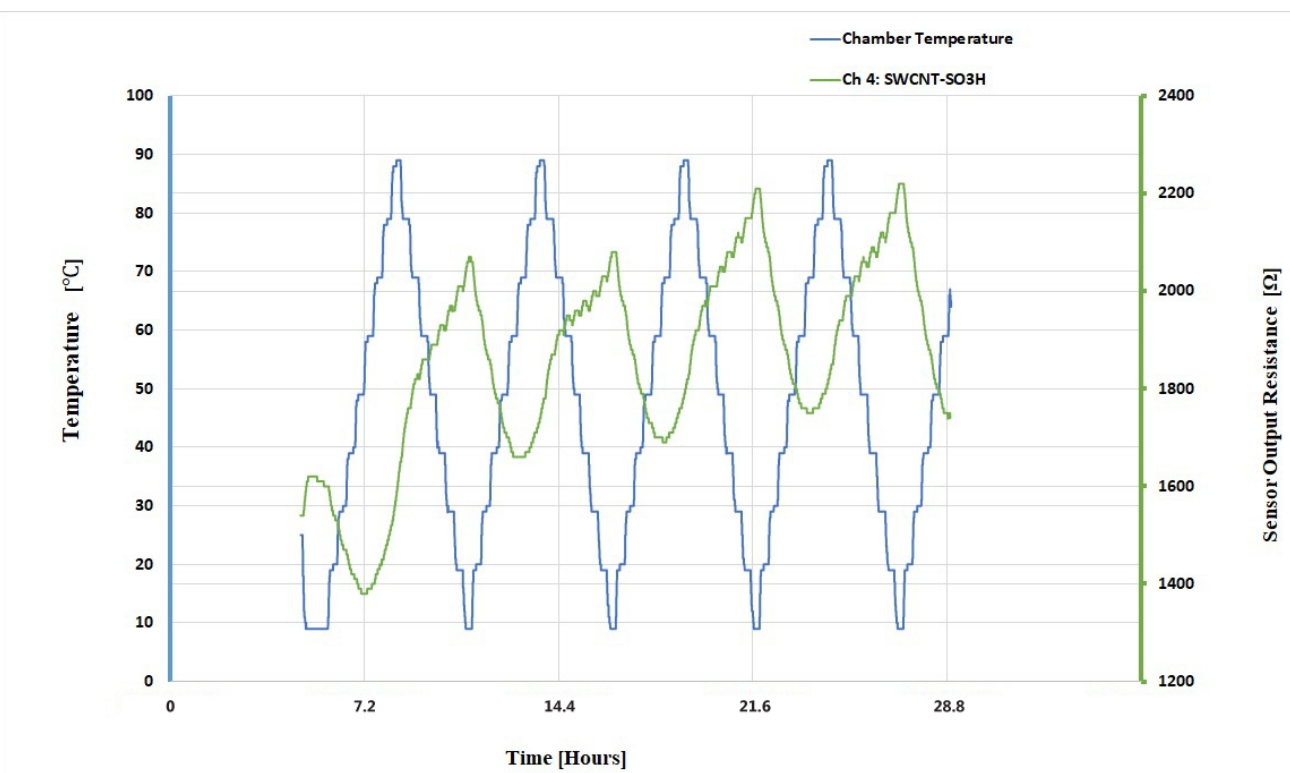
Graph 3.1. Ch 1: SWCNT resistive response to temperature.



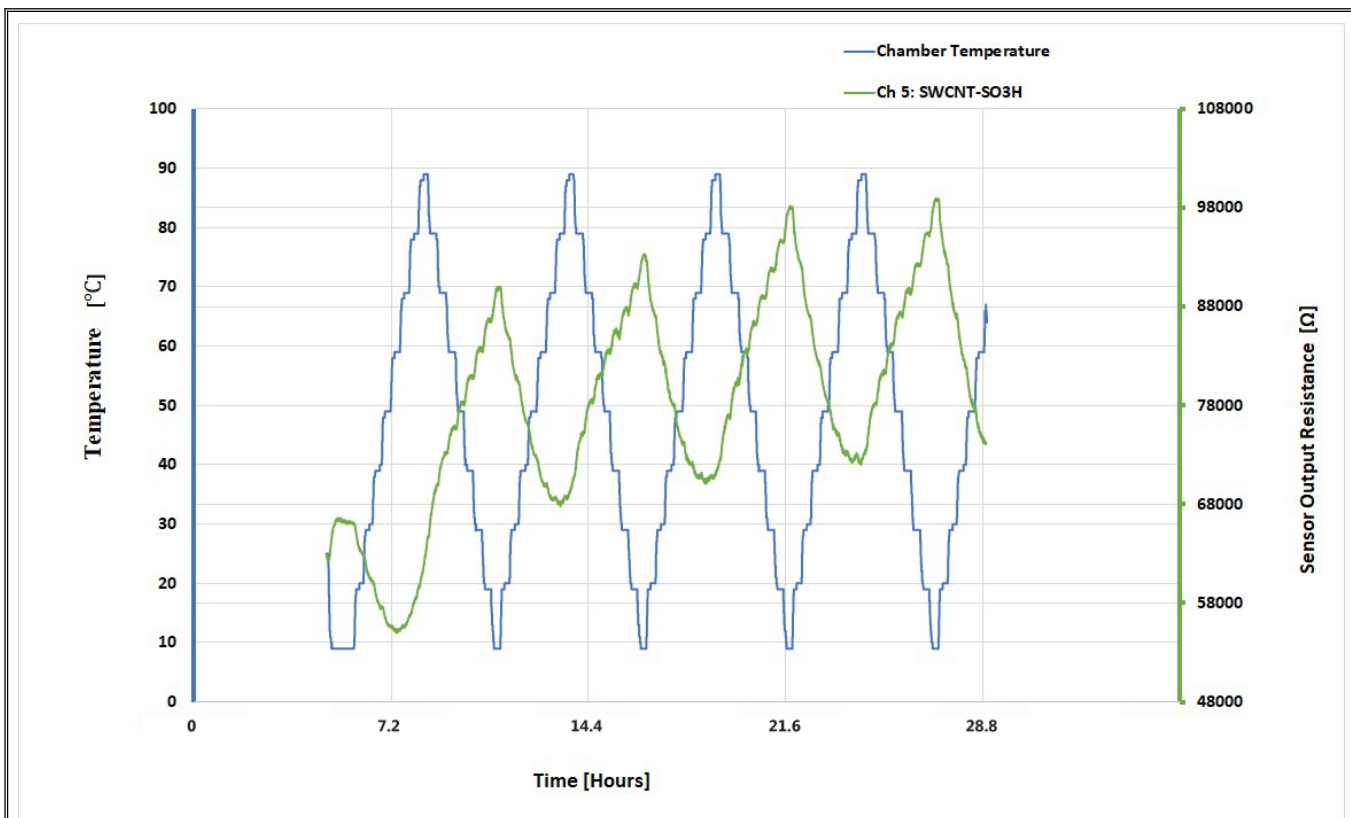
Graph 3.2.: SWCNT resistive response to temperature.



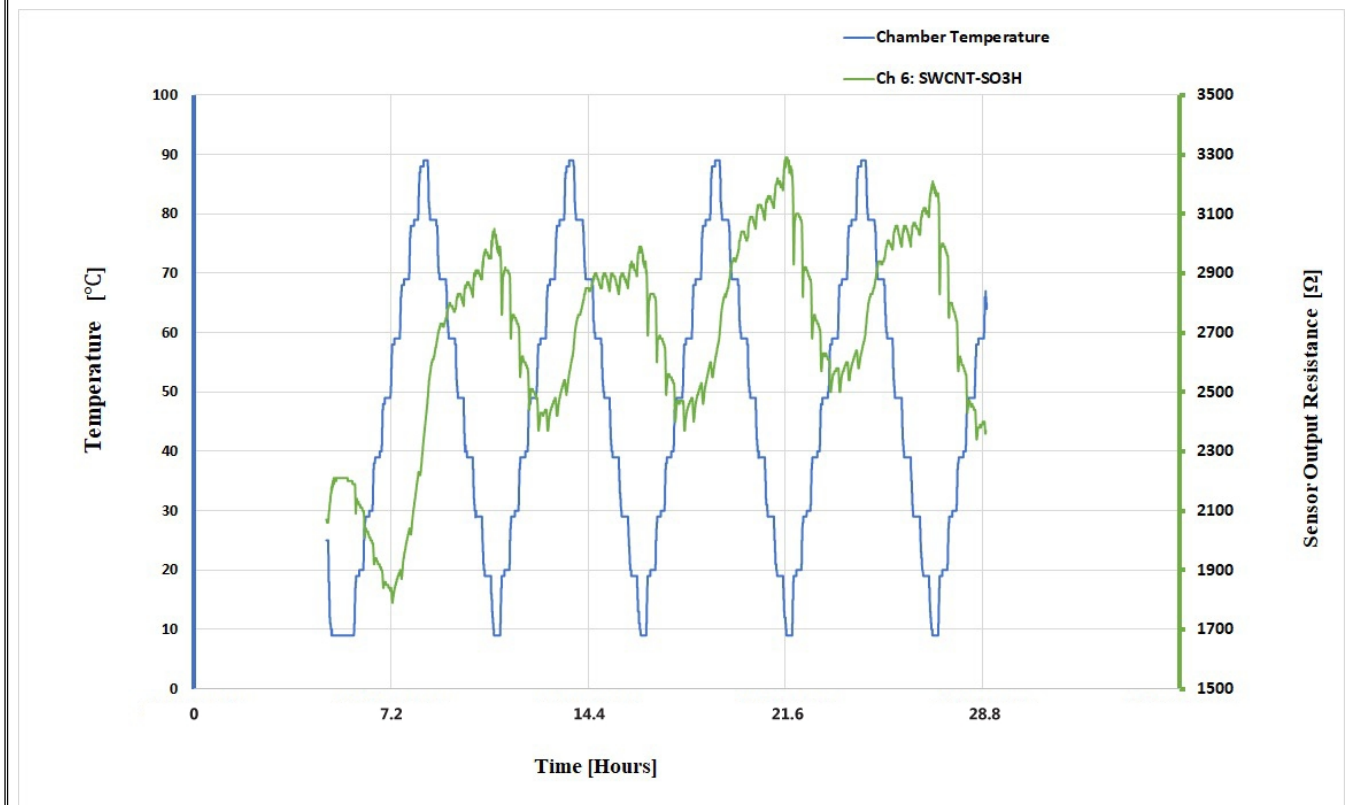
Graph 3.3.. Ch 3: SWCNT resistive response to temperature.



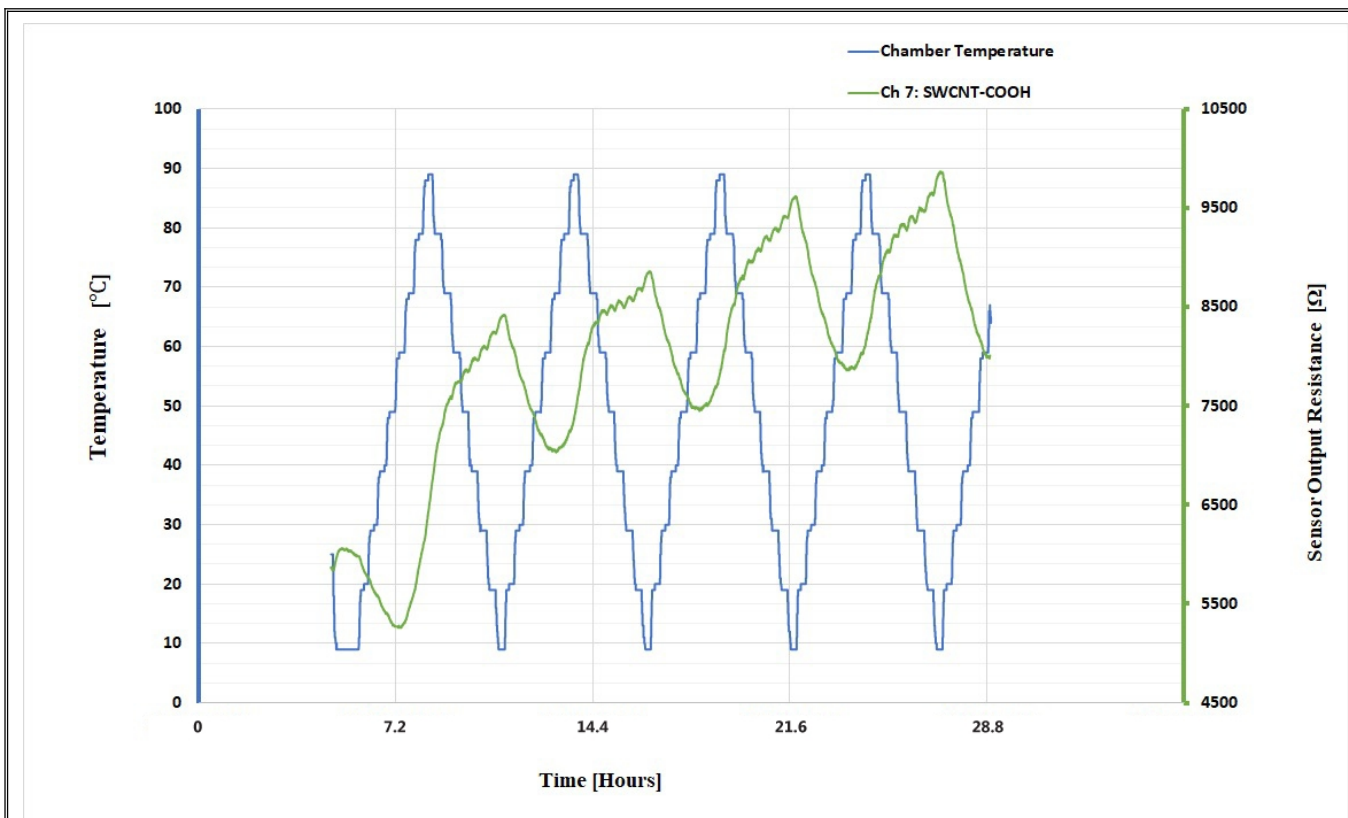
Graph 3.4. Ch 4: SWCNT-SO₃H resistive response to temperature.



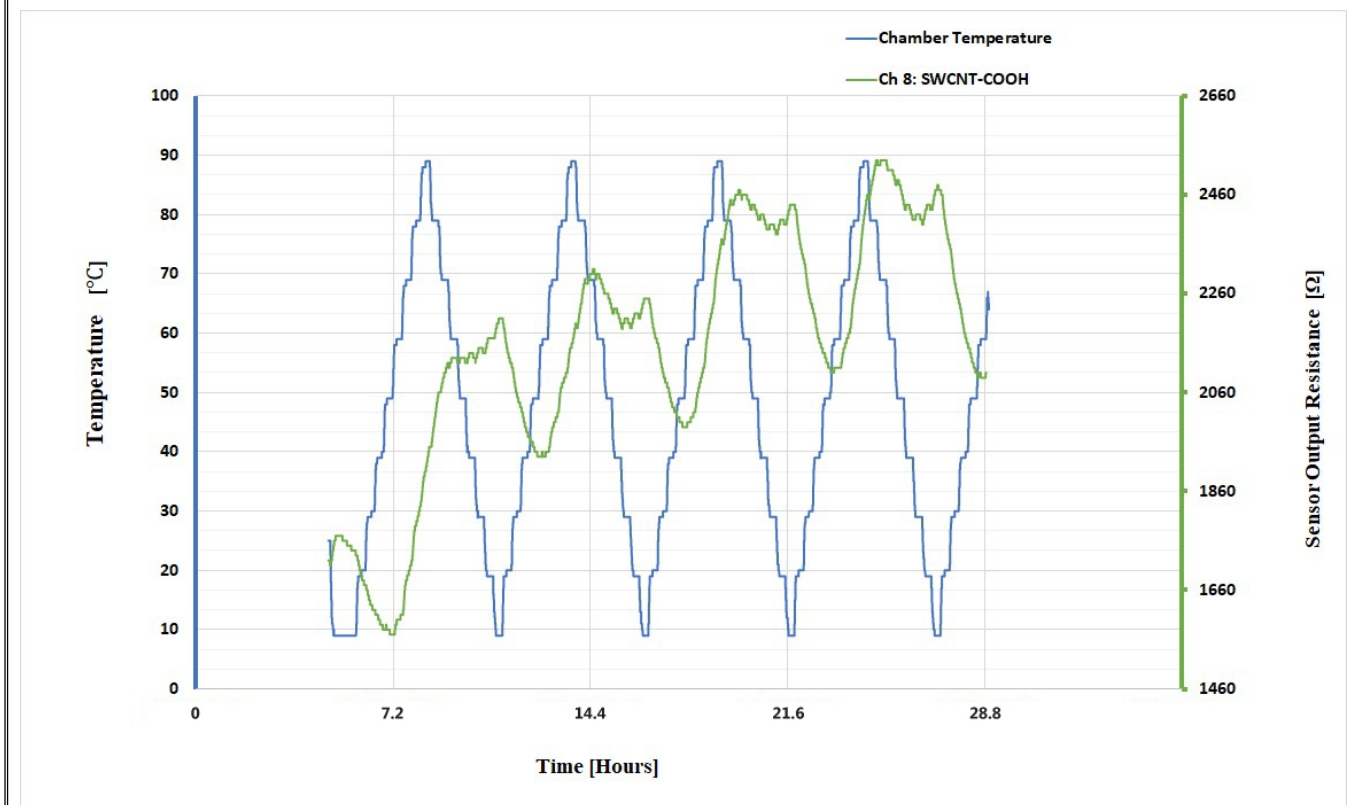
Graph 3.5. Ch 5: SWCNT-SO3H resistive response to temperature.



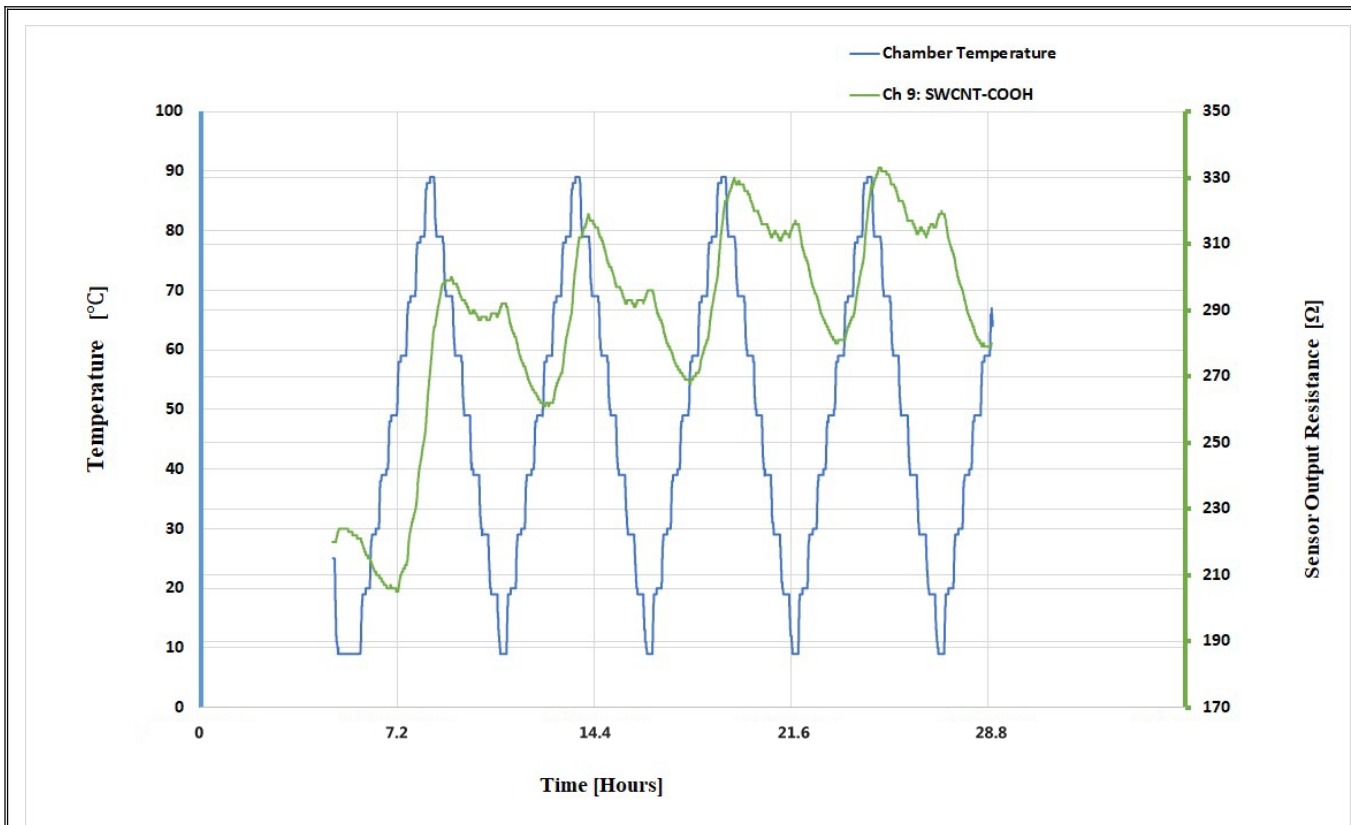
Graph 3.6. Ch 6: SWCNT-SO3H resistive response to temperature.



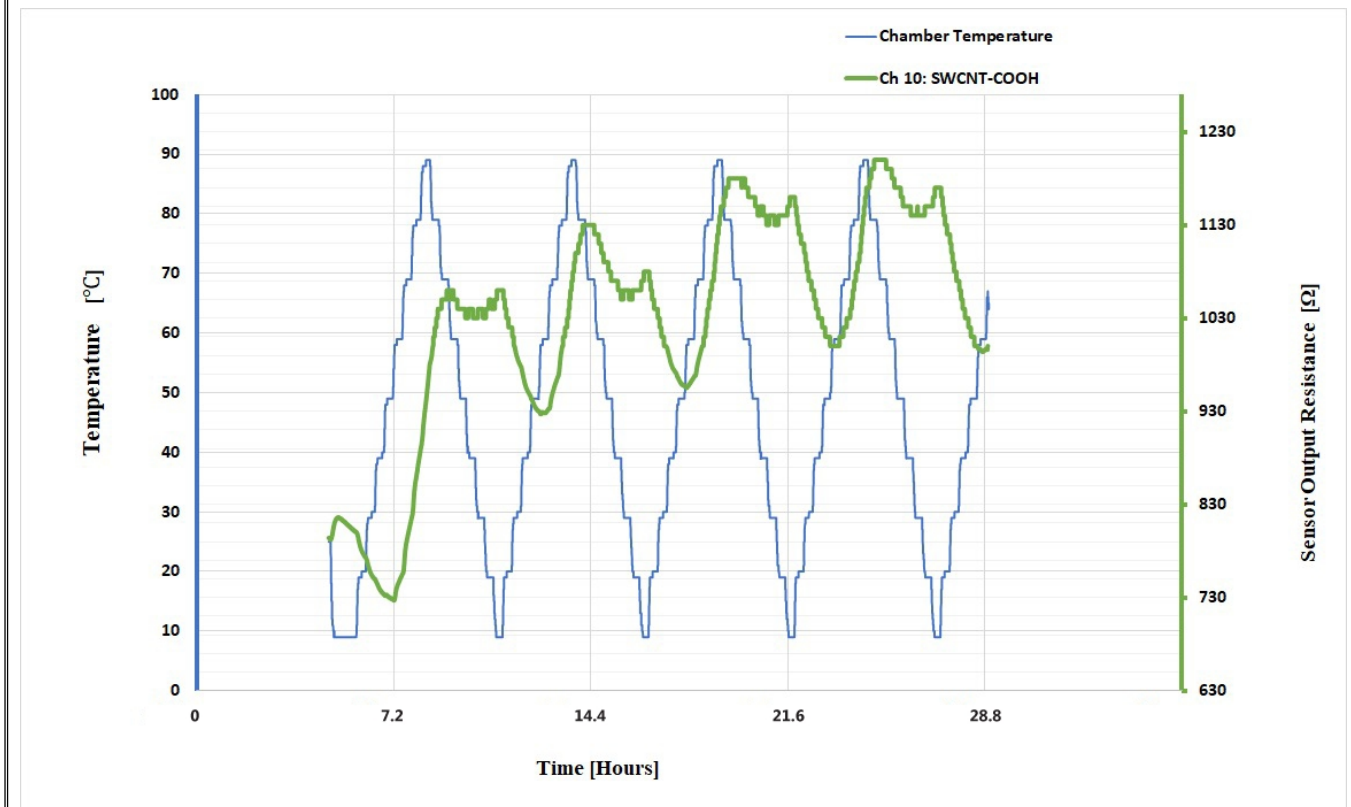
Graph 3.7. Ch 7: SWCNT-COOH resistive response to temperature.



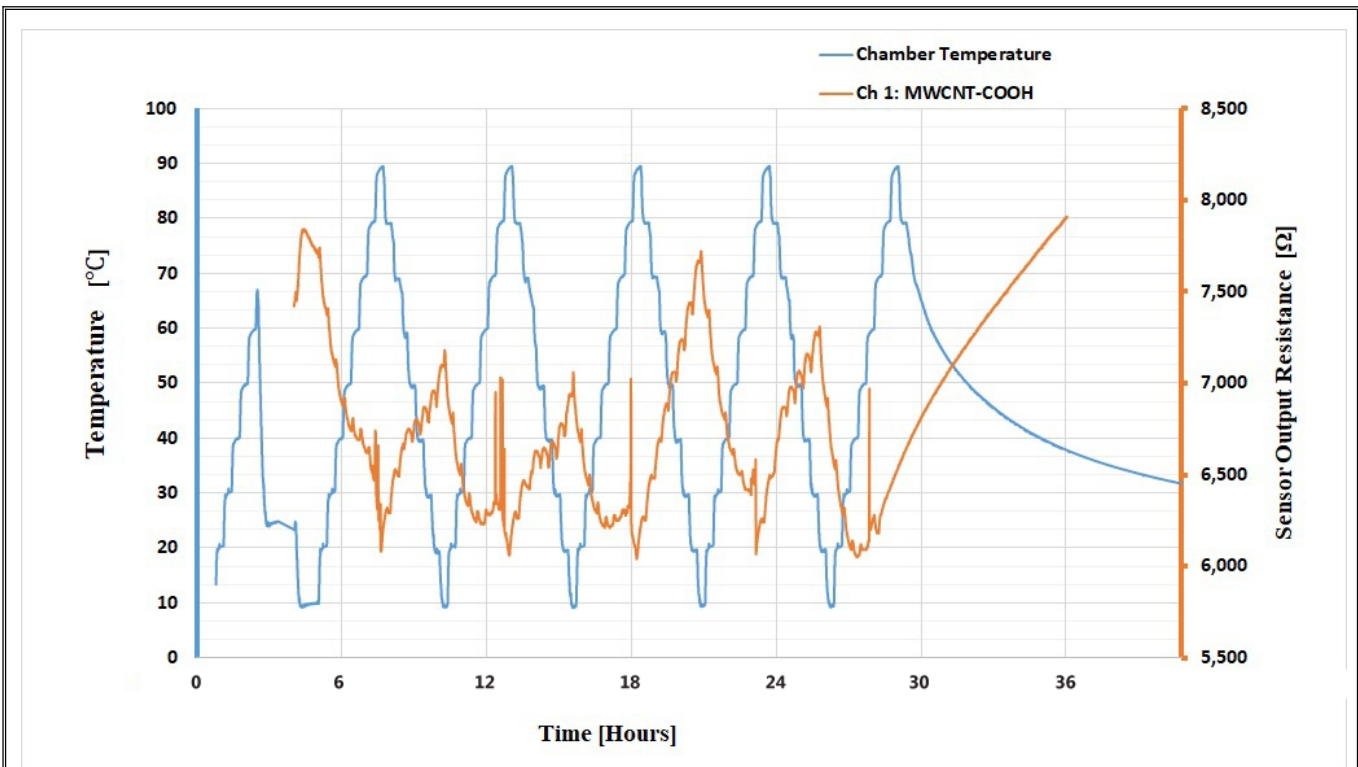
Graph 3.8. Ch 8: SWCNT-COOH resistive response to temperature.



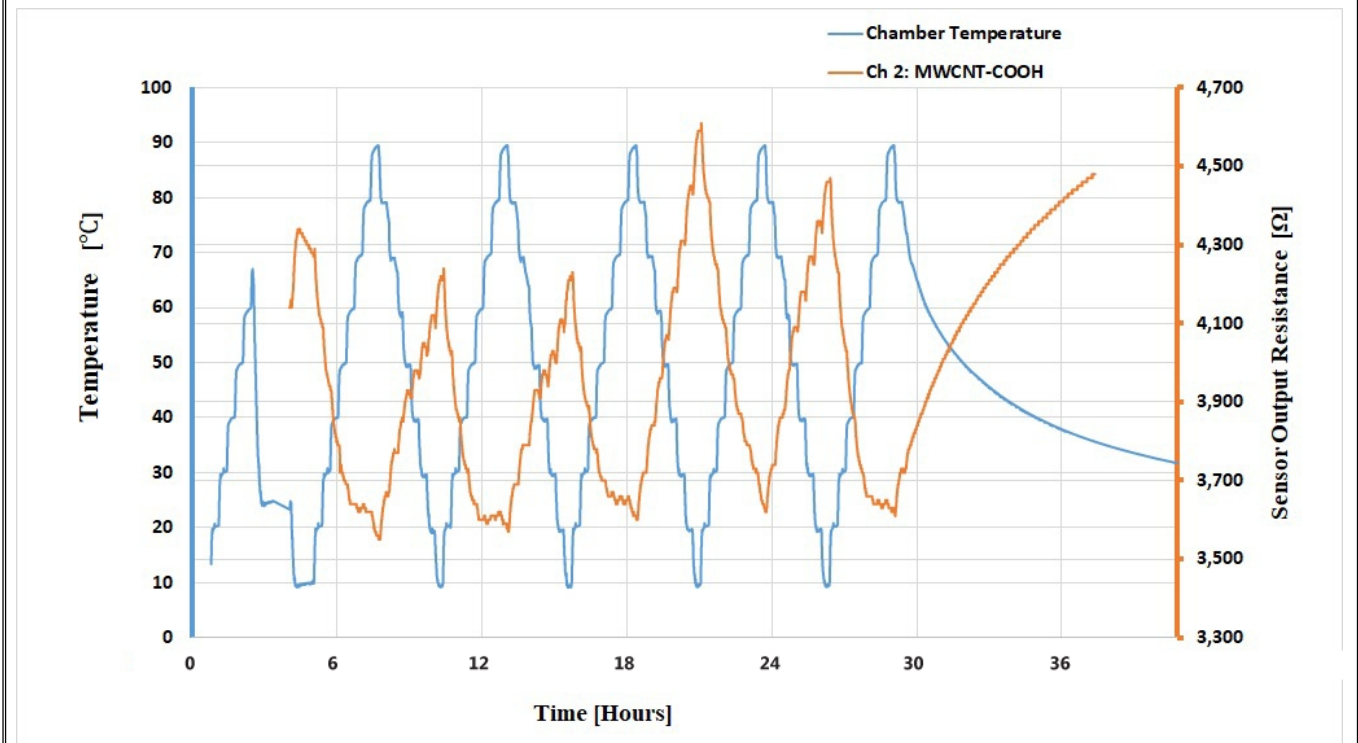
Graph 3.9. Ch: SWCNT-COOH resistive response to temperature.



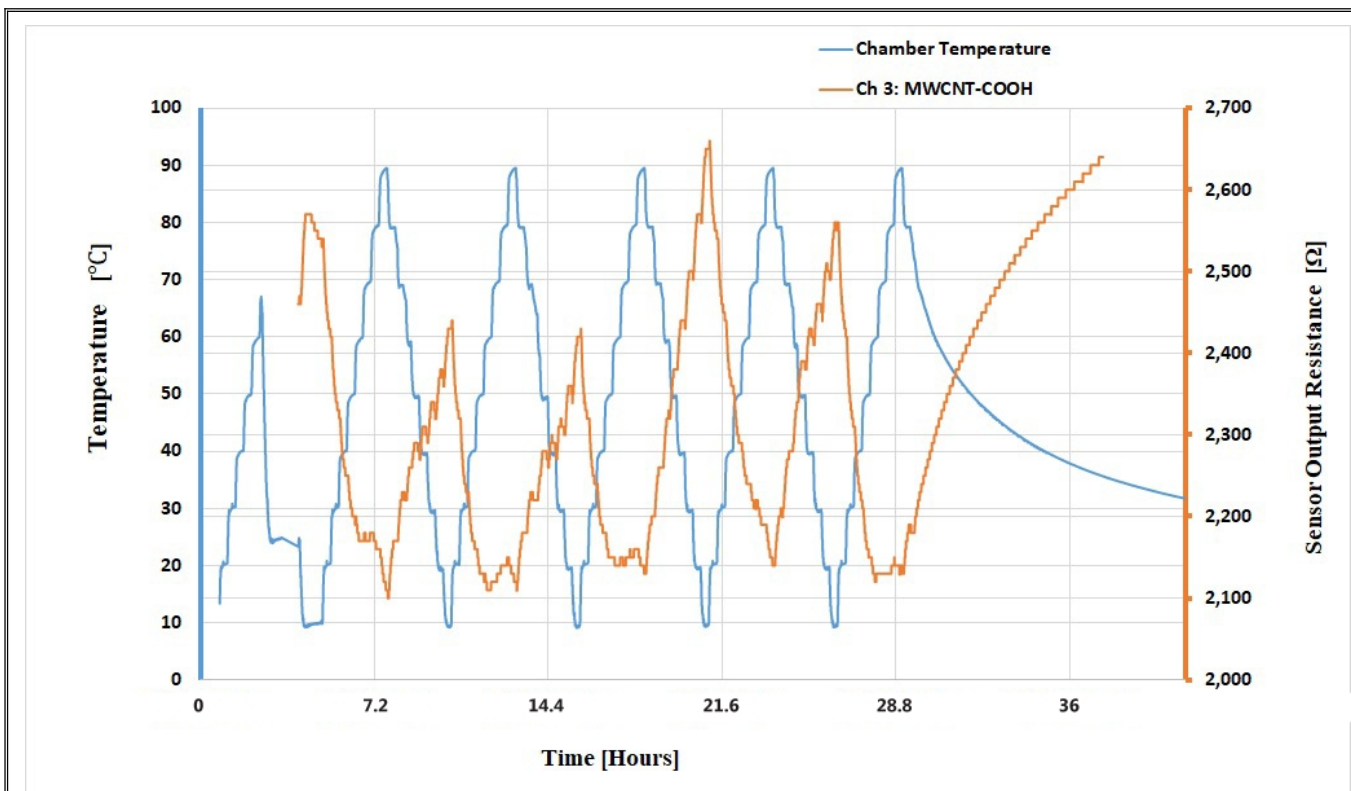
Graph 3.10. Ch 10: SWCNT-COOH resistive response to temperature.



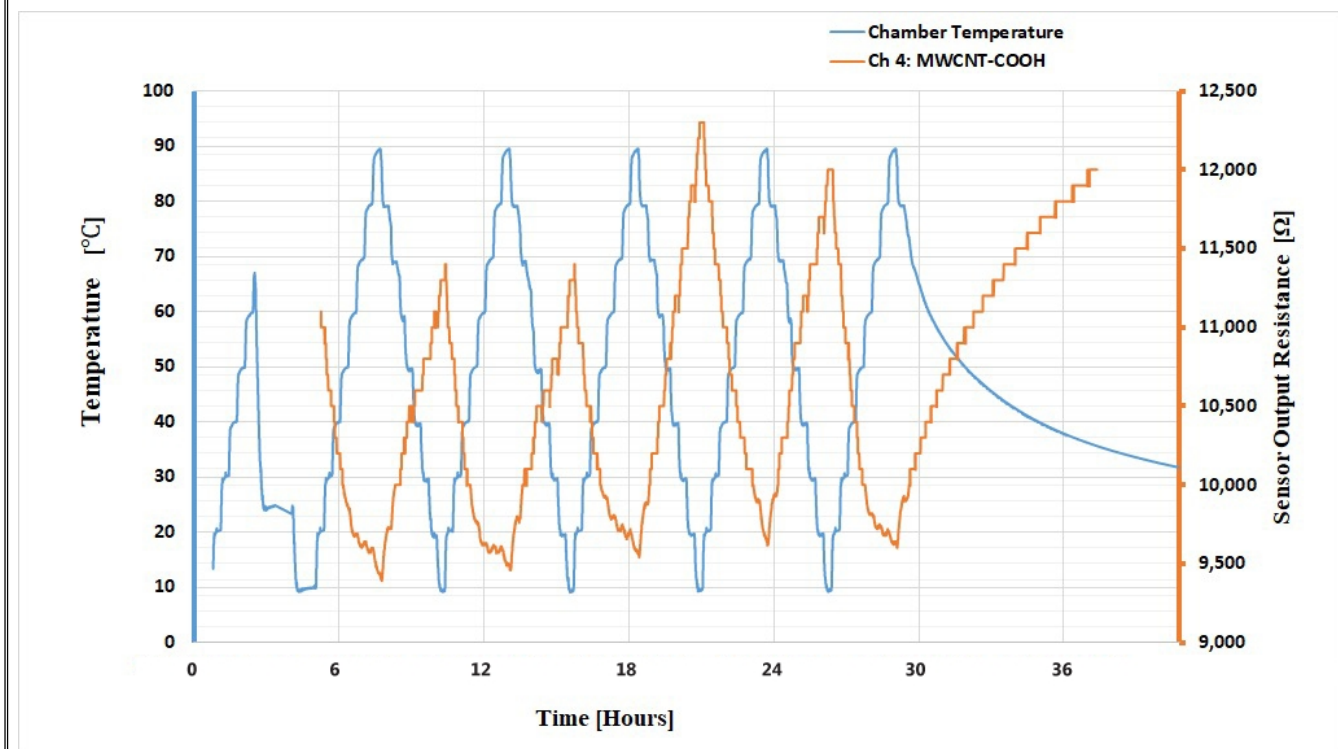
Graph 11. Ch 1: MWCNT-COOH resistive response to temperature.



Graph 12. Ch 2: MWCNT-COOH resistive response to temperature.



Graph 13 Ch 3: MWCNT-COOH resistive response to temperature.



Graph 14. Ch 4: MWCNT-COOH resistive response to temperature.

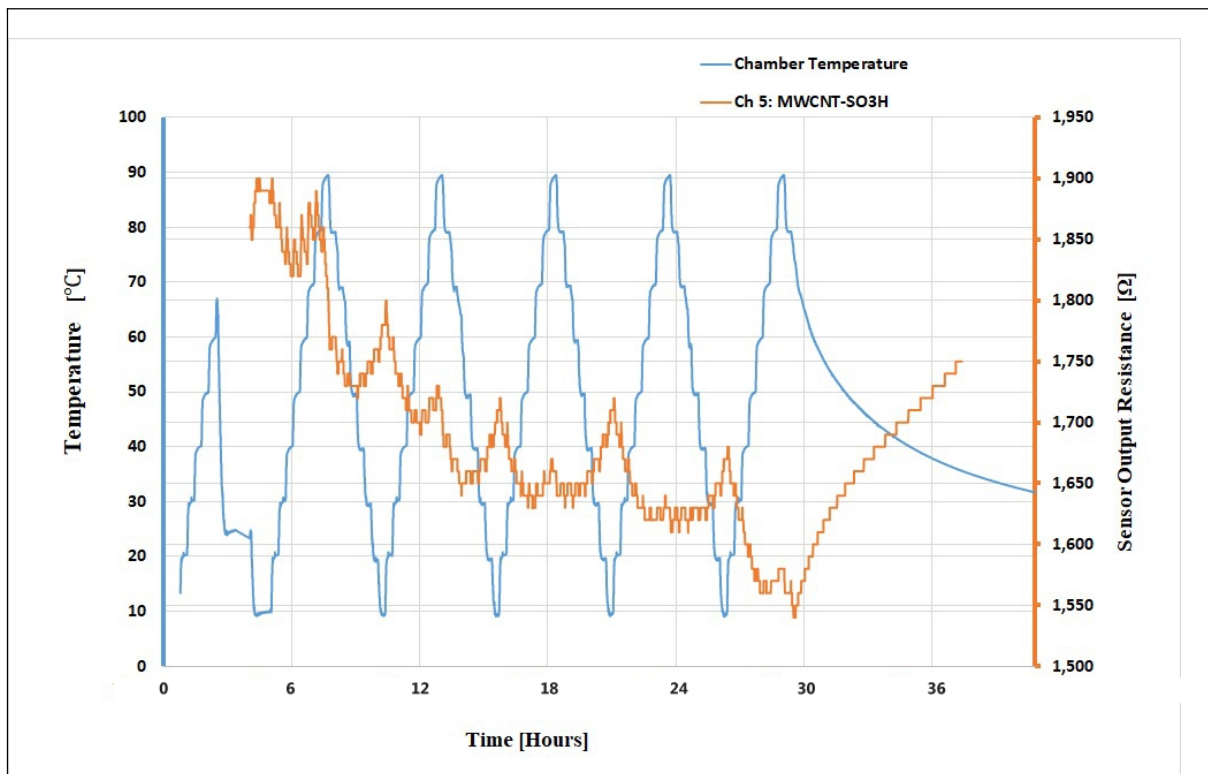
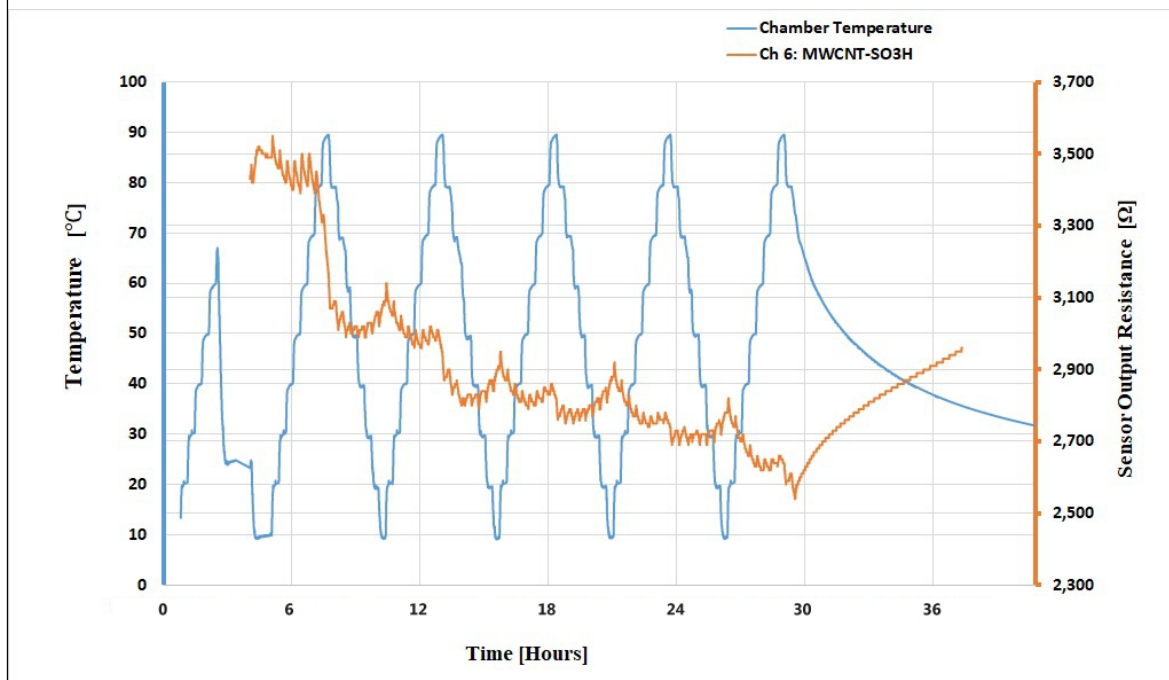
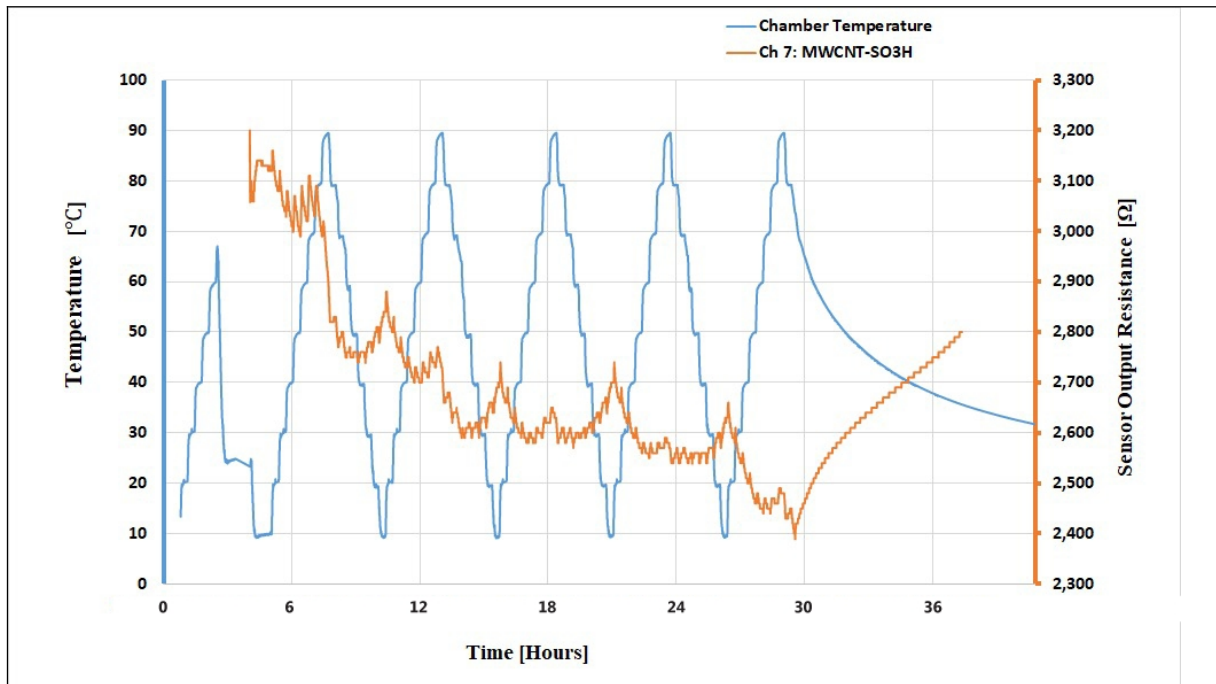


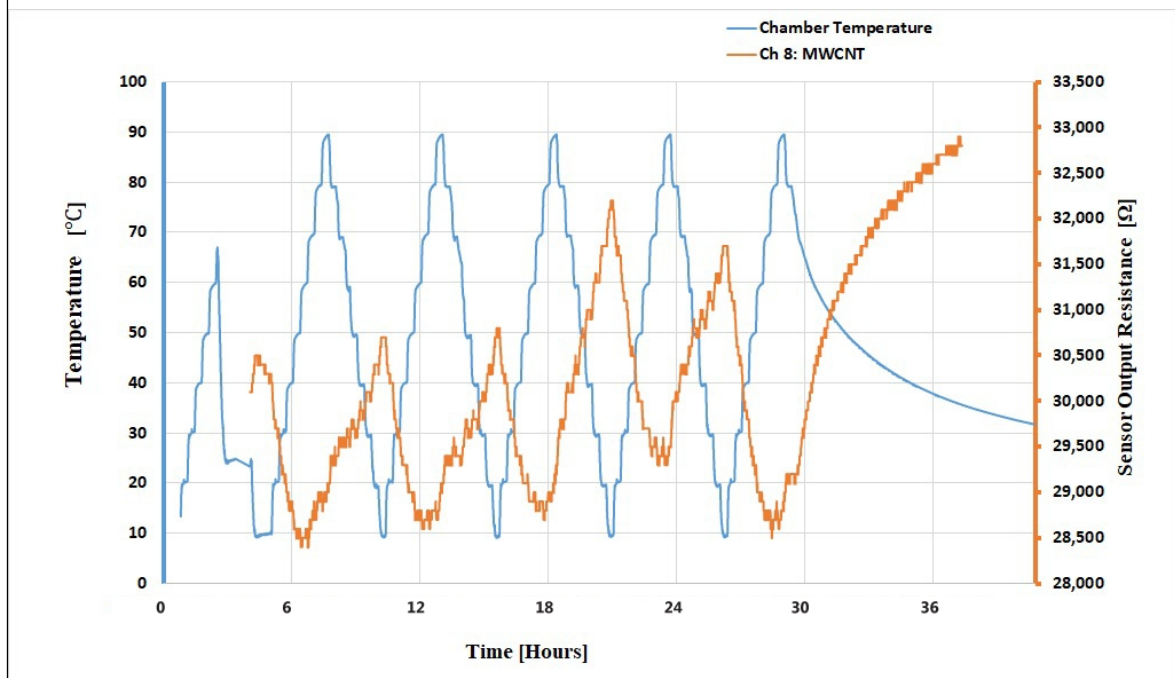
Figure Graph 15 Ch 5: MWCNT-SO3H resistive response to temperature.



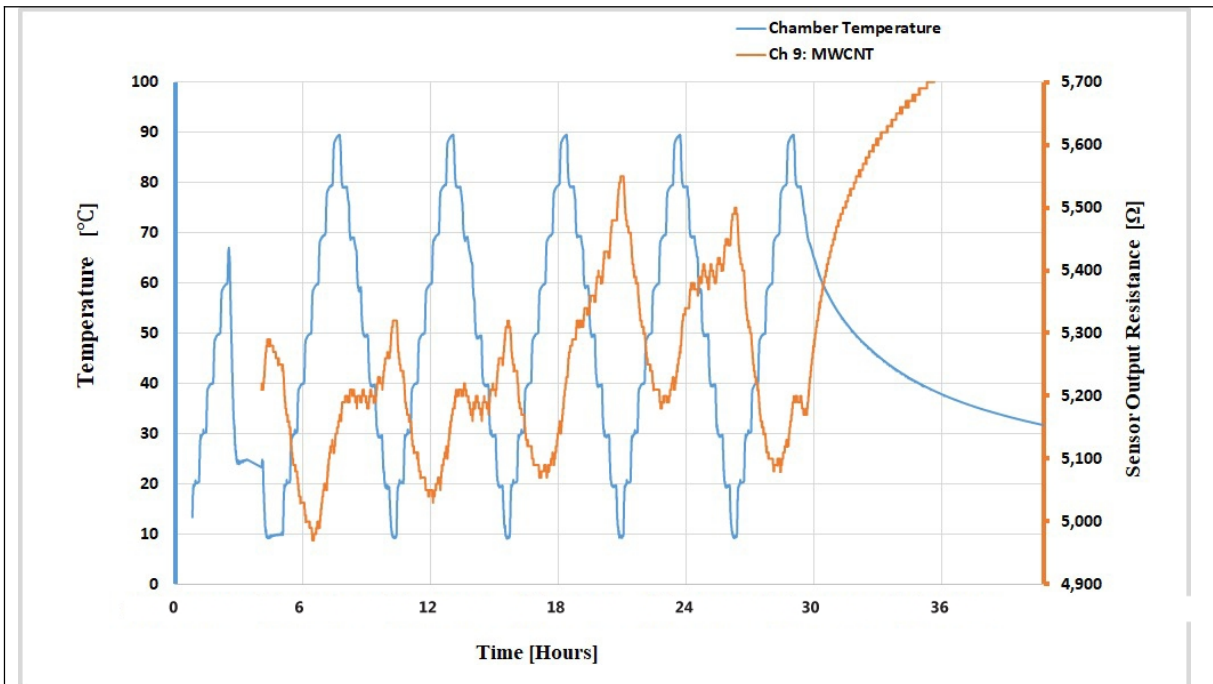
Graph 16. Ch 6: MWCNT-SO3H resistive response to temperature.



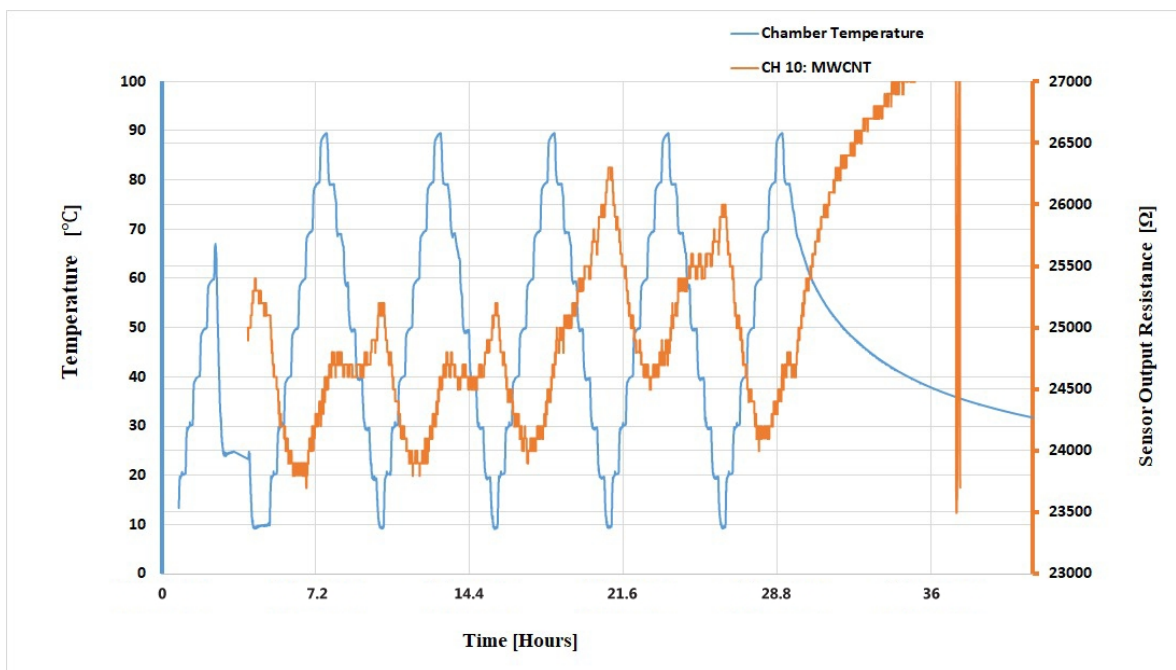
Graph 17 Ch 7: MWCNT-SO3H resistive response to temperature.



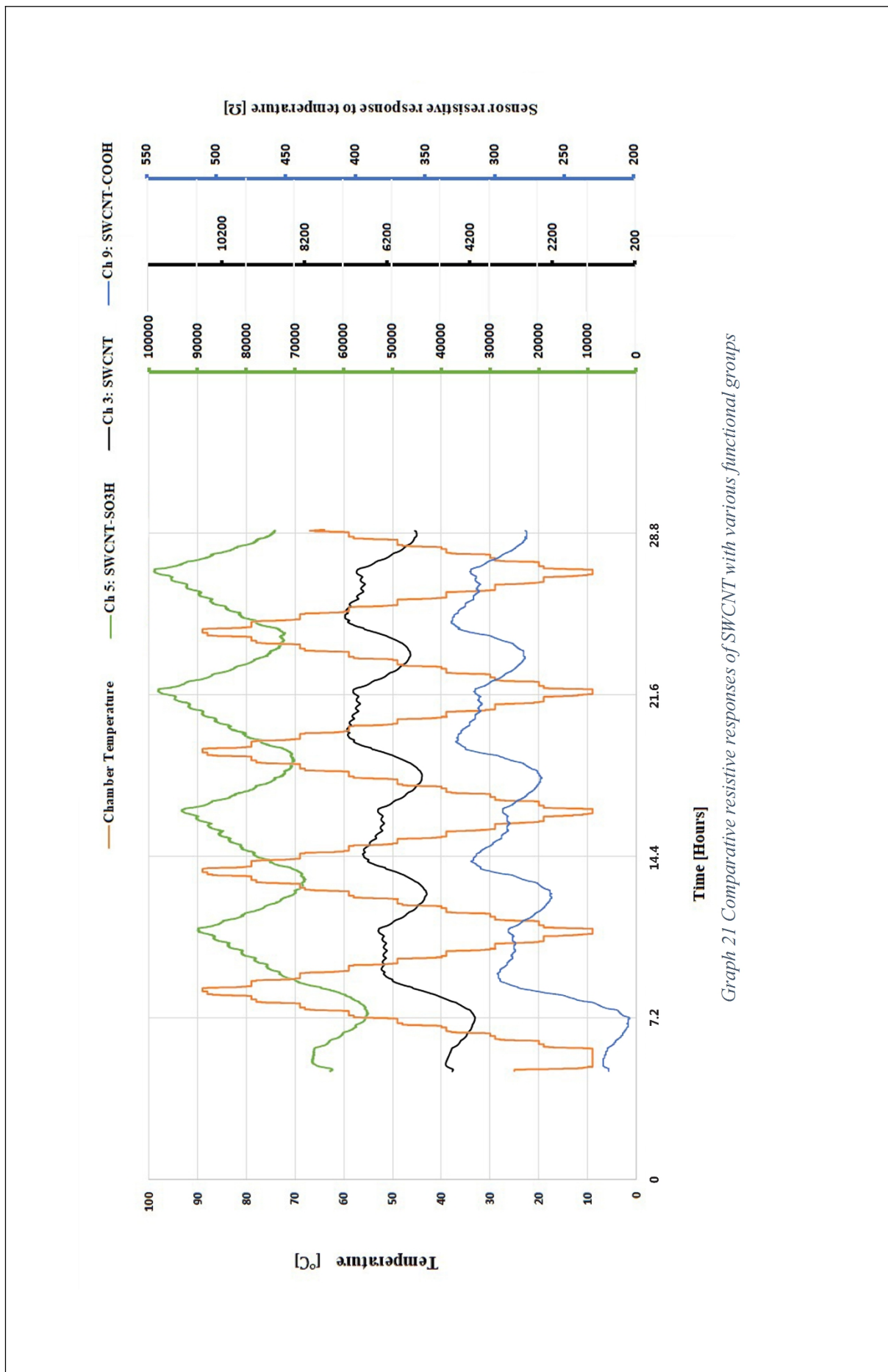
Graph 18. Ch 8: MWCNT resistive response to temperature.



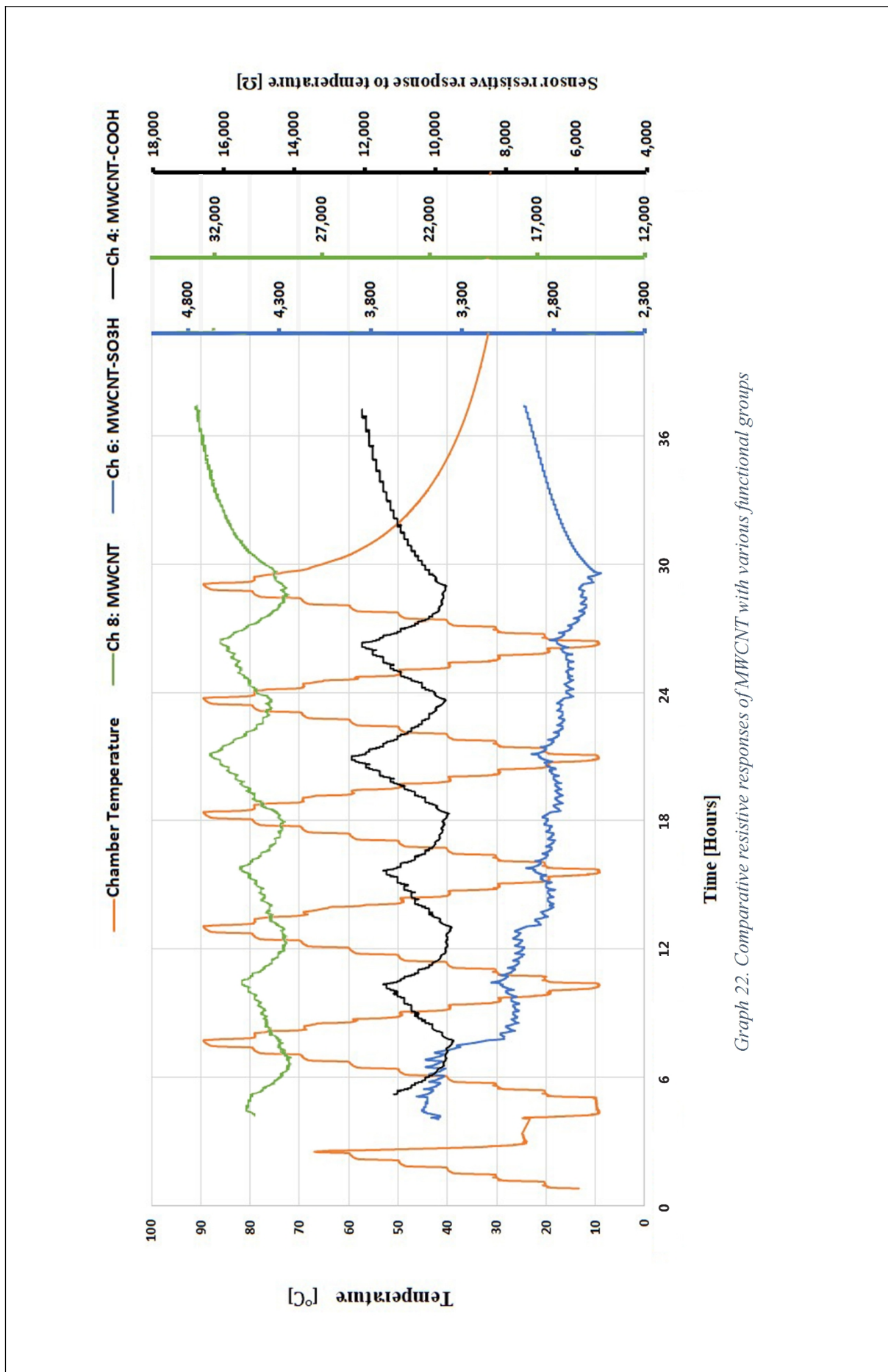
Graph 19. Ch 9: MWCNT resistive response to temperature.



Graph 20. Ch 10: MWCNT resistive response to temperature.



Graph 21 Comparative resistive responses of SWCNT with various functional groups



Graph 22. Comparative resistive responses of MWCNT with various functional groups

Data Analysis

From graphical data displayed, it is clear that CNTs generally exhibit a negative temperature coefficient (NTC).

Among the SWCNTs it was observed that for the same change in temperature, SWCNT-SO₃H showed the highest sensitivity followed by SWCNT and then SWCNT-COOH. At steady state, the approximate average electrical resistance of SWCNT-SO₃H was 80 k Ω , SWCNT 50 k Ω and SWCNT-COOH 290 Ω . A gradual rise in the steady state minimum values attained by all the three functionalization sample groups was observed to increase in value at all three local minimum points showing inconsistent repeatability temperature detection. This trend is observed to extend during all the climatic chamber cycles. All three functionalization, under the same climatic chamber conditions, are observed to attain steady state behavior at the same time and present patterns that vary in a similar manner (increase in local maximum a minimum value with time).

The functionalization of SWCNTs with -COOH lowers the temperature sensitivity of SWCNTs therefore making them suitable for use in applications such as gas sensors. Kim et al. [177] demonstrates how acid or base treated SWCNT-COOH can be modified to make highly sensitive carbon dioxide and ammonia sensors. The sensitivity displayed by SWCNT-SO₃H make it ideal for the construction of the detection of carbon monoxide gas sensors at ambient temperatures as is illustrated by Hannon et al [178].

Among the MWCNTs it was observed that under identical climatic chamber conditions, unfunctionalized MWCNT sensors showed the greatest responsivity and output range for a given temperature change. In this respect MWCNT-COOH had yet a higher responsivity than did MWCNT-SO₃H sensors. MWCNT and MWCNT-COOH showed more consistent repeatability than did MWCNT-SO₃H. MWCNT-SO₃H displayed every decreasing local maximum and minimum values with time. At steady state, the approximate average electrical resistance of MWCNT was 29 k Ω , MWCNT-COOH 11 k Ω and MWCNT-SO₃H 2.8 k Ω .

Compared to the unfunctionalized MWCNT, -COOH and -SO₃H functional groups improve the conductivity of the MWCNT as is seen in the combined MWCNT graph.

In comparison, it can be concluded from the graphs that when functionalized with -COOH and SO₃H functional groups, the electric properties of SWCNT and MWCNT are tuned differently with respect temperature. Studying these kinds of graphs may help with the evaluation of suitable CNM functionalization for a given application as per required temperature range of operation.

References

- [1] P. S. Karthik, A. L. Himaja, and S. P. Singh, "Carbon-allotropes: Synthesis methods, applications and future perspectives," *Carbon Letters*, vol. 15, no. 4. pp. 219–237, 2014, doi: 10.5714/CL.2014.15.4.219.
- [2] N. Malik, T. Arfin, and A. U. Khan, "Graphene nanomaterials: Chemistry and pharmaceutical perspectives," in *Nanomaterials for Drug Delivery and Therapy*, Elsevier, 2019, pp. 373–402.
- [3] U. Kamran, Y.-J. Heo, J. W. Lee, and S.-J. Park, "Functionalized carbon materials for electronic devices: A review," *Micromachines*, vol. 10, no. 4, 2019, doi: 10.3390/mi10040234.
- [4] S. Nasir, M. Z. M. Z. Hussein, Z. Zainal, and N. A. N. A. Yusof, "Carbon-based nanomaterials/allotropes: A glimpse of their synthesis, properties and some applications," *Materials (Basel)*., vol. 11, no. 2, p. 295, 2018, doi: 10.3390/ma11020295.
- [5] M. C. Roco, "Environmentally responsible development of nanotechnology," *Environ. Sci. Technol.*, vol. 39, no. 5, pp. 106A-112A, 2005, [Online]. Available: https://scholar.google.com/scholar?hl=en&as_sdt=2005&cites=8055011134892914671&scipsc=&q=Environmentally+responsible+development+of+nanotechnology+cite&btnG=.
- [6] L. Dai, "Chapter 1 - From conventional technology to carbon nanotechnology: The fourth industrial revolution and the discoveries of C60, carbon nanotube and nanodiamond," L. B. T.-C. N. Dai, Ed. Amsterdam: Elsevier, 2006, pp. 3–11.
- [7] S. H. Hajiabadi, H. Aghaei, M. Kalateh-Aghamohammadi, and M. Shorgasthi, "An overview on the significance of carbon-based nanomaterials in upstream oil and gas industry," *Journal of Petroleum Science and Engineering*, vol. 186. Elsevier B.V., p. 106783, Mar. 01, 2020, doi: 10.1016/j.petrol.2019.106783.

- [8] Y. Yang, X. Yang, Y. Yang, and Q. Yuan, "Aptamer-functionalized carbon nanomaterials electrochemical sensors for detecting cancer relevant biomolecules," *Carbon*, vol. 129. Elsevier Ltd, pp. 380–395, Apr. 01, 2018, doi: 10.1016/j.carbon.2017.12.013.
- [9] S. Hanna Varghese *et al.*, "Sensors based on carbon nanotubes and their applications: a review," *Curr. Nanosci.*, vol. 6, no. 4, pp. 331–346, 2010.
- [10] "Richard P. Feynman - Biographical." <https://www.nobelprize.org/prizes/physics/1965/feynman/biographical/> (accessed May 09, 2021).
- [11] J. E. Hulla, S. C. Sahu, and A. W. Hayes, "Nanotechnology: History and future," *Hum. Exp. Toxicol.*, vol. 34, no. 12, pp. 1318–1321, Nov. 2015, doi: 10.1177/0960327115603588.
- [12] H. W. Kroto, J. R. Heath, S. C. O'Brien, R. F. Curl, and R. E. Smalley, "C₆₀: Buckminsterfullerene," *Nature*, vol. 318, no. 6042, pp. 162–163, 1985, doi: 10.1038/318162a0.
- [13] S. Iijima, "Helical microtubules of graphitic carbon," *Nature*, vol. 354, no. 6348, pp. 56–58, 1991.
- [14] R. G. R. G. Mendes *et al.*, "Carbon nanostructures as a multi-functional platform for sensing applications," *Chemosensors*, vol. 6, no. 4, 2018, doi: 10.3390/chemosensors6040060.
- [15] V. D. N. Bezzon *et al.*, "Carbon Nanostructure-based Sensors: A Brief Review on Recent Advances," *Adv. Mater. Sci. Eng.*, vol. 2019, 2019, doi: 10.1155/2019/4293073.
- [16] C. C. Villarreal, T. Pham, P. Ramnani, and A. Mulchandani, "Carbon allotropes as sensors for environmental monitoring," *Current Opinion in Electrochemistry*, vol. 3, no. 1. Elsevier B.V., pp. 106–113, Jun. 01, 2017, doi: 10.1016/j.coelec.2017.07.004.

- [17] M. del P. L. López, J. L. V. Palomino, M. L. S. Silva, and A. R. Izquierdo, “Optimization of the Synthesis Procedures of Graphene and Graphite Oxide,” in *Recent Advances in Graphene Research*, InTech.
- [18] T. E. Saraswati, U. H. Setiawan, M. R. Ihsan, I. Isnaeni, and Y. Herbani, “The Study of the Optical Properties of C60 Fullerene in Different Organic Solvents,” *Open Chem.*, vol. 17, no. 1, pp. 1198–1212, 2019.
- [19] I. Lahiri, S. Das, C. Kang, and W. Choi, “Application of carbon nanostructures—Energy to electronics,” *JOM*, vol. 63, no. 6, pp. 70–76, 2011, doi: 10.1007/s11837-011-0095-1.
- [20] Z. Wang, S. Wu, J. Wang, A. Yu, and G. Wei, “Carbon nanofiber-based functional nanomaterials for sensor applications,” *Nanomaterials*, vol. 9, no. 7, p. 1045, 2019.
- [21] F. R. Baptista, S. A. Belhout, S. Giordani, and S. J. Quinn, “Recent developments in carbon nanomaterial sensors,” *Chem. Soc. Rev.*, vol. 44, no. 13, pp. 4433–4453, 2015.
- [22] D. Jariwala, V. K. Sangwan, L. J. Lauhon, T. J. Marks, and M. C. Hersam, “Carbon nanomaterials for electronics, optoelectronics, photovoltaics, and sensing,” *Chem. Soc. Rev.*, vol. 42, no. 7, pp. 2824–2860, 2013, doi: 10.1039/c2cs35335k.
- [23] N. P. Shetti, A. Mishra, S. Basu, and T. M. Aminabhavi, “Versatile fullerenes as sensor materials,” *Materials Today Chemistry*, vol. 20. Elsevier Ltd, p. 100454, Jun. 01, 2021, doi: 10.1016/j.mtchem.2021.100454.
- [24] Y. Gogotsi, *Nanomaterials Handbook*, 2nd ed. Boca Raton: CRC Press., 2017.
- [25] H. Ehtesabi, “Application of carbon nanomaterials in human virus detection,” *Journal of Science: Advanced Materials and Devices*, vol. 5, no. 4. Elsevier B.V., pp. 436–450, Dec. 01, 2020, doi: 10.1016/j.jsamd.2020.09.005.
- [26] K. K. Li, G. Y. Liu, L. S. Zheng, J. Jia, Y. Y. Zhu, and Y. T. Zhang, “Coal-derived

- carbon nanomaterials for sustainable energy storage applications,” *Xinxing Tan Cailiao/New Carbon Materials*, vol. 36, no. 1. Institute of Metal Research Chinese Academy of Sciences, pp. 133–154, Feb. 01, 2021, doi: 10.1016/S1872-5805(21)60010-0.
- [27] Z. Peng *et al.*, “Advances in the application, toxicity and degradation of carbon nanomaterials in environment: A review,” *Environment International*, vol. 134. Elsevier Ltd, p. 105298, Jan. 01, 2020, doi: 10.1016/j.envint.2019.105298.
- [28] P. R. Riley and R. J. Narayan, “Recent advances in carbon nanomaterials for biomedical applications: A review,” *Curr. Opin. Biomed. Eng.*, vol. 17, p. 100262, Jan. 2021, doi: 10.1016/j.cobme.2021.100262.
- [29] M. Kim, J. Jang, and C. Cha, “Carbon nanomaterials as versatile platforms for theranostic applications,” *Drug Discovery Today*, vol. 22, no. 9. Elsevier Ltd, pp. 1430–1437, Sep. 01, 2017, doi: 10.1016/j.drudis.2017.05.004.
- [30] Z. Yang, J. Tian, Z. Yin, C. Cui, W. Qian, and F. Wei, “Carbon nanotube- and graphene-based nanomaterials and applications in high-voltage supercapacitor: A review,” *Carbon*, vol. 141. Elsevier Ltd, pp. 467–480, Jan. 01, 2019, doi: 10.1016/j.carbon.2018.10.010.
- [31] R. K. Thines, N. M. Mubarak, S. Nizamuddin, J. N. Sahu, E. C. Abdullah, and P. Ganesan, “Application potential of carbon nanomaterials in water and wastewater treatment: A review,” *Journal of the Taiwan Institute of Chemical Engineers*, vol. 72. Taiwan Institute of Chemical Engineers, pp. 116–133, Mar. 01, 2017, doi: 10.1016/j.jtice.2017.01.018.
- [32] M. Giorcelli, P. Savi, and A. Tagliaferro, “Concept, methodologies and tools for carbon for sensing devices,” in *2018 IEEE 8th International Nanoelectronics Conferences (INEC)*, 2018, pp. 33–34, doi: 10.1109/INEC.2018.8441917.
- [33] R. T. Sataloff, M. M. Johns, and K. M. Kost, “Carbon Nanotechnology Recent Developments in Chemistry, Physics, Materials Science and Device Applications.”

- [34] E. H. L. Falcao and F. Wudl, "Carbon allotropes: beyond graphite and diamond," *J. Chem. Technol. Biotechnol. Int. Res. Process. Environ. Clean Technol.*, vol. 82, no. 6, pp. 524–531, 2007.
- [35] J. Sengupta, "Carbon nanotube fabrication at industrial scale: Opportunities and challenges," *Handb. Nanomater. Ind. Appl.*, pp. 172–194, 2018.
- [36] A. Hirsch, "The era of carbon allotropes," *Nat. Mater.*, vol. 9, no. 11, pp. 868–871, 2010.
- [37] A. Streitwieser, C. H. Heathcock, E. M. Kosower, and P. J. Corfield, *Introduction to organic chemistry*, no. 547 STR. Macmillan New York, 1992.
- [38] Y. Chen, Y. Xie, X. Yan, M. L. Cohen, and S. Zhang, "Topological carbon materials: A new perspective," *Physics Reports*, vol. 868. Elsevier B.V., pp. 1–32, Jul. 03, 2020, doi: 10.1016/j.physrep.2020.05.003.
- [39] E. A. Belenkov and V. A. Greshnyakov, "Classification schemes for carbon phases and nanostructures," *New Carbon Mater.*, vol. 28, no. 4, pp. 273–282, 2013, doi: [https://doi.org/10.1016/S1872-5805\(13\)60081-5](https://doi.org/10.1016/S1872-5805(13)60081-5).
- [40] D. Demarchi and A. Tagliaferro, *Carbon for sensing devices*. Springer International Publishing., 2015.
- [41] Q. Zhang, J. Huang, W. Qian, Y. Zhang, and F. Wei, "The road for nanomaterials industry: A review of carbon nanotube production, post-treatment, and bulk applications for composites and energy storage," *Small*, vol. 9, no. 8, pp. 1237–1265, 2013.
- [42] H. Hwang, J. Jeong, Y. Kim, and M. Chang, "Carbon Nanomaterials as Versatile Platforms for Biosensing Applications," *Micromachines*, vol. 11, p. 814, Aug. 2020, doi: 10.3390/mi11090814.
- [43] V. Georgakilas, J. Perman, J. Tucek, and R. Zboril, "Broad Family of Carbon

- Nanoallotropes: Classification, Chemistry, and Applications of Fullerenes, Carbon Dots, Nanotubes, Graphene, Nanodiamonds, and Combined Superstructures,” *Chem. Rev.*, vol. 115, May 2015, doi: 10.1021/cr500304f.
- [44] F. Xie, M. Yang, M. Jiang, X. J. Huang, W. Q. Liu, and P. H. Xie, “Carbon-based nanomaterials – A promising electrochemical sensor toward persistent toxic substance,” *TrAC - Trends Anal. Chem.*, vol. 119, p. 115624, 2019, doi: 10.1016/j.trac.2019.115624.
- [45] C. S. Jon, L. Y. Meng, and D. Li, “Recent review on carbon nanomaterials functionalized with ionic liquids in sample pretreatment application,” *TrAC - Trends in Analytical Chemistry*, vol. 120. Elsevier B.V., p. 115641, Nov. 01, 2019, doi: 10.1016/j.trac.2019.115641.
- [46] G. B. Kauffman, “Inorganic Chemistry, (Miessler, Gary L.; Tarr, Donald A.)” ACS Publications, 2000.
- [47] S. Tiwari, V. Kumar, A. Huczko, R. Oraon, A. De Adhikari, and G. Nayak, “Magical Allotropes of Carbon: Prospects and Applications,” *Crit. Rev. Solid State Mater. Sci.*, vol. 41, Nov. 2015, doi: 10.1080/10408436.2015.1127206.
- [48] E. Osawa, “Superaromaticity,” *Kagaku*, vol. 25, pp. 854–863, 1970.
- [49] S. Thakral and R. M. Mehta, “Fullerenes: An introduction and overview of their biological properties,” *Indian J. Pharm. Sci.*, vol. 68, no. 1, p. 13, 2006, doi: 10.1002/chin.200637226.
- [50] T. C. Dinadayalane and J. Leszczynski, “Fundamental structural, electronic, and chemical properties of carbon nanostructures: graphene, fullerenes, carbon nanotubes, and their derivatives,” *Handb. Comput. Chem.*, vol. 2, pp. 793–867, 2012.
- [51] A. A. Taherpour and F. Mousavi, “Carbon nanomaterials for electroanalysis in pharmaceutical applications,” in *Fullerenes, Graphenes and Nanotubes: A Pharmaceutical Approach*, Elsevier, 2018, pp. 169–225.

- [52] “Press release: The 1996 Nobel Prize in Chemistry.”
<https://www.nobelprize.org/prizes/chemistry/1996/press-release/> (accessed May 10, 2021).
- [53] M. Mojica, J. A. Alonso, and F. Méndez, “Synthesis of fullerenes,” *J. Phys. Org. Chem.*, vol. 26, no. 7, pp. 526–539, 2013.
- [54] H. Prinzbach *et al.*, “Gas-phase production and photoelectron spectroscopy of the smallest fullerene, C₂₀,” *Nature*, vol. 407, no. 6800, pp. 60–63, 2000.
- [55] R. Taylor, J. P. Hare, A. K. Abdul-Sada, and H. W. J. Kroto, “chem. Soc,” *Chem. Commun*, pp. 1423–1425, 1990.
- [56] M. Azizi-Lalabadi, H. Hashemi, J. Feng, and S. M. Jafari, “Carbon nanomaterials against pathogens; the antimicrobial activity of carbon nanotubes, graphene/graphene oxide, fullerenes, and their nanocomposites,” *Advances in Colloid and Interface Science*, vol. 284. Elsevier B.V., p. 102250, Oct. 01, 2020, doi: 10.1016/j.cis.2020.102250.
- [57] “Fullerene Hybridization Is More Complex Than You Think -MSTnano.com.”
<https://mstnano.com/fullerene-hybridization-is-more-complex-than-you-think/> (accessed Apr. 19, 2021).
- [58] M. A. Lebedeva, T. W. Chamberlain, and A. N. Khlobystov, “Harnessing the synergistic and complementary properties of fullerene and transition-metal compounds for nanomaterial applications,” *Chem. Rev.*, vol. 115, no. 20, pp. 11301–11351, 2015.
- [59] A. Masuhara, Z. Tan, H. Kasai, H. Nakanishi, and H. Oikawa, “Fullerene fine crystals with unique shapes and controlled size,” *Jpn. J. Appl. Phys.*, vol. 48, no. 5R, p. 50206, 2009.
- [60] C.-T. Hsieh *et al.*, “Post-assembly dimension-dependent face-selective etching of fullerene crystals,” *Mater. Horizons*, vol. 7, no. 3, pp. 787–795, 2020.

- [61] L. Becker, J. L. Bada, R. E. Winans, J. E. Hunt, T. E. Bunch, and B. M. French, "Fullerenes in the 1.85-billion-year-old Sudbury impact structure," *Science (80-.)*, vol. 265, no. 5172, pp. 642–645, 1994.
- [62] S. Pizzarello *et al.*, "The organic content of the Tagish Lake meteorite," *Science (80-.)*, vol. 293, no. 5538, pp. 2236–2239, 2001.
- [63] W. Zhenxia *et al.*, "Fullerenes in the fossil of dinosaur egg," *Fuller. Sci. Technol.*, vol. 6, no. 4, pp. 715–720, 1998.
- [64] D. Heymann, L. P. F. Chibante, R. R. Brooks, W. S. Wolbach, and R. E. Smalley, "Fullerenes in the Cretaceous-Tertiary boundary layer," *Science (80-.)*, vol. 265, no. 5172, pp. 645–647, 1994.
- [65] P. R. Buseck, S. J. Tsipursky, and R. Hettich, "Fullerenes from the geological environment," *Science (80-.)*, vol. 257, no. 5067, pp. 215–217, 1992.
- [66] P. R. Buseck, "Geological fullerenes: Review and analysis," *Earth Planet. Sci. Lett.*, vol. 203, no. 3–4, pp. 781–792, Nov. 2002, doi: 10.1016/S0012-821X(02)00819-1.
- [67] D. Felder-Flesch, "(Endo) Fullerenes: From Production to Isolation," in *Fullerenes*, 2011, pp. 3–11.
- [68] W. Krätschmer, L. D. Lamb, K. Fostiropoulos, and D. R. Huffman, "Solid C 60: a new form of carbon," *Nature*, vol. 347, no. 6291, pp. 354–358, 1990.
- [69] R. E. Haufler *et al.*, "Efficient production of C60 (buckminsterfullerene), C60H36, and the solvated buckide ion," *J. Phys. Chem.*, vol. 94, no. 24, pp. 8634–8636, Nov. 1990, doi: 10.1021/j100387a005.
- [70] A. Nimibofa, E. A. Newton, A. Y. Cyprain, and W. Donbebe, "Fullerenes: synthesis and applications," *J Mater Sci*, vol. 7, pp. 22–33, 2018.
- [71] G. N. Churilov, "Plasma synthesis of fullerenes," *Instruments Exp. Tech.*, vol. 43, no.

- 1, pp. 1–10, 2000.
- [72] R. E. Smalley, “Self-assembly of the fullerenes,” *Acc. Chem. Res.*, vol. 25, no. 3, pp. 98–105, 1992.
- [73] C. M. Lieber and C. C. Chen, “Preparation of Fullerenes and Fullerene-Based Materials,” *Solid State Phys. - Adv. Res. Appl.*, vol. 48, no. C, pp. 109–148, Jan. 1994, doi: 10.1016/S0081-1947(08)60578-0.
- [74] W. Krätschmer, “The story of making fullerenes,” *Nanoscale*, vol. 3, no. 6, pp. 2485–2489, 2011.
- [75] R. Kour, S. Arya, S.-J. Young, V. Gupta, P. Bandhoria, and A. Khosla, “Review—Recent Advances in Carbon Nanomaterials as Electrochemical Biosensors,” *J. Electrochem. Soc.*, vol. 167, no. 3, p. 37555, 2020, doi: 10.1149/1945-7111/ab6bc4.
- [76] S. Afreen, K. Muthoosamy, S. Manickam, and U. Hashim, “Functionalized fullerene (C₆₀) as a potential nanomediator in the fabrication of highly sensitive biosensors,” *Biosens. Bioelectron.*, vol. 63, pp. 354–364, 2015.
- [77] E. Castro, A. H. Garcia, G. Zavala, and L. Echegoyen, “Fullerenes in biology and medicine,” *J. Mater. Chem. B*, vol. 5, no. 32, pp. 6523–6535, 2017.
- [78] A. Mateo-Alonso, D. Bonifazi, and M. Prato, “Functionalization and applications of [60]fullerene,” in *Carbon Nanotechnology*, Elsevier, 2006, pp. 155–189.
- [79] M. Fouskaki and N. Chaniotakis, “Fullerene-based electrochemical buffer layer for ion-selective electrodes,” *Analyst*, vol. 133, no. 8, pp. 1072–1075, 2008.
- [80] W. Zhilei, L. Zaijun, S. Xiulan, F. Yinjun, and L. Junkang, “Synergistic contributions of fullerene, ferrocene, chitosan and ionic liquid towards improved performance for a glucose sensor,” *Biosens. Bioelectron.*, vol. 25, no. 6, pp. 1434–1438, 2010.

- [81] R. S. Ruoff and A. L. Ruoff, "The bulk modulus of C60 molecules and crystals: a molecular mechanics approach," *Appl. Phys. Lett.*, vol. 59, no. 13, pp. 1553–1555, 1991.
- [82] G. T. Hermanson, "Buckyballs, Fullerenes, and Carbon Nanotubes," in *Bioconjugate Techniques*, Elsevier, 2013, pp. 741–755.
- [83] N. Furuuchi, R. G. Shrestha, Y. Yamashita, T. Hirao, K. Ariga, and L. K. Shrestha, "Self-assembled fullerene crystals as excellent aromatic vapor sensors," *Sensors (Switzerland)*, vol. 19, no. 2, pp. 1–12, 2019, doi: 10.3390/s19020267.
- [84] A. Kausar, "Advances in Polymer/Fullerene Nanocomposite: A Review on Essential Features and Applications," *Polym. - Plast. Technol. Eng.*, vol. 56, no. 6, pp. 594–605, 2017, doi: 10.1080/03602559.2016.1233278.
- [85] A. E. M. A. Mohamed and M. A. Mohamed, "Carbon nanotubes: Synthesis, characterization, and applications," in *Carbon Nanomaterials for Agri-food and Environmental Applications*, Elsevier, 2019, pp. 21–32.
- [86] S. Iijima and T. Ichihashi, "Single-shell carbon nanotubes of 1-nm diameter," *Nature*, vol. 363, no. 6430, pp. 603–605, 1993.
- [87] S. H. K. S. H. K. Yap, K. K. K. K. Chan, S. C. S. C. Tjin, and K. T. K.-T. Yong, "Carbon allotrope-based optical fibers for environmental and biological sensing: A review," *Sensors (Switzerland)*, vol. 20, no. 7, 2020, doi: 10.3390/s20072046.
- [88] M. J. Yee *et al.*, "Carbon nanomaterials based films for strain sensing application—A review," *Nano-Structures and Nano-Objects*, vol. 18. Elsevier B.V., p. 100312, Apr. 01, 2019, doi: 10.1016/j.nanoso.2019.100312.
- [89] W. Q. Neves *et al.*, "Effects of pressure on the structural and electronic properties of linear carbon chains encapsulated in double wall carbon nanotubes," *Carbon N. Y.*, vol. 133, pp. 446–456, Jul. 2018, doi: 10.1016/j.carbon.2018.01.084.

- [90] S. Kruss, A. J. Hilmer, J. Zhang, N. F. Reuel, B. Mu, and M. S. Strano, "Carbon nanotubes as optical biomedical sensors," *Advanced Drug Delivery Reviews*, vol. 65, no. 15. Elsevier, pp. 1933–1950, Dec. 01, 2013, doi: 10.1016/j.addr.2013.07.015.
- [91] B. Peng *et al.*, "Measurements of near-ultimate strength for multiwalled carbon nanotubes and irradiation-induced crosslinking improvements," *Nat. Nanotechnol.*, vol. 3, no. 10, pp. 626–631, 2008.
- [92] B. Abdallah, A. M. A. Elhissi, W. Ahmed, and M. Najlah, "Carbon nanotubes drug delivery system for cancer treatment," in *Advances in Medical and Surgical Engineering*, Elsevier, 2020, pp. 313–332.
- [93] Q. Zhao, Z. Gan, and Q. Zhuang, "Electrochemical sensors based on carbon nanotubes," *Electroanal. An Int. J. Devoted to Fundam. Pract. Asp. Electroanal.*, vol. 14, no. 23, pp. 1609–1613, 2002.
- [94] J. J. Davis, R. J. Coles, and H. A. O. Hill, "Protein electrochemistry at carbon nanotube electrodes," *J. Electroanal. Chem.*, vol. 440, no. 1–2, 1997.
- [95] E. K. Wujcik and C. N. Monty, "Nanotechnology for implantable sensors: carbon nanotubes and graphene in medicine," *Wiley Interdiscip. Rev. Nanomedicine Nanobiotechnology*, vol. 5, no. 3, pp. 233–249, 2013.
- [96] H. Kim *et al.*, "Tensile properties of millimeter-long multi-walled carbon nanotubes," *Sci. Rep.*, vol. 7, no. 1, pp. 1–7, 2017.
- [97] X. L. Xie, Y. W. Mai, and X. P. Zhou, "Dispersion and alignment of carbon nanotubes in polymer matrix: A review," *Materials Science and Engineering R: Reports*, vol. 49, no. 4. Elsevier Ltd, pp. 89–112, May 19, 2005, doi: 10.1016/j.mser.2005.04.002.
- [98] E. Joselevich, H. Dai, J. Liu, K. Hata, and A. H. Windle, "Carbon nanotube synthesis and organization," *Carbon Nanotub.*, pp. 101–165, 2007.

- [99] J. An, Z. Zhan, and L. Zheng, “Controllable Synthesis of Carbon Nanotubes,” in *Industrial Applications of Carbon Nanotubes*, Elsevier Inc., 2017, pp. 1–45.
- [100] J. T. W. Yeow and N. Sinha, “Carbon nanotube and fullerene sensors,” in *Sensors Based on Nanostructured Materials*, Springer, 2009, pp. 11–28.
- [101] N. Rajesh Jesudoss Hynes *et al.*, “Synthesis, properties, and characterization of carbon nanotube-reinforced metal matrix composites,” in *Nanocarbon and its Composites: Preparation, Properties and Applications*, Elsevier, 2018, pp. 805–830.
- [102] T. W. Ebbesen and P. M. Ajayan, “Large-scale synthesis of carbon nanotubes,” *Nature*, vol. 358, no. 6383, pp. 220–222, 1992.
- [103] D. S. Bethune *et al.*, “Cobalt-catalysed growth of carbon nanotubes with single-atomic-layer walls,” *Nature*, vol. 363, no. 6430, pp. 605–607, 1993.
- [104] C. E. Baddour and C. Briens, “Carbon nanotube synthesis: a review,” *Int. J. Chem. React. Eng.*, vol. 3, no. 1, 2005.
- [105] M. Ishigami, J. Cumings, A. Zettl, and S. Chen, “A simple method for the continuous production of carbon nanotubes,” *Chem. Phys. Lett.*, vol. 319, no. 5–6, pp. 457–459, Mar. 2000, doi: 10.1016/S0009-2614(00)00151-2.
- [106] T. Guo, P. Nikolaev, A. Thess, D. T. Colbert, and R. E. Smalley, “Catalytic growth of single-walled nanotubes by laser vaporization,” *Chem. Phys. Lett.*, vol. 243, no. 1–2, pp. 49–54, Sep. 1995, doi: 10.1016/0009-2614(95)00825-O.
- [107] H. Dai, J. H. Hafner, A. G. Rinzler, D. T. Colbert, and R. E. Smalley, “Nanotubes as nanoprobe in scanning probe microscopy,” *Nature*, vol. 384, no. 6605, pp. 147–150, 1996.
- [108] V. Choudhary, B. P. Singh, and R. B. Mathur, “Carbon nanotubes and their composites,” *Synth. Appl. carbon Nanotub. their Compos.*, no. 9, pp. 193–222, 2013.

- [109] M. Jahanshahi and A. D. Kiadehi, "Fabrication, purification and characterization of carbon nanotubes: Arc-discharge in liquid media (ADLM)," *Synth. Appl. Carbon Nanotub. Their Compos.*, pp. 55–76, 2013.
- [110] W. E. Sawyer and A. Man, "US Pat. 229335 (June 29, 1880) on pyrolytic carbon," *Aylsworth, JW, US Pat*, vol. 553296.
- [111] R. Haubner, "The history of hard CVD coatings for tool applications at the University of Technology Vienna," *Int. J. Refract. Met. Hard Mater.*, vol. 41, pp. 22–34, 2013.
- [112] M. José-Yacamán, M. Miki-Yoshida, L. Rendon, and J. G. Santiesteban, "Catalytic growth of carbon microtubules with fullerene structure," *Appl. Phys. Lett.*, vol. 62, no. 6, pp. 657–659, 1993.
- [113] S. Zhang, Z. Li, C. Yang, Y. Xu, and J. Zhou, "Application of image stitching method in corrosion morphology analysis," *J. Electron. Imaging*, vol. 28, no. 1, p. 13045, 2019.
- [114] M. Patila, N. Chalmpes, E. Dounousi, H. Stamatis, and D. Gournis, "Use of functionalized carbon nanotubes for the development of robust nanobiocatalysts," in *Methods in Enzymology*, vol. 630, Academic Press Inc., 2020, pp. 263–301.
- [115] T. R. Shojaei and S. Azhari, "Fabrication, functionalization, and dispersion of carbon nanotubes," in *Emerging Applications of Nanoparticles and Architectural Nanostructures: Current Prospects and Future Trends*, Elsevier Inc., 2018, pp. 501–531.
- [116] V. Biju, "Chemical modifications and bioconjugate reactions of nanomaterials for sensing, imaging, drug delivery and therapy," *Chem. Soc. Rev.*, vol. 43, no. 3, pp. 744–764, 2014.
- [117] S. Beg *et al.*, "Emergence in the functionalized carbon nanotubes as smart nanocarriers for drug delivery applications," in *Fullerenes, Graphenes and*

- Nanotubes: A Pharmaceutical Approach*, Elsevier, 2018, pp. 105–133.
- [118] L. Fernández-García *et al.*, “Graphene anchored palladium complex as efficient and recyclable catalyst in the Heck cross-coupling reaction,” *J. Mol. Catal. A Chem.*, vol. 416, pp. 140–146, May 2016, doi: 10.1016/j.molcata.2016.02.023.
- [119] N. Maheshwari *et al.*, “Functionalized Carbon Nanotubes for Protein, Peptide, and Gene Delivery,” in *Biomaterials and Bionanotechnology*, Elsevier, 2019, pp. 613–637.
- [120] L. Bacakova *et al.*, “Applications of Nanocellulose/Nanocarbon Composites: Focus on Biotechnology and Medicine,” *NANOMATERIALS*, vol. 10, no. 2, 2020, doi: 10.3390/nano10020196.
- [121] M. Kaur, M. Kaur, and V. K. Sharma, “Nitrogen-doped graphene and graphene quantum dots: A review on synthesis and applications in energy, sensors and environment,” *Advances in Colloid and Interface Science*, vol. 259. Elsevier B.V., pp. 44–64, Sep. 01, 2018, doi: 10.1016/j.cis.2018.07.001.
- [122] K. S. Novoselov *et al.*, “Electric field effect in atomically thin carbon films,” *Science (80-.)*, vol. 306, no. 5696, pp. 666–669, 2004.
- [123] X. Jin *et al.*, “Review on exploration of graphene in the design and engineering of smart sensors, actuators and soft robotics,” *Chem. Eng. J. Adv.*, vol. 4, p. 100034, Dec. 2020, doi: 10.1016/j.ceja.2020.100034.
- [124] E. Gerstner, “Nobel prize 2010: Andre geim & konstantin novoselov,” *Nat. Phys.*, vol. 6, no. 11, p. 836, 2010.
- [125] P. R. Wallace, “The band theory of graphite,” *Phys. Rev.*, vol. 71, no. 9, p. 622, 1947.
- [126] A. K. Geim, “Graphene prehistory,” *Phys. Scr.*, vol. T146, p. 14003, 2012, doi: 10.1088/0031-8949/2012/t146/014003.

- [127] H. P. Boehm, R. Setton, and E. Stumpp, “Nomenclature and terminology of graphite intercalation compounds (IUPAC Recommendations 1994),” *Pure Appl. Chem.*, vol. 66, no. 9, pp. 1893–1901, 1994.
- [128] Q. Li, X. Li, S. Wageh, A. A. Al-Ghamdi, and J. Yu, “CdS/graphene nanocomposite photocatalysts,” *Adv. Energy Mater.*, vol. 5, no. 14, p. 1500010, 2015.
- [129] Y. Zhu *et al.*, “Graphene and graphene oxide: synthesis, properties, and applications,” *Adv. Mater.*, vol. 22, no. 35, pp. 3906–3924, 2010.
- [130] A. Iwan and A. Chuchmała, “Perspectives of applied graphene: Polymer solar cells,” *Progress in Polymer Science*, vol. 37, no. 12. Pergamon, pp. 1805–1828, Dec. 01, 2012, doi: 10.1016/j.progpolymsci.2012.08.001.
- [131] J. Liu, L. Cui, and D. Losic, “Graphene and graphene oxide as new nanocarriers for drug delivery applications,” *Acta Biomater.*, vol. 9, no. 12, pp. 9243–9257, 2013.
- [132] Q. He, S. Wu, Z. Yin, and H. Zhang, “Graphene-based electronic sensors,” *Chem. Sci.*, vol. 3, no. 6, pp. 1764–1772, 2012.
- [133] N. F. Atta, A. Galal, and E. H. El-Ads, “Graphene—a platform for sensor and biosensor applications,” *Biosensors-Micro Nanoscale Appl.*, vol. 9, pp. 38–84, 2015.
- [134] D. G. Papageorgiou, I. A. Kinloch, and R. J. Young, “Mechanical properties of graphene and graphene-based nanocomposites,” *Progress in Materials Science*, vol. 90. Elsevier Ltd, pp. 75–127, Oct. 01, 2017, doi: 10.1016/j.pmatsci.2017.07.004.
- [135] J. Xie, Q. Chen, H. Shen, and G. Li, “Wearable graphene devices for sensing,” *J. Electrochem. Soc.*, vol. 167, no. 3, p. 37541, 2020, doi: 10.1149/1945-7111/ab67a4.
- [136] L. A. Falkovsky, “Optical properties of graphene,” in *Journal of Physics: conference series*, 2008, vol. 129, no. 1, p. 12004.
- [137] J. Chang, G. Zhou, E. R. Christensen, R. Heideman, and J. Chen, “Graphene-based

- sensors for detection of heavy metals in water : a review,” pp. 3957–3975, 2014, doi: 10.1007/s00216-014-7804-x.
- [138] A. J. S. Ahammad, T. Islam, and M. M. Hasan, “Graphene-based electrochemical sensors for biomedical applications,” in *Biomedical Applications of Graphene and 2D Nanomaterials*, Elsevier, 2019, pp. 249–282.
- [139] L. A. Ponomarenko *et al.*, “Chaotic Dirac billiard in graphene quantum dots,” *Science (80-.)*, vol. 320, no. 5874, pp. 356–358, 2008.
- [140] J. Liu, Z. Liu, C. J. Barrow, and W. Yang, “Molecularly engineered graphene surfaces for sensing applications: A review,” *Analytica Chimica Acta*, vol. 859. Elsevier, pp. 1–19, Feb. 15, 2015, doi: 10.1016/j.aca.2014.07.031.
- [141] W. Choi, I. Lahiri, R. Seelaboyina, and Y. S. Kang, “Synthesis of graphene and its applications: a review,” *Crit. Rev. Solid State Mater. Sci.*, vol. 35, no. 1, pp. 52–71, 2010.
- [142] B. Raval and I. Banerjee, “Functionalized Graphene Nanocomposite in Gas Sensing,” in *Functionalized Graphene Nanocomposites and Their Derivatives: Synthesis, Processing and Applications*, Elsevier, 2018, pp. 295–322.
- [143] V. Singh, D. Joung, L. Zhai, S. Das, S. I. Khondaker, and S. Seal, “Graphene based materials: past, present and future,” *Prog. Mater. Sci.*, vol. 56, no. 8, pp. 1178–1271, 2011.
- [144] D. V Kosynkin *et al.*, “Longitudinal unzipping of carbon nanotubes to form graphene nanoribbons,” *Nature*, vol. 458, no. 7240, pp. 872–876, 2009.
- [145] B. Shen, J. Ding, X. Yan, W. Feng, J. Li, and Q. Xue, “Influence of different buffer gases on synthesis of few-layered graphene by arc discharge method,” *Appl. Surf. Sci.*, vol. 258, no. 10, pp. 4523–4531, 2012.
- [146] S. William, J. R. Hummers, and R. E. Offeman, “Preparation of graphitic oxide,” *J.*

- Am. Chem. Soc.*, vol. 80, no. 6, p. 1339, 1958.
- [147] K. Sheng, Y. Xu, L. I. Chun, and G. Shi, “High-performance self-assembled graphene hydrogels prepared by chemical reduction of graphene oxide,” *New Carbon Mater.*, vol. 26, no. 1, pp. 9–15, 2011.
- [148] V. Georgakilas *et al.*, “Functionalization of graphene: covalent and non-covalent approaches, derivatives and applications,” *Chem. Rev.*, vol. 112, no. 11, pp. 6156–6214, 2012.
- [149] T. Kuilla, S. Bhadra, D. Yao, N. H. Kim, S. Bose, and J. H. Lee, “Recent advances in graphene based polymer composites,” *Prog. Polym. Sci.*, vol. 35, no. 11, pp. 1350–1375, 2010.
- [150] M. M. Velázquez, T. Alejo, D. López-Díaz, B. Martín-García, and M. D. Merchán, “Langmuir-Blodgett Methodology: A Versatile Technique to Build 2D Material Films,” in *Two-dimensional Materials - Synthesis, Characterization and Potential Applications*, InTech, 2016.
- [151] M. S. Kim, L. Ma, Z. Choudhury, S. S. Moganty, S. Wei, and L. A. Archer, “Fabricating multifunctional nanoparticle membranes by a fast layer-by-layer Langmuir–Blodgett process: Application in lithium–sulfur batteries,” *J. Mater. Chem. A*, vol. 4, no. 38, pp. 14709–14719, 2016.
- [152] E. B. Aydin, M. Aydin, and M. K. Sezginurk, “Immobilization Techniques of Nanomaterials,” in *New Developments in Nanosensors for Pharmaceutical Analysis*, Elsevier, 2019, pp. 47–78.
- [153] “Depositing Monolayers & Thin Films of Nanoparticles – nanoComposix.” <https://nanocomposix.com/pages/depositing-monolayers-and-thin-films-of-nanoparticles#target> (accessed May 16, 2021).
- [154] M. N. Norizan *et al.*, “Carbon nanotubes: functionalisation and their application in chemical sensors,” *RSC Adv.*, vol. 10, no. 71, pp. 43704–43732, 2020.

- [155] A. Kaliyaraj Selva Kumar, Y. Zhang, D. Li, and R. G. Compton, “A mini-review: How reliable is the drop casting technique?,” *Electrochemistry Communications*, vol. 121. Elsevier Inc., p. 106867, Dec. 01, 2020, doi: 10.1016/j.elecom.2020.106867.
- [156] A. R. Boccaccini, J. Cho, J. A. Roether, B. J. C. Thomas, E. Jane Minay, and M. S. P. Shaffer, “Electrophoretic deposition of carbon nanotubes,” *Carbon*, vol. 44, no. 15. Pergamon, pp. 3149–3160, Dec. 01, 2006, doi: 10.1016/j.carbon.2006.06.021.
- [157] M. Atiq Ur Rehman, Q. Chen, A. Braem, M. S. P. Shaffer, and A. R. Boccaccini, “Electrophoretic deposition of carbon nanotubes: recent progress and remaining challenges,” *Int. Mater. Rev.*, pp. 1–30, 2020.
- [158] A. Sarkar and D. Hah, “Electrophoretic deposition of carbon nanotubes on silicon substrates,” *J. Electron. Mater.*, vol. 41, no. 11, pp. 3130–3138, 2012.
- [159] P. Zhao, L. J. LeSergent, J. Farnese, J. Z. Wen, and C. L. Ren, “Electrophoretic deposition of carbon nanotubes on semi-conducting and non-conducting substrates,” *Electrochem. commun.*, vol. 108, p. 106558, Nov. 2019, doi: 10.1016/j.elecom.2019.106558.
- [160] Š. František and H. Petra, “Layer-by-Layer method – Chobotix.” <https://www.chobotix.cz/research-2/finished-or-inactive-projects/layer-by-layer-method/> (accessed May 17, 2021).
- [161] I. A. Neacșu, A. I. Nicoară, O. R. Vasile, and B. Ș. Vasile, “Inorganic micro- and nanostructured implants for tissue engineering,” in *Nanobiomaterials in Hard Tissue Engineering: Applications of Nanobiomaterials*, Elsevier Inc., 2016, pp. 271–295.
- [162] K. Kakaei, M. D. Esrafil, and A. Ehsani, “Graphene and Anticorrosive Properties,” in *Interface Science and Technology*, vol. 27, Elsevier B.V., 2019, pp. 303–337.
- [163] Q. Zheng, Z. Li, J. Yang, and J. K. Kim, “Graphene oxide-based transparent conductive films,” *Progress in Materials Science*, vol. 64. Elsevier Ltd, pp. 200–247, Jul. 01, 2014, doi: 10.1016/j.pmatsci.2014.03.004.

- [164] D. Lončarević and Ž. Čupić, “The perspective of using nanocatalysts in the environmental requirements and energy needs of industry,” in *Industrial Applications of Nanomaterials*, Elsevier, 2019, pp. 91–122.
- [165] X. Wang, L. Zhi, and K. Müllen, “Transparent, conductive graphene electrodes for dye-sensitized solar cells,” *Nano Lett.*, vol. 8, no. 1, pp. 323–327, 2008.
- [166] A. Abdellah *et al.*, “Flexible carbon nanotube based gas sensors fabricated by large-scale spray deposition,” *IEEE Sens. J.*, vol. 13, no. 10, pp. 4014–4021, 2013.
- [167] X. Wang, J. Sparkman, and J. Gou, “Strain sensing of printed carbon nanotube sensors on polyurethane substrate with spray deposition modeling,” *Commun. Commun.*, vol. 3, pp. 1–6, Mar. 2017, doi: 10.1016/j.coco.2016.10.003.
- [168] J. R. Creighton and P. Ho, “Introduction to chemical vapor deposition (CVD),” *Chem. Vap. Depos.*, vol. 2, pp. 1–22, 2001.
- [169] “Chemical Vapour Deposition (CVD) - An Introduction.”
<https://www.azom.com/article.aspx?ArticleID=1552> (accessed May 18, 2021).
- [170] L. Sun *et al.*, “Chemical vapour deposition,” *Nat. Rev. Methods Prim.*, vol. 1, no. 1, pp. 1–20, 2021.
- [171] T. Wang *et al.*, “A review on graphene-based gas/vapor sensors with unique properties and potential applications,” *Nano-Micro Lett.*, vol. 8, no. 2, pp. 95–119, 2016.
- [172] Y. M. Manawi, A. Samara, T. Al-Ansari, and M. A. Atieh, “A review of carbon nanomaterials’ synthesis via the chemical vapor deposition (CVD) method,” *Materials (Basel)*, vol. 11, no. 5, p. 822, 2018.
- [173] S. Kleckley *et al.*, “Fullerenes and polymers produced by the chemical vapor deposition method,” ACS Publications, 1998.

- [174] A. Sanginario, B. Miccoli, and D. Demarchi, "Carbon Nanotubes as an Effective Opportunity for Cancer Diagnosis and Treatment," *Biosensors*, vol. 7, no. 1. 2017, doi: 10.3390/bios7010009.
- [175] G. J. M. Fehine *et al.*, "Direct dry transfer of chemical vapor deposition graphene to polymeric substrates," *Carbon N. Y.*, vol. 83, pp. 224–231, Mar. 2015, doi: 10.1016/j.carbon.2014.11.038.
- [176] as aaaaaas, "Senzorová platforma BI2," Palackého 644, 388 15 Blatná. Accessed: May 25, 2021. [Online]. Available: http://www.tesla-blatna.cz/_soubory/katalogovy_list_bi2.pdf.
- [177] B. Kim, T. J. Norman, R. S. Jones, D. Moon, J. Han, and M. Meyyappan, "Carboxylated single-walled carbon nanotube sensors with varying pH for the detection of ammonia and carbon dioxide using an artificial neural network," *ACS Appl. Nano Mater.*, vol. 2, no. 10, pp. 6445–6451, 2019.
- [178] A. Hannon, Y. Lu, J. Li, and M. Meyyappan, "Room Temperature Carbon Nanotube Based Sensor for Carbon Monoxide Detection," *J. Sensors Sens. Syst.*, vol. 3, pp. 349–354, Dec. 2014, doi: 10.5194/jsss-3-349-2014.
- [179] H. Ehtesabi, "Carbon nanomaterials for salivary-based biosensors: a review," *Materials Today Chemistry*, vol. 17. Elsevier Ltd, p. 100342, Sep. 01, 2020, doi: 10.1016/j.mtchem.2020.100342.
- [180] "Allotropes of Carbon - Study Material for IIT JEE | askIITians." <https://www.askiitians.com/iit-jee-s-and-p-block-elements/allotropes-of-carbon/> (accessed May 08, 2021).
- [181] A. Krueger, *Carbon materials and nanotechnology*. John Wiley & Sons, 2010.
- [182] T. M. B. F. Oliveira *et al.*, "Current overview and perspectives on carbon-based (bio)sensors for carbamate pesticides electroanalysis," *TrAC - Trends in Analytical Chemistry*, vol. 124. Elsevier B.V., p. 115779, Mar. 01, 2020, doi:

- 10.1016/j.trac.2019.115779.
- [183] S. Pilehvar and K. De Wael, “Recent advances in electrochemical biosensors based on fullerene-C60 nano-structured platforms,” *Biosensors*, vol. 5, no. 4, pp. 712–735, 2015.
- [184] T. C. Hirschmann *et al.*, “Characterization of bundled and individual triple-walled carbon nanotubes by resonant Raman spectroscopy,” *ACS Nano*, vol. 7, no. 3, pp. 2381–2387, Mar. 2013, doi: 10.1021/nn3055708.
- [185] L. Y. Jun *et al.*, “An overview of functionalised carbon nanomaterial for organic pollutant removal,” *J. Ind. Eng. Chem.*, vol. 67, pp. 175–186, Nov. 2018, doi: 10.1016/j.jiec.2018.06.028.
- [186] R. Bogue, “Graphene sensors: a review of recent developments,” *Sens. Rev.*, 2014.
- [187] G. Barroso, Q. Li, R. K. Bordia, and G. Motz, “Polymeric and ceramic silicon-based coatings—a review,” *J. Mater. Chem. A*, vol. 7, no. 5, pp. 1936–1963, 2019.
- [188] L. Fu and A. M. Yu, “Carbon nanotubes based thin films: fabrication, characterization and applications,” *Rev. Adv. Mater. Sci*, vol. 36, no. 1, pp. 40–61, 2014.
- [189] “Deposition Technologies: An Overview,” in *Handbook of Deposition Technologies for Films and Coatings*, Elsevier Inc., 2010, pp. 1–31.

